Robust Decentralized L. F. C. with Online Interaction Trajectory Improvement

by

Ali Abdel-Gader Cherid

A Thesis Presented to the

FACULTY OF THE COLLEGE OF GRADUATE STUDIES

KING FAHD UNIVERSITY OF PETROLEUM & MINERALS

DHAHRAN, SAUDI ARABIA

In Partial Fulfillment of the
Requirements for the Degree of

MASTER OF SCIENCE

In

ELECTRICAL ENGINEERING

June, 1983

Order Number 1355728

Robust decentralized L.F.C. with online interaction trajectory improvement

Cherid, Ali Abdel-Gader, M.S.

King Fahd University of Petroleum and Minerals (Saudi Arabia), 1983

U·M·I
300 N. Zeeb Rd.
Ann Arbor, MI 48106

ROBUST DECENTRALIZED L.F.C. WITH ONLINE INTERACTION TRAJECTORY IMPROVEMENT

BY

ALI ABDEL-GADER CHERID

THESIS

PRESENTED TO THE FACULTY OF THE COLLEGE OF GRADUATE STUDIES

UNIVERSITY OF PETROLEUM AND MINERALS

DHAHRAN, SAUDI ARABIA.

IN PARTIAL FULFILLMENT OF THE

REQUIREMENTS FOR THE DEGREE OF

MASTER OF SCIENCE IN ELECTRICAL ENGINEERING

JUNE 1983

UNIVERSITY OF PETROLEUM AND MINERALS

DHAHRAN, SAUDI ARABIA.

This thesis, written by

ALI ABDEL-GADER CHERID

under the direction of his Thesis Committee, and approved by all its members, has been presented to and accepted by the Dean, College of Graduate Studies, in partial fulfillment of the requirements for the degree of

MASTER OF SCIENCE IN ELECTRICAL ENGINEERING

Dean, College of Graduate Studies

Date:

Department Chairman

THESIS COMMITTEE

Chairman

Member

Member

بسم الله الرحمن الرحيم

اقرأ باسم ربك الذي خلق

خلق الإنسان من علق

اقرأ وربك الأكرم الذي علم بالقلم

علم الإنسان ما لم يعلم

العلق : ١ - ٥

This thesis is dedicated to my parents

ACKNOWLEDGEMENTS

Acknowledgement is due to the University of Petroleum and Minerals for support of this research.

I wish to express my appreciation to Dr. Y.L. Abdel-Magid, Assistant Professor of Electrical Engineering, who served as my major advisor. I also wish to thank the other members of my Thesis Committee, Prof. A.H. El-Abiad and Dr. G.M. Aly, Assoc. Professor of Systems Engineering.

Thanks are also due to Mr. M.K. Butt, Secretary of Electrical Engineering Department, for his excellent typing of the thesis and sincere cooperation.

TABLE OF CONTENTS

Page

LIST OF FIGURES

ABSTRACT

A Model-following decentralized algorithm to design near-optimal load frequency regulator for large interconnected dynamic power systems is considered. By using a simple reduced-order model for the interaction between subsystems, a decentralized controller whose parameters are independent of initial states and which can accommodate constant disturbances, is designed. No information transfer between different sub-systems is necessary. The choice of the crude model of the interaction is scrutinized in order to develop a feedback controller which fits the load frequency problem.

The decentralized algorithm is applied to a multi-area power system to control the load and frequency. The performance of the resulting controller is compared to that of the known integrated optimal controller. The algorithm is also tested on different system configurations to prove its efficiency.

بسم الله الرحمن الرحيم

الموجز

تدور هذه الاطروحة حول تصميم منظّم يعمل على التحكم في ذبذبات الحمل – في شبكات الطاقة الديناميكية المترابطة الكبيرة – ليجعل مسارها منضبطا .

سنرى أنّه بواسطة أستخدامنا لنموذج بسيط ذي الدرجة المبسّطة للتفاعل بين الشبكات الجزئية ، فإنه يمكن تصميم المنظّم اللامركزي ذي المعاملات المستقلّة عن الحالات البدائية ، والذى يمكنه أن يتلائم مع الاضطرابات الثابتة ، وكما أنّه لايوجد ضرورة لنقل معلومات بين الشبكات الفرعية المختلفة .

ويتمّ التأكد والتدقيق في أختبار النموذج الخام ، للتفاعل بين الشبكات الفرعية للتمكّن من أنشاءمنظّم ذي التغذية الخلفية المغلقة والذي يناسب مسألة تذبذب الحمل .

إنّ النظام اللّامركزي يجدي تطبيقه في شبكات الطاقة ذات المناطق المتعدّدة للتحكم بتذبذب الحمل .

إنّ آداء هذا المنظّم يتمّمقارنته مع آداء المنظّم المتكامل ذى الحالة الأمثل المعروفة ، ويتمّ أيضا فحص النّظام على هيئات متعددة لشبكات مختلفة لاثبات فاعليّة هذا النظام .

1. INTRODUCTION

1.1 GENERAL OVERVIEW

Man's demand for consumption of energy has increased steadily. A major portion of the energy need of modern society is supplied in the form of electrical energy. Very complex power systems have been built to satisfy this increasing demand. Now, there is tendency toward an interconnected network of transmission lines linking generators and loads into a large interconnected system. Many advantages can be derived from operating the system into a large interconnected system. If for example a small group of power system say of 1000-MW rating loses 300-MW (which represents 30% of its rating) and if operating alone, will be in big trouble. If the same system was part of large group, say 100,000-MW capacity the same 300-MW generation failure would represent only a 0.3% loss of the total rating capacity. The frequency would be saved and by mutual assistance the 300-MW would instantaneously flow into the crippled area via the tie-lines which are connected to it. Moreover the system size reduces the need for reserve power among the individual area.

This vast enterprise of supplying electrical energy presents many engineering problems. The design, planning and operation of such systems are exceedingly complex. The entire design must be based on automatic control and not on the slow response of human operators.

The load and frequency control (L F C) problem has been one of the major subject concerning power system engineers. It is becoming now much more significant in accordance with increasing size and complexity of interconnected power systems. Until now much work [1-9] has been carried out to improve the design of load and frequency controller.

In classical control, the dynamical and transient system response of the closed loop are not guaranteed to be stable. From previous study and practical results [12] it was found that, the response of the interconnected power system depends mainly on the choice of K_I and B which are respectively the gain of the area control error (ACE) and the frequency bias constant. Consequently, the designer task is to select the parameters K_I and B to obtain a satisfactory response and obtain a controllable closed-loop system. However there is no standard method of solving such problem especially in large systems.

Actually, the design of such problem involves trial and error analysis. Moreover there is no sufficient condition which guarantees the existence of the optimal controller.

Accordingly, to be able to predict the performance of such large and complex systems, it is required to seek even more powerful tools of analysis and synthesis. One way of handling such large systems is by using modern control. The optimal control theory has been successfully applied in power systems by many authors [1,2]. However the applications of these techniques brought new difficulties to the analysis and, synthesis of the newly developed controllers.

Recently many authors have tackled the subject of L F C. from the decentralized point of view [4,6-8]. Numerous problems facing previous methods have been solved, examples are computation time and memory storage.

1.2 OBJECTIVE

The thesis objective is to design an efficient robust decentralized regulator for the LFC problem. The problem is formulated using for each subsystemm a low-order model for the interactions. The output of the interaction model is improved online using a model-following technique [13]. Specifically, the following points will be investigated:

a) The choice of the crude model for the interaction.

b) The effect of the weighting matrices of the states and the control.

c) Introducing a sub-optimality measure.

d) The application of the algorithm to a multi-area power system of different configurations:

   * radial
   * cascaded
   * system containing loops

e) Simulation of the system on the computer for comparison with different existing methods.

1.3 THESIS OUTLINE

The thesis consists of six chapters.

- The first chapter gives an introduction to the thesis of large interconnected power systems. It also includes the advantages of interconnecting the power system into large interconnected system.
- The second chapter presents a literature review of various existing control methods applied to L F C.
- The third chapter gives in sufficient detail the model following algorithms. It also includes the design of the robust decentralized controller.
- In chapter four a description of the power system is considered. It also includes the state space representation of the model.
- In chapter five, a complete simulation of a two area-power system is presented. The results and conclusion are given.

- In chapter six the algorithm is applied to a four areas power system with different configurations. Simulation results are also given.

2. LITERATURE REVIEW

2.1 INTRODUCTION

In the last few years many techniques have been developed to improve the response of the system with optimum time and cost using simple algorithms [3-7]. One way is by using decentralized controllers. There are various efficient methods which have been developed to design these sub-optimal controllers. However, there are many associated problems which require detailed study. The main problem in decentralized control is the decomposition of large systems. The interaction state variables which are not available to the system can be introduced by imposing constraints on the appropriate subsystem model. In some cases sufficient conditions for stability have been developed.

2.2 CLASSICAL L F C.

The basic approach of classical control is to find the best value of the parameters K_I, gain of the area control error (ACE) integration and B, the frequency bias, in the sense to minimize the integral square error (ISE) criterion [10,11].

The error is defined as the tie-line power deviation from scheduled value and the frequency deviation from nominal value. The regulator consists of a conventional integral control of the area control error (ACE) used as the feedback signal. The area control error is defined mathematically as

$$ACE = \Delta P_{tie} + B\ \Delta F \tag{2-1}$$

and the speed changer command ΔP_C is of the form:

$$\Delta P_c = -K_I \int (\Delta P_{tie} + B\ \Delta F)\ dt \tag{2-2}$$

$$= -K_I \int ACE\ dt$$

where ΔP_{tie} is the sum of all the tie-lines power connected to the controlled area and ΔF is the frequency deviation.

Many authors [3-5] have tried to improve the response of L F C using only classical control, and with more detailed mathematical description of the power system, however the response did not drastically improve.

2.3 DESIGN OF REGULATOR USING MODERN OPTIMAL CONTROL

In [1], a new approach of the power system control problem has been reported. This approach is based on the design method of modern control theory.

A model of multi-area power system was derived in the state space form and can be stated as follows:

Given the cost function:

$$C = 1/2 \int (x^t\ Q\ x + u^t\ R\ u)\ dt \qquad (2\text{-}3)$$

where: Q nxn positive semi-definite symmetric state weighting matrix.

R mxm positive definite symmetric control weighting matrix.

x nx1 state vector.

u mx1 control vector.

Find the control vector u that minimizes the cost function C and which is constrained to the system dynamics.

$$\dot{x} = Ax + Bu \tag{2-4}$$

where A and B are state distribution matrix and the control distribution matrix with proper dimensions respectively.

If the system is observable and controllable, the control vector u, which minimizes the cost function always exists in the form:

$$u = -Kx \tag{2-5}$$

where $K = R^{-1}B^{t}p$

The feedback gain K is calculated in the sense to minimize the specified cost function (Performance Index).

The matrix p is obtained by solving a matrix Riccati differential equation. For the infinite time problem the Riccati equation has a steady state solution. Since the gain matrix is constant, the optimally controlled system can be expressed in a simple form.

The optimal controller assumes that the information about all the states is always available. The structure of an integrated controller is shown in Fig. (2-1).

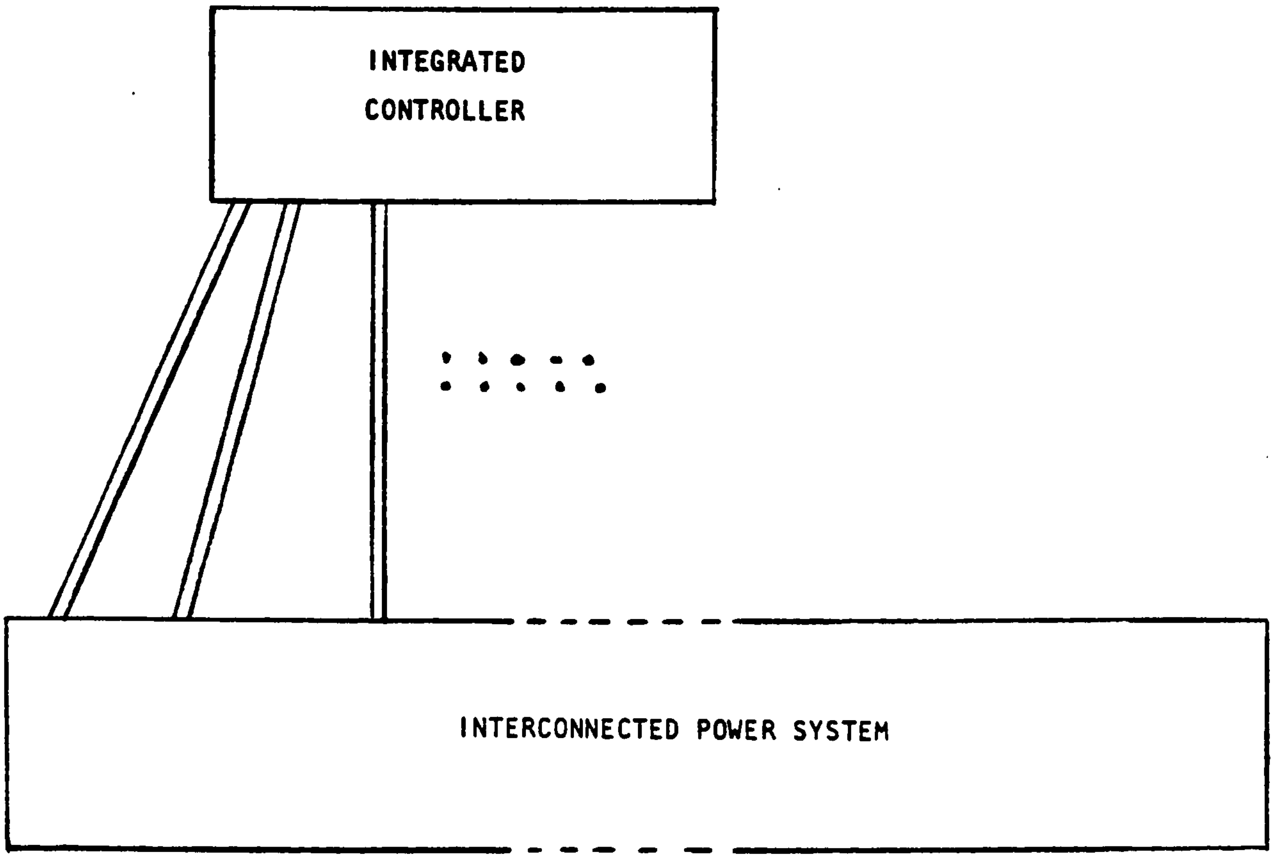

Figure (2-1). Integrated Controller.

2.4 DECENTRALIZED REGULATORS

Decentralized and multilevel control system seems to solve many of the problems (as complexity of the controller, computation time etc.) encountered in the integrated controller. Two major factors contributed to the growth and subsequent rapid development of the theory in this area in the past years are:

1. The finite length of computation time and the increasing complexity of the control system.

2. The decentralized control system has numerous potential advantages over the centralized one for large scale systems such as:

   - ease of design,
   - parallel computation,
   - system reliability,
   - incorporation of micro or mini-computer.

Moreover the structure of large power system occurring in practice can be identified as an interconnection of subsystems. This suggests the use of many controllers to accomplish the control function instead of one integrated controller. Two structures of decentralized control system have been proposed in Figs. (2-2) and (2-3).

The basic feature of decentralized control approach is the problem of decomposition. A large scale system may be decoupled into a set of smaller and independent subsystems which can be solved independently.

Then the optimization problem becomes:

$$\min_{u} J = \sum_{i=1}^{N} \frac{1}{2} \int_{0}^{\infty} \{||x_i||^2_{Q_i} + ||u_i||^2_{R_i}\} \, dt \qquad (2\text{-}6)$$

Subject to

$$\dot{x}_i = A_i x_i + B_i u_i + C_i z_i \qquad (2\text{-}7)$$

$$z_i = \sum_{j=1}^{N} L_{ij} x_j \qquad \text{for } i=1,2, \text{---} N \qquad (2\text{-}8)$$

Various techniques [4,6-9] have been applied to large interconnected power systems such as two-level and

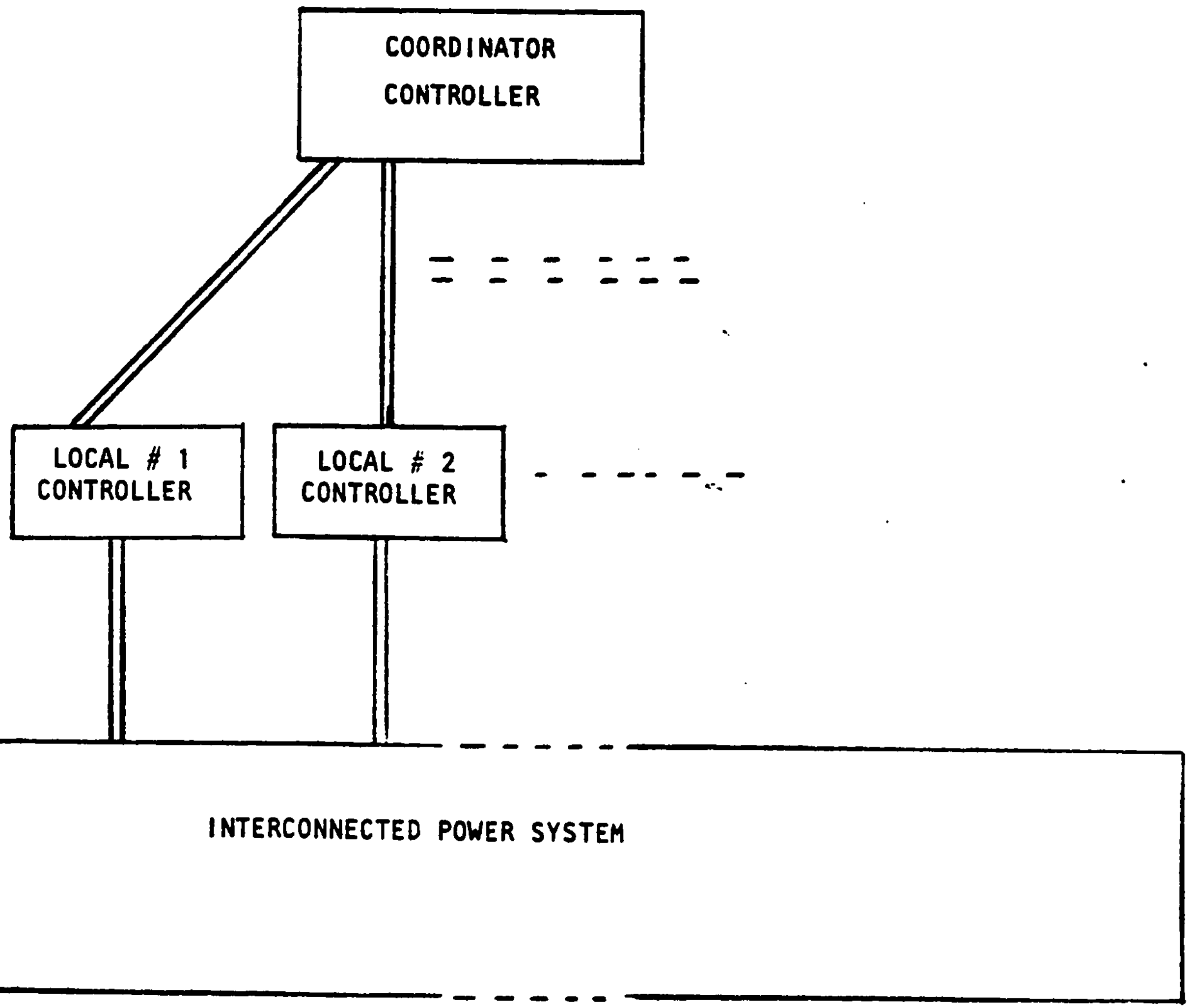

Figure (2-2). Two-level controller.

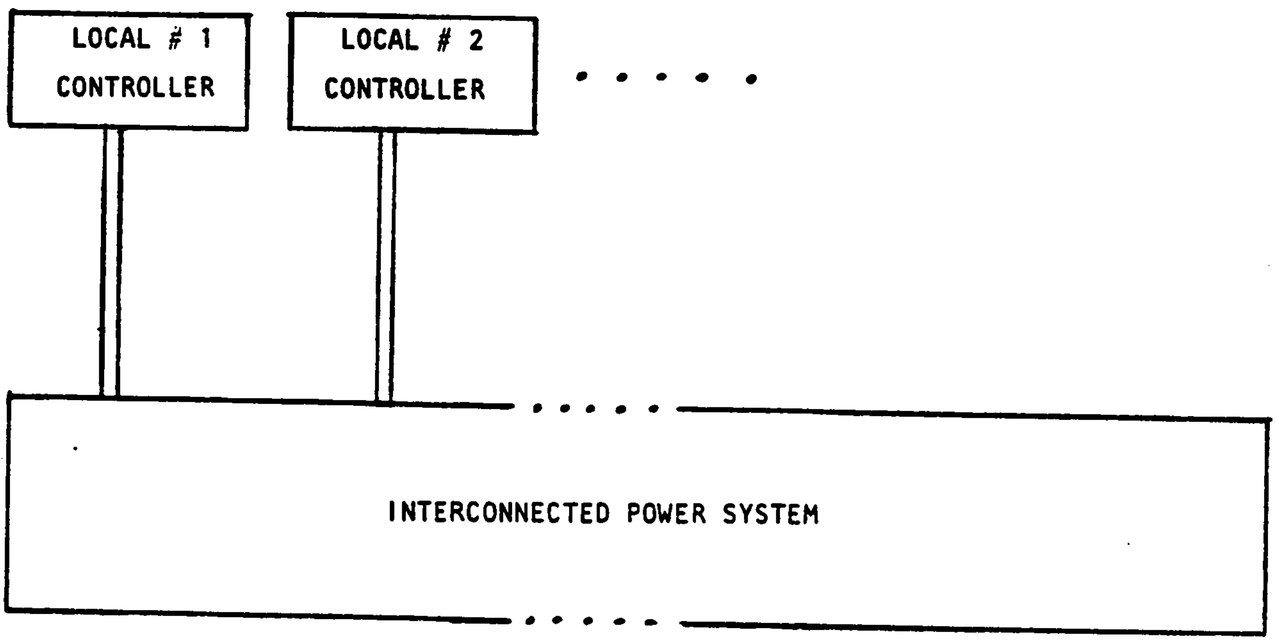

Figure (2-3). Completely decentralized controller.

complete decentralized control. Some of these techniques will be discussed, and a brief comparison will be presented.

2.4.1 Multi-level Control Structure

In [8] a two-level method was applied to a two-area power system. The basic approach in the two-level technique is to form two processing levels where on the lower level n independent sub-problems are solved (i.e. neglecting the interaction or constraints equation between different sub-system). The parameters of the lower level sub-optimal controller are computed from the subsystem information. The second-level controller is computed in order to take into account the interaction between sub-systems.

The total control force of the ith subsystem can be expressed as:

$$u_i = u_{\ell i} + u_{gi} \qquad (2\text{-}9)$$

where $u_{\ell i}$ is the first level control signal (or local control signal) and is computed using the well known relation:

$$u_{\ell i} = -R_i^{-1} B^t P_i x_i \qquad (2\text{-}10)$$

where the matrix P is the solution of the Riccati equation

$$P_i A_i + A_i^t P_i - P_i B_i R_i^{-1} B_i^t P_i + Q_i = 0 \qquad (2\text{-}11)$$

and the second level controller is obtained in the following way. Let us assume

$$A = A_d + A_o$$

where $A_d = \text{diag}\ (A_1, A_2, \ldots\ldots, A_N)$

and A_o containing the off-diagonal blocks.

Then the controlled system can be written as:

$$\left.\begin{aligned} dx/dt &= (A_d + A_o)\ x + B(u_\ell + u_g) \\ &= A_d\ x + B\ u_\ell + A_o\ x + B\ u_g \end{aligned}\right\} \quad (2\text{-}12)$$

The last two terms can be compensated if the following condition is satisfied

$$\left.\begin{aligned} &A_o\, x + B\, u_g = 0 \\ \text{so} \quad &u_g = -(B^t\, B)^{-1}\, B^t\, A_o\, x \end{aligned}\right\} \qquad (2\text{-}13)$$

$$\text{or} \quad u_g = -G\, x$$

$$\text{where} \quad G = (B^t\, B)^{-1}\, B^t\, A_o \qquad (2\text{-}14)$$

The two-level structure is shown in Fig. (2-4).

2.4.2 Completely Decentralized Controllers

Many methods [3,4,6,7] have been developed to eliminate complete transfer of information between subsystems.

In [3] the solution to the LFC problem is based on the conventional tie-line bias control (TBC). The regulator consists of conventional integral control part, and an additional proportional and derivative control parts with the area control error (A C E) used as a feedback signal. The feedback scheme is shown in Fig. (2-5).

The design approach of the controller is as follows:

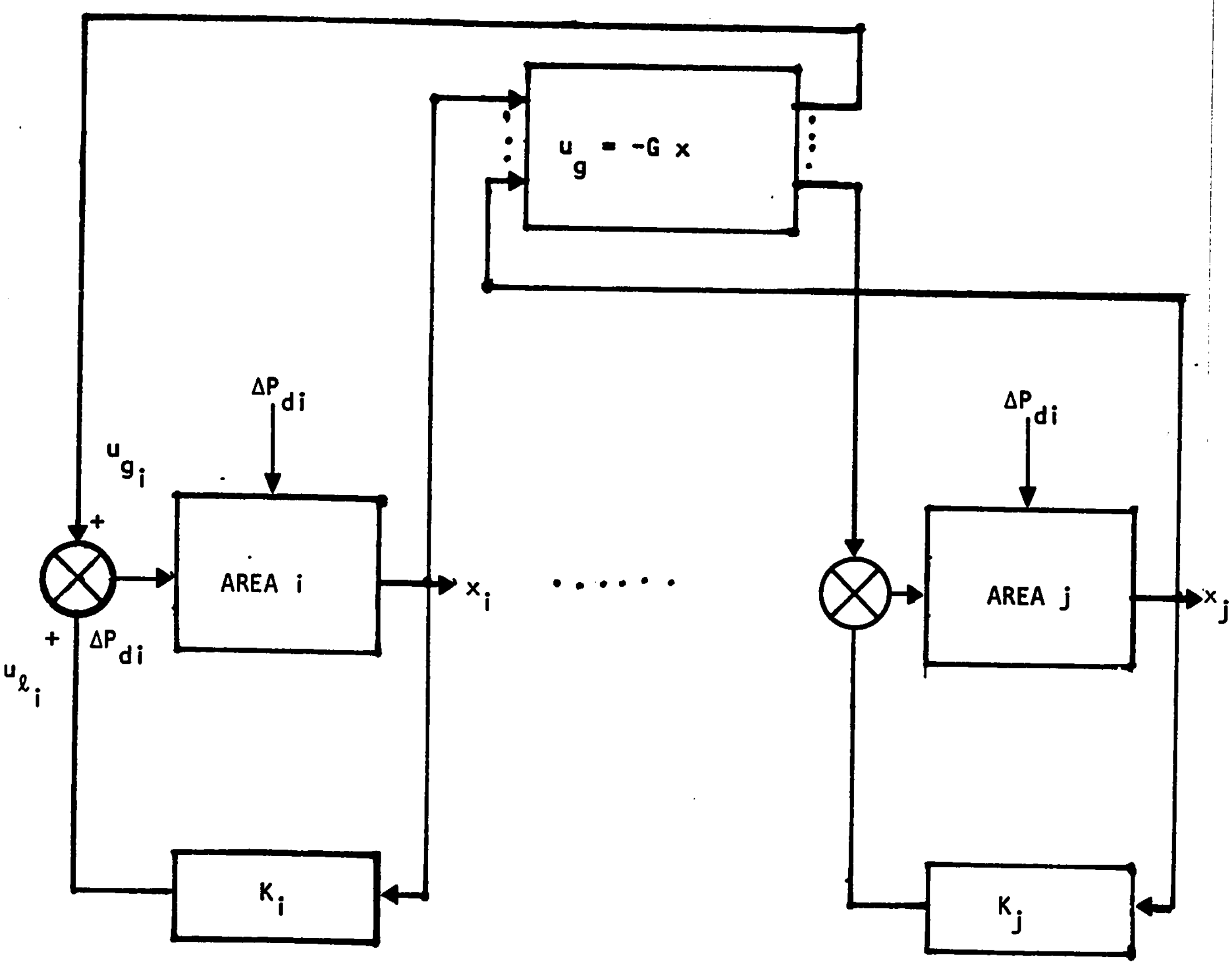

Figure 2-4. Two-level control.

$$\text{Min } J = \frac{1}{2}\int_0^\infty x^t Q x \, dt \qquad (2\text{-}15)$$

where Q is positive semi-definite symmetric matrix subject to the constraints

$$\dot{x} = A(h)\, x \qquad (2\text{-}16)$$

where x, A and h are the state vector, the system matrix and the feedback gain vector, respectively. The vector gain h is selected in the sense of minimizing the performance index J. The feedback gains of the decentralized regulator are determined by Newton interactive algorithm. Additional limiters are added to prevent excessive control action.

The problem can be replaced by the following optimization problem

$\min_h J = Tr(K\, X_o)$ subjected to Liapunov equation:

$$A^t\, K + K\, A = -Q \qquad (2\text{-}17)$$

where $T_r(\ .\ )$ is the trace operator.

K denotes the positive definite matrix solution of equation (2-17).

The matrix X_o is defined as:

$$X_o = x_o x_o^t \qquad (2\text{-}18)$$

x_o = initial value of state vector x.

The necessary conditions for optimality are given by

$$dJ/dh_i = Tr\ (dK/dh_i\ X_o) = 0 \qquad (2\text{-}19)$$

for all i.

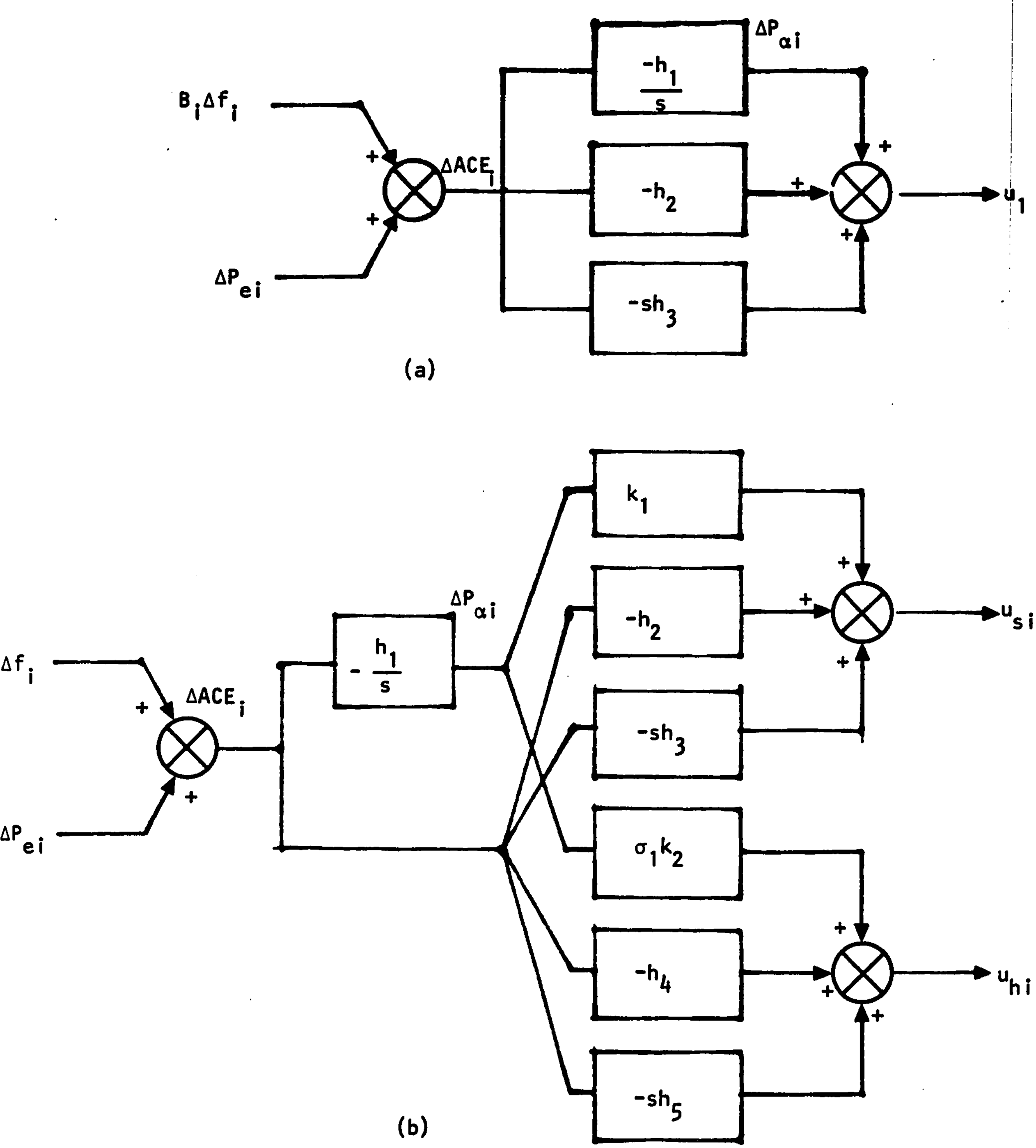

Figure 2-5(a). Block diagram of decentralized regulator for model containing only nonreheat turbine.

Figure 2-5(b). Block diagram of decentralized regulator for model containing reheat turbine and hydroplant.

The regulator gain h can be modified recursively by Newton Raphson algorithm along the direction of correction Δh, determined by the following equation, until the optimal conditions in Eqn. (2-19) are satisfied:

$$\Delta h = -M^{-1} d \qquad (2\text{-}20)$$

$$m_{ij} = m_{ji} = \partial^2 J/(\partial h_i \partial h_j) = \mathrm{Tr}\,[\partial^2 k/(\partial h_i \partial h_j)\ X_o]$$

$$= (i,j) \text{ element of Jacobian matrix } M.$$

$$d_i = \frac{\partial J}{\partial h_i} = \mathrm{Tr}\,[\frac{\partial k}{\partial h_i}\ X_o] = i\text{th element of column vector } d.$$

In [7] an approach was developed to solve the load and frequency control problem by shifting the closed-loop eigenvalues to the left. A class of minimum order robust decentralized controllers which solve the general multi-area load frequency problems are obtained.

In [6], the area decomposition method is applied to multi-area L F C system. The system is divided into subsystems which are controlled individually.

After decomposition some of the subsystems may not be controllable. These are called peculiar systems. The system is made to be controllable by adding matrices to the distribution state matrices of sub-systems which are not controllable.

2.5 DISCUSSION

The conventional way of solving the load and frequency control problem is not likely to be significantly improved by assuming that a detailed mathematical description of the power system is available or by using more complex controller [9]. Moreover the classical control is based on trial and error analysis.

The optimal controller of the integrated system involves many difficulties which can be summarized as follows:

- the computation time for large system is extremely large.
- The required storage may exceed the capacity of the available computers. For an n area power system, the minimum number of state variables necessary to describe the system is 3n.

For interconnected power system, more state variables are required to describe adequately the system.

The state distribution matrix A is of dimension 3n x 3n which represents $9xn^2$ memory location to store the matrix A.

Moreover the controller is very complex and difficult to maintain. The implementation cost is highly expensive due to the telemetring of the required data to the central controller when the system is spread over large geographical area which might be the case for an interconnected power system.

The reliability of large systems decreases very rapidly with increasing complexity.

There are limits on the speed of computation beyond which no process can be done.

The multi-level method requires the solution of the global system to compute the second level controller.

Moreover it requires the transfer of information to the second level controller.

In [3] a complicated algorithm was developed. The system response was found to be far from the optimal control (the integrated optimal control). There is no condition for stability and the system response is very oscillatory.

Moreover the controller is not optimal in the sense that the controlled system (i.e. interconnected power system) includes constraints on the control force which was not taken into account. Finally the decomposition was not mentioned.

In [6-7] the required constraints are not explicitly expressed. Second, the method requires the computation of the poles and zeros of the global system, moreover the condition of stability of the system depends on the integrated system. From the simulation, the incremental change of the frequency reaches a peak of 0.008 at time equal to 4.0-seconds. The system remains oscillating 16-second with a minimum peak of 0.002, which is far from the optimal integrated control.

Based on references [13] an attempt is being made to come up with an efficient algorithm for designing decentralized controller for LFC of multi-area system.

3. MODEL-FOLLOWING DECENTRALIZED CONTROLLERS

3.1 INTRODUCTION

The purpose of load and frequency control is to maintain the frequency and tie-line at certain preselected values. The suggested control strategy is to decentralize the controller using modern control theory. The control obtained is a linear in function of the state variables of the controlled sub-system only.

The interaction state variables unavailable to the controller will be estimated using an appropriately designed crude model. Using model-following techniques, the interaction state variables are corrected online, before being used to generate the feedback control force.

To apply modern control theory, it is required to represent the controlled system into state variable form, and specify the desired performance index mathematically in terms of a cost function to be minimized. The controller obtained is optimal in the sense of minimizing the specified cost function.

The method will be applied to a multi-area power system. Sufficient conditions to guarantee the stability of the closed-loop system have been developed [12].

3.2 LINEAR SYSTEM

Linear and time invariant systems can be represented mathematically in the form

$$\dot{x} = Ax + Bu \tag{3-1}$$

Where x is the state vector, u is the command input to the system. A and B are distribution matrices of the state vector and control vector respectively.

The state space model describes the actual physical system operating under small perturbation.

3.3 SYSTEM COST

The performance of the system is specified in terms of a cost that is to be minimized. The weighting matrices Q and R are chosen depending on the design criteria.

Q penalizes the state deviation from its scheduled values, and R penalizes excessive control efforts. The choice of Q and R is of primary importance.

3.4 OPTIMAL CONTROLLER

The optimal control function that minimizes a quadratic cost in state of control variable is a linear function of the present states of the system. The control vector can be represented mathematically by:

$$u = -Kx = -R^{-1}B^{t}P\,x \tag{3-2}$$

The matrix P is determined by solving the matrix Riccatti equation [1], given by

$$\dot{P}(t) \; -P(t)\,A - A^{t}\,P(t) + Q + P(t)\,BR^{-1}B^{t}\,P(t) \tag{3-3}$$

For infinite duration process, the optimal control law P is stationary and can be obtained from solving the matrix equation

$$0 = -PA - A^{t}P - Q + PBR^{-1}B^{t}\,P \tag{3-4}$$

obtained by setting $\dot{P}(t) = 0$ in Eqn. (3-3).

The representation of the optimal controller is as shown in Fig. (3-1).

The optimally controlled system can be expressed in the closed-loop form:

$$\dot{x} = A_c x \tag{3-5}$$

where $A_c = A - BK$ (3-6)

3.5 MODEL-FOLLOWING CONTROL SYSTEM SYNTHESIS TECHNIQUES

The model-following control system is utilized to make the actual system behave like a prespecified ideal system or model.

Let the linear system be defined by

$$\dot{x}_p = A_p x_p + Bu \tag{3-7}$$

and the ideal system or model described by

$$\dot{x}_m = H x_m \tag{3-8}$$

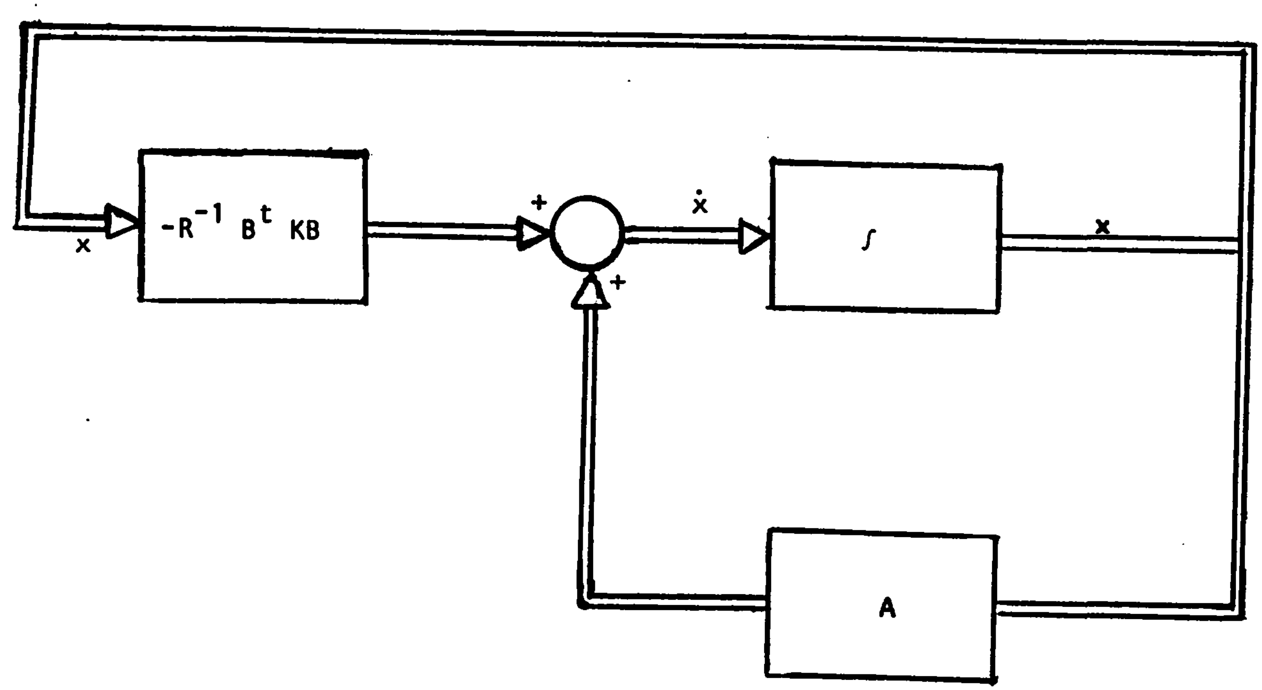

Figure 3.1. Plant and optimal feedback controller.

where the elements of the coefficient matrix H are specified by the designer, x_m and x_p have the same dimension.

Various optimization techniques are available to design model following control. In the next section two of the these techniques are discussed.

3.6 REAL-MODELL-FOLLOWING

In this technique, the plant equations and the dynamic equations defining the ideal system are combined into a single system so that a performance criterion that penalizes the difference between the plant and the model state variables can be selected. Combining these equations into a single system by writing

$$x = \begin{bmatrix} x_p \\ \vdots \\ x_m \end{bmatrix} \qquad (3\text{-}9)$$

gives $$\dot{x} = \begin{bmatrix} A & 0 \\ 0 & H \end{bmatrix} x + \begin{bmatrix} B \\ 0 \end{bmatrix} u \qquad (3\text{-}10)$$

Now an approximate performance criterion for achieving model following is

$$\min_u \int_0^\infty \{(x_p - x_m)^t Q(x_p - x_m) + u^t Ru\} dt$$

$$= \min_u \int_0^\infty \left(\left\{ x^t \begin{bmatrix} Q & -Q \\ -Q & Q \end{bmatrix} \right\} x + u^t R u \right) dt \qquad (3\text{-}11)$$

The computation of the optimal-control law parameters is straight forward. If the system is controllable and observable, then the closed-loop control system is obtained for any prespecified model.

The optimal control law that results from this problem formulation can be written as

$$u = [D_{\text{feed-back}}] x_p + [D_{\text{feed-forward}}] x_m \qquad (3\text{-}12)$$

which can be represented by Fig. (3-2).

3.7 IMPLICIT MODEL-FOLLOWING

A quite different approach to optimal model following is to use the performance criterion to minimize the dynamical differences

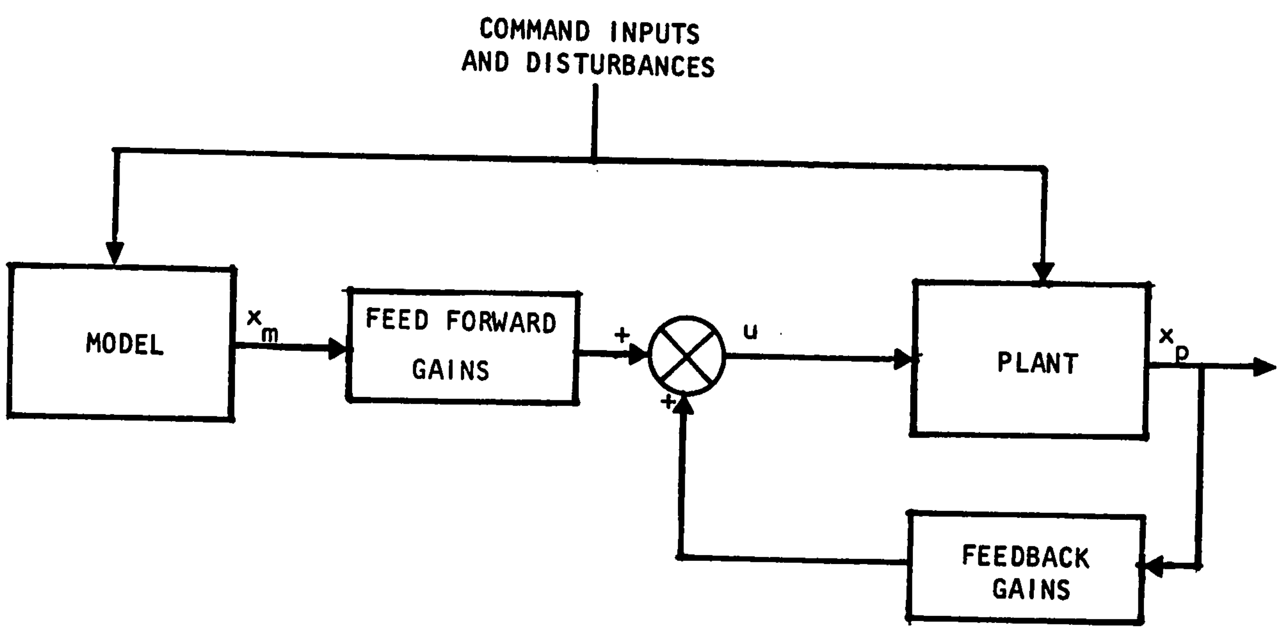

Figure 3-2. Real-model following optimal-control system.

between the ideal and actual systems. Thus the following criterion is used

$$\min_u \int_0^T \{(Ax_p + Bu - Hx_m)^t Q(Ax_p + Bu - Hx_m) + u^t Ru\} \, dt \qquad (3\text{-}13)$$

The first term weighs the difference between the plant rate (dynamics) and the rate that would occur if the controlled system were identical to the ideal system. By minimizing the error between the system, it is made to behave like the specified model.

The resulting control law matches the entire dynamic characteristics of the model system as specified in the performance criterion, and the solution is unique.

3.8 DECENTRALIZED ALGORITHM

Hassan and Singh [13] have developed an approach based on model-following, in which only subsystems level calculation are made. This is done by modelling the interactions with other subsystems via a crude low-order model whose output is improved online before it is used to generate the decentralized sub-optimal control vector. As a result, we obtain a complete, decentralized controller. The question of how the crude model is to be chosen will be clarified.

3.9 MODEL-FOLLOWING ALGORITHM

The basic problem is to minimize the cost function

$$\min_u J = \sum_{i=1}^{N} \frac{1}{2} \int_0^\infty \{\|x_i\|^2_{Q_i} + \|u_i\|^2_{R_i}\} \, dt \tag{3-14}$$

subject to

$$\dot{x}_i = A_i x_i + B_i u_i + C_i z_i \tag{3-15}$$

$$z_i = \sum_{j=1}^{N} L_{ij} x_j \tag{3-16}$$

Where x_i is the n_i-dimensional state vector of the ith subsystem, u_i is the m_i-dimensional control vector and z_i is the q_i-dimensional interconnection vector. We will assume that the pair (A_i, B_i) is completely controllable.

Let us suppose initially that z_i can be represented by the following dynamical model

$$\dot{z}_i = A_{zi} z_i \tag{3-17}$$

Where A_{zi} may be chosen to be the block of the global A matrix corresponding to the vector z_i. To clarify this idea of the choice of A_{zi}, let us consider the integrated forms of Eqns. (3-15) and (3-16), i.e.

$$\dot{x} = Ax + Bu + Cz$$

$$z = Lx$$

The global matrix A is given by (A + CL)

Then, we can modify our optimization problem to the approximate form:

$$\min J = \frac{1}{2} \sum_{i=1}^{N} \int_0^{\infty} \{\|y_i\|^2_{\tilde{Q}_i} + \|u_i\|^2_{R_i}\} \, dt \tag{3-18}$$

subject to

$$\dot{y}_i = \tilde{A}_i y_i + \tilde{B}_i u_i \tag{3-19}$$

where

$$y_i = \begin{bmatrix} x_i \\ \hline z_i \end{bmatrix}, \quad \tilde{A}_i = \left[\begin{array}{c|c} A_i & C_i \\ \hline 0 & A_{zi} \end{array}\right]$$

$$\tilde{B}_i = \begin{bmatrix} B_i \\ \hline 0 \end{bmatrix}, \quad \tilde{Q}_i = \left[\begin{array}{c|c} Q_i & 0 \\ \hline 0 & 0 \end{array}\right] \tag{3-20}$$

In this case, the resulting gain matrix will depend on the chosen matrix A_{zi}, and on the trajectories of z_i, since the control u_i will be a function of both x_i, and z_i. Now, since z_i is not available for measurement, we will not try to improve the model for z_i. Rather, we shall try to modify its trajectories.

If we assume that $(\tilde{A}_i, \tilde{B}_i)$ is controllable, and $(\tilde{A}_i, \tilde{Q}_i)$ are observable, then the solution of Eqn. (3-18) subject to Eqn. (3-19) is given by

$$u_i = -R_i^{-1} \tilde{B}_i^t P_i y_i \tag{3-21}$$

Where P_i is the solution of a matrix Riccati equations. We can rewrite the optimal control as

$$u_i^* = -G_{i1} x_i - G_{i2} z_i \tag{3-22}$$

From the above equation, we see that the gain matrix is a function of the approximate system model, and the optimal control u_i^* is a function of the subsystem x_i and the interconnection input vector z_i.

Even if we can obtain z_i from the interconnection model this model is a relatively crude one. It is therefore required to improve the trajectory online.

To do this, let us consider a subsystem model whose input $\hat{z}_i$ is provided by the crude model i.e.

$$\dot{\hat{x}}_i = A_i\hat{x}_i + B_i\, u_i + C_i\hat{z}_i \tag{3-23}$$

Where $\hat{x}_i$ is the state vector of the subsystem model. Then if we substitute for u_i in Eqns.(3-15) and (3-23), after having replaced z_i by $\hat{z}_i$ in Eqn. (3-22), we have

$$\dot{x}_i' = (A_i - B_iG_{i1})\; x_i' + C_iz_i - B_iG_{i2}\hat{z}_i$$

or $$\dot{x}_i' = \hat{A}_i\; x_i' + C_iz_i - B_iG_{i2}\hat{z}_i \tag{3-24}$$

where $$\hat{A}_i = A_i - B_iG_{i1} \tag{3-25}$$

where x_i' is the sub-optimal state of subsystem i resulting from using $\hat{z}_i$ instead of z_i and

$$\dot{\hat{x}}_i' = \hat{A}_i\hat{x}_i' + C_i\hat{z}_i - B_iG_{i2}\hat{z}_i \tag{3-26}$$

let $$\tilde{x}_i = x_i' - \hat{x}_i' \tag{3-27}$$

$$\hat{z}_i = z_i - \hat{z}_i \tag{3-28}$$

Thus, substracting Eqn. (3-26) from Eqn. (3-24) we obtain

$$\dot{\tilde{x}}_i = \hat{A}_i\tilde{x}_i + C_i\tilde{z}_i \qquad (3\text{-}2\ \ )$$

and our aim is to minimize the error $\dot{x}_i$ and $\tilde{z}_i$. For this problem, we can construct another optimization problem, which is:

$$\min J_i = \frac{1}{2}\int_0^\infty (\|\tilde{x}_i\|^2_{H_i} + \|\tilde{z}_i\|^2_{S_i})\, dt \tag{3-30}$$

subject to the constraint Eqn. (3-28) where H_i and S_i are positive semi-definite and positive-definite matrices respectively.

The solution of this problem is

$$\tilde{z}_i^* = -S_i^{-1} C_i^t K_i \tilde{x}_i \tag{3-31}$$

where K_i is a solution of an appropriate Riccati-type equation.

Using Eqns. (3-29) and (3-31) one obtains

$$z_i = \hat{z}_i - S_i^{-1} C_i^t K_i \tilde{x}_i \tag{3-32}$$

and we will use this to generate the control. Thus the dynamical equation for the subsystem will be

$$\begin{aligned}
\dot{x}_i &= \hat{A}_i x_i + C_i z_i - B_i G_{i2} [\hat{z}_i - S_i^{-1} C_i^t K_i \tilde{x}] \\
\dot{\hat{x}}_i &= \hat{A}_i \hat{x}_i + (C_i - B_i G_{i2}) \hat{z}_i \\
\dot{\hat{z}}_i &= A_{z_i} \hat{z}_i
\end{aligned} \tag{3-33}$$

and which could be represented by Fig. (2-3).

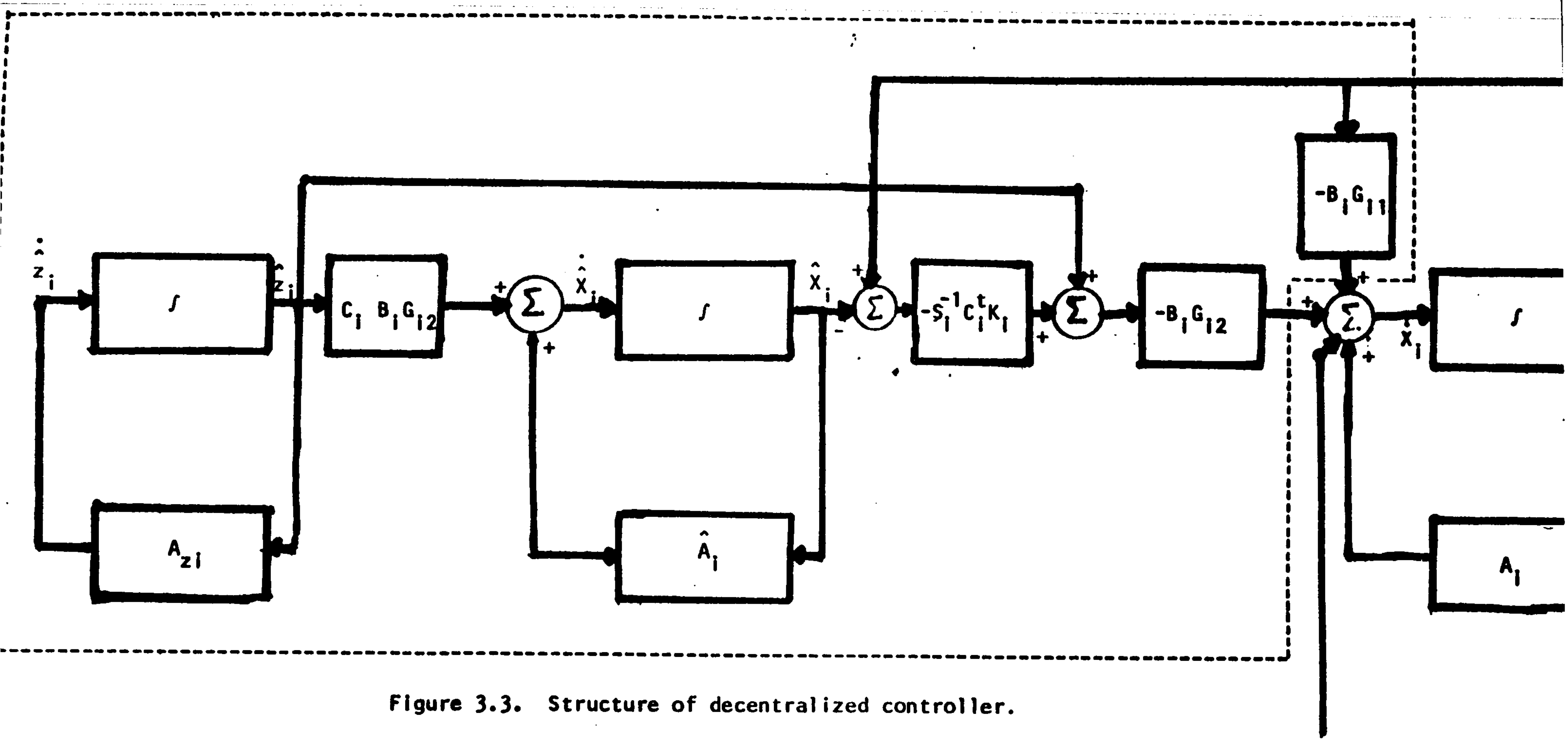

Figure 3.3. Structure of decentralized controller.

This approach can be characterised by the following: (a) The decentralized controller has gains which are independent of the initial conditions. (b) The sub-optimality in the controller design arises from the fact that: (i) The controller does not take into account all the states of the overall system (ii) The decentralized gain matrix G_i depends on the approximate interconnection model. (iii) Although we improve the outputs of the interconnection model, there always remains a difference between z^* and z. (c) The controller is easy to compute, as we see from Fig. (3-3), we only need to work sub-system by subsystem and the global solution is not required. The blocks of Fig. (3-3) are easy to calculate.

4. POWER SYSTEM MODEL

4.1 INTRODUCTION

A power system is an enterprise of supplying electrical energy. It consists generally of a large number of generators interconnected into a network of distribution. With the increasing demand in electrical energy, more generators are required. Moreover, for economical and other problems discussed earlier, there is tendency toward an interconnected network. Consequently the planning, implementation,and operation of such systems become exceedingly complex. To simplify the problem, the power system is subdivided into control areas connected by tie lines as it is shown in Fig. (4-1).

4.2 DEFINITION OF CONTROL AREA

The concept of "control area" is in reality a relative one. It assumes that the coupling between generators within an area is strong enough to constitute a coherent group i.e. all generators of a single area have the same frequency, or at least the coupling is stronger than the one between distinct control areas.

4.3 DYNAMIC OF POWER SYSTEM

We shall first develop a dynamic model describing the incremental load and frequency dynamics of a control area i, connected to neighbouring areas via tie-lines as shown in Fig. (4-1). Practically, all power systems today are tied together with neighbouring area.

If the area experiences a load change of magnitude ΔP_{D_i}, the turbine controller increases the output of the turbine by an amount ΔP_{G_i} (MW). The net power surplus in the area therefore equals $\Delta P_{G_i} - \Delta P_{D_i}$, and this power will be absorbed in three ways.

1- By increasing the area kinetic energy $W_{kin,i}$.

2- By an increased load consumption represented by $D_i\ \Delta f_i$.

3- By increasing the export of power via tie-lines, with the total amount $\Delta P_{tie,i}$.

We can express this situation mathematically by

$$\Delta P_{G_i} - \Delta P_{D_i} = \frac{d}{dt}(W_{kin,i}) + D_i.\Delta f_i + \Delta P_{tie,i} \qquad (4\text{-}1)$$

All terms are in MW. It is more practical to divide the equation by P_{r_i}, the total rated area power expressed in megawatt. The equation then takes on the form:

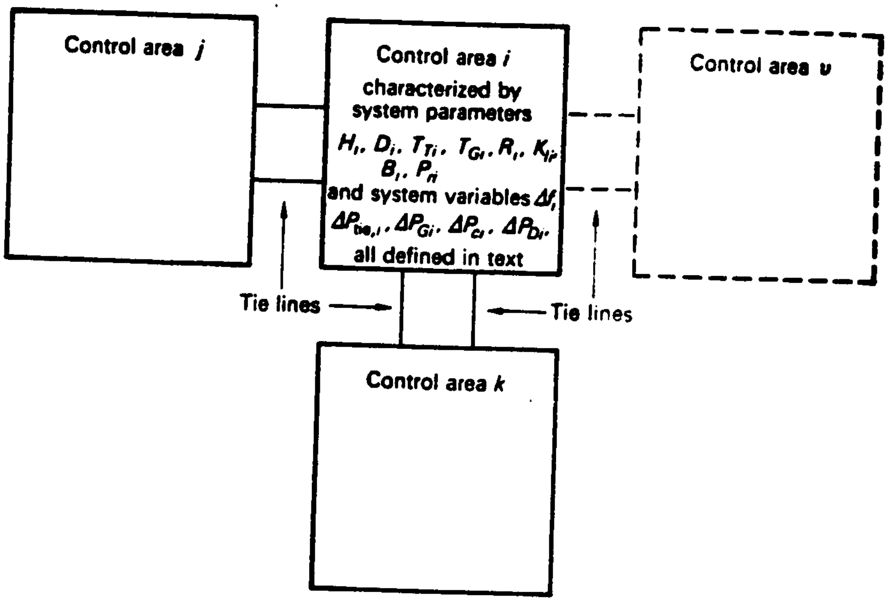

Figure 4.1. Interconnected control areas.

$$\Delta P_{G_i} - \Delta P_{D_i} = (2H_i/f^*) \frac{d}{dt} (\Delta f_i) + D_i \, \Delta f_i + \Delta P_{tie,i} \qquad (4\text{-}2)$$

where the inertia constant H_i is defined as

$$H_i = \frac{W_{kin,i}}{P_{r_i}} \qquad (4\text{-}3)$$

The differential Eqn. (4-2) is linear with constant coefficient, and by laplace transformation, it takes on the form:

$$[\Delta P_{G_i}(s) - \Delta P_{D_i}(s) - \Delta P_{tie,i}(s)] \frac{K_{p_i}}{1 + sT_{p_i}} = \Delta F_i(s) \qquad (4\text{-}4)$$

where, the following new parameters have been introduced to simplify its notation:

$$T_{p_i} = \frac{2H_i}{f^* D_i} \quad \text{(Sec.)} \qquad (4\text{-}5)$$

$$K_{pi} = \frac{1}{D_i} \text{ (Hz/pu MV)} \qquad (4\text{-}6)$$

The area transfer function will be of the form

$$G_{pi}(s) = \frac{K_{pi}}{1 + sT_{pi}} \qquad (4\text{-}7)$$

4.4 INCREMENTAL TIE-LINE POWER $\Delta P_{tie,i}$

The total real power exported from area i, $P_{tie,i}$, equals the sum of all out flowing line powers, $P_{tie,i\nu}$, in the lines connecting area i, with the neighboring areas i.e.

$$P_{tie,i} = \sum_{\nu} P_{tie,i\nu} \tag{4-8}$$

If the line losses are neglected, the individual line powers can be written in the form

$$P_{tie,i\nu} = \frac{|V_i|\ |V_\nu|}{X_{i\nu}\ P_{ri}} \sin\ (\delta_i - \delta_\nu)$$

$$= P_{tie,max\ i\nu}\ \text{Sin}\ (\delta_i - \delta_\nu) \tag{4-9}$$

where $V_i = |V_i|\ e^{j\ \delta_i}$

$$V_\nu = |V_\nu| e^{j\ \delta_\nu}$$

are terminal bus voltages of the line, and $X_{i\nu}$ its reactances. The maximum value $P_{tie,\ max\ i\nu}$ represents the maximum real power that can be transmitted via tie-lines.

If the phase angles deviate from their nominal values δ_i^* and δ_ν^* by an amount $\Delta\delta_i$ & $\Delta\delta_\nu$ respectively, we obtain

$$\Delta P_{tie,i\nu} = \frac{\partial P_{tie,i}}{\partial(\delta_i - \delta_\nu)} (\Delta\delta_i - \Delta\delta_\nu) \tag{4-10}$$

Thus $$\Delta P_{tie,i\nu} = \frac{|V_i| \ |V_\nu|}{X_i \ \ P_{ri}} \text{Cos}(\delta_i^* - \delta_\nu^*)(\Delta\delta_i - \Delta\delta_\nu) \tag{4-11}$$

Since the phase angles are related to the area frequency change by:

$$\Delta\delta_i = 2\pi \int \Delta f_i \, dt \tag{4-12}$$

By combining Eqns. (3-11) & (3-12), we obtain

$$\Delta P_{tie,i\nu} = T_{i\nu} \left(\int \Delta f_i \, dt - \int \Delta f_\nu \, dt\right) \tag{4-13}$$

where $$T_{i\nu} = 2\pi \frac{|V_i| \ |V_\nu|}{X_{i\nu} \ P_{ri}} \text{Cos } (\delta_i^* - \delta_\nu^*) \tag{4-14}$$

is the synchronizing coefficient, or the electrical stiffness of the tie-line.

By Laplace transforming Eqn. (4-13), we obtain

$$\Delta P_{tie,i\nu} (s) = \frac{T_{i\nu}}{s} (\Delta F_i(s) - \Delta F_\nu(s)) \tag{4-15}$$

The total increment in exported power for area i is finally obtained from Eqn. (4-8).

$$\Delta P_{tie,i}(s) = \frac{1}{s} \sum_{\nu} T^{*}_{i\nu}[\Delta F_i(s) - \Delta F_{\nu}(s)] \tag{4-16}$$

4.5 INCREMENTAL GENERATED POWER ΔP_{Gi}

Under load disturbances (load increases or decreases), the system experience changes in the nominal values of the frequency, voltage and phase angle. To keep this nominal state or some of them (in our case the frequency), the generators increase the generated power to compensate for the increase in demand.

A study of the turbine control [12] reveals that for small signals around the nominal settings the system (that is the generator, turbine and governor system) may be represented by two time constants T_{G_i} & T_{T_i}. T_{G_i} represents the time constant of the governor, and T_{T_i} represents the time lag of the turbine. The generator response is considered to be instanteneous in comparison with the time constants of the turbine and governor. It can be stated mathematically that:

$$\frac{d}{dt} \Delta P_{G_i} = \frac{1}{T_{T_i}} \Delta P_{G_i} + \frac{1}{T_{T_i}} \Delta X_{G_i} \tag{4-17}$$

$$\frac{d}{dt} \Delta X_{G_i} = \frac{1}{T_{G_i}} \Delta X_{G_i} - \frac{1}{T_{G_i} R_i} \Delta F_i + \frac{1}{T_{G_i}} \Delta P_{G_i} \tag{4-18}$$

where ΔP_{G_i} is incremental change in generation in per unit MW, ΔX_{G_i} is incremental change in the governor valve position in per unit MW, R_i is the self-regulation of the governor in Hz/pu MW, and ΔP_{C_i} is the incremental change in the speed change position in p.u. MW.

Taking the laplace transformation of Eqns. (4-17) & (4-18) one can obtain

$$\Delta P_{G_i}(s) = \frac{1}{1 + sT_{T_i}} \Delta X_{E_i}(s) \tag{4-19}$$

$$\Delta X_{G_i}(s) = \frac{1}{1 + sT_{G_i}} \left(\Delta P_{C_i}(s) - \frac{1}{R_i} \Delta F_i(s)\right) \tag{4-20}$$

4.6 OVERALL SINGLE-AREA SYSTEM MODEL

Upon combining Eqns. (4-17), (4-16) and (4-20), one obtains the overall single-area for small perturbation. The model is shown in Fig. (4-2). This type of model will be used in the overall analysis of L.F.C.

4.7 BLOCK DIAGRAM OF A TWO-AREA SYSTEM

By combining two single-area model that we have developed already, we obtain a two-area system. A block diagram of two-area

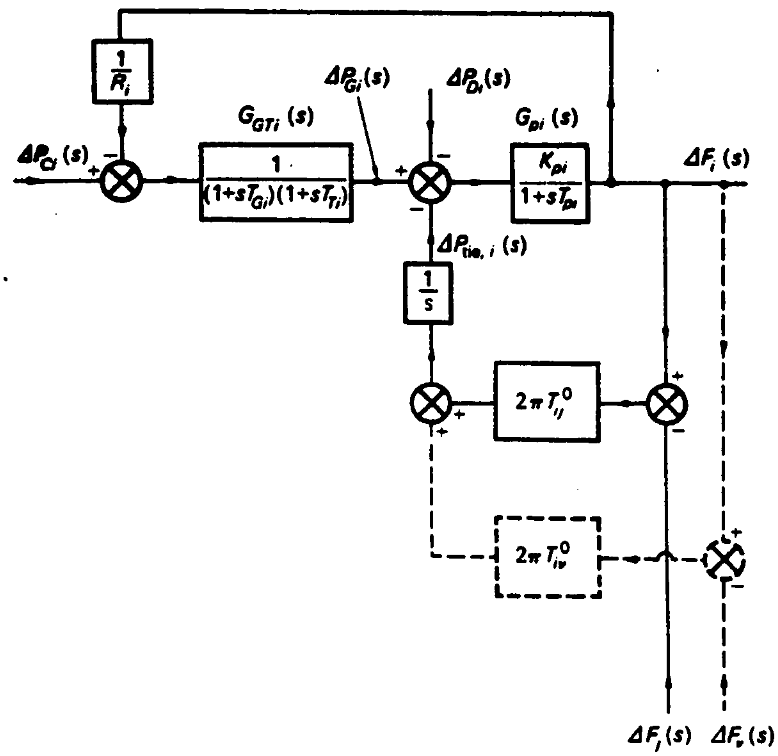

Figure 4.2. Complete block-diagram representation of control area i.

system is shown in Fig. (4-3).

Before proceeding further, let us explain the presence of the block containing the transfer a_{12}. This transfer parameter is equal to the following expression

$$a_{12} = -\frac{P_{r_1}}{P_{r_2}} \tag{4-21}$$

i.e., the negative ratio between rated megawatts of area 1 and 2 respectively. It is necessary to include it in the block diagram because the term $\Delta P_{tie,1}$ in Eqn. (4-21) represents the tie-line power change out from area 1 expressed in per unit of area, rating P_{r_1}.

4.8 STATE SPACE REPRESENTATION

4.8.1 State space variable

Let us first give a brief introduction to state space representation. Any linear system can be represented mathematically by

$$\dot{x} = Ax + Bu + \Gamma p \tag{4-22}$$

where x, is the state vector. These state variables are the minimum number of variable containing sufficient information about the past history of the system, to allow the calculation of the future state of the system assuming the control input known. The state variables are not purely mathematical representation but have true physical meaning. Some of these states are not obtained directly but various methods are available to estimate these terms.

4.8.2 Representation of a Two Area System

Taking the equation of the power equilibrium, the incremental tie-line flow, the change in generation, and position of the speed governor in area i, which after assembling them we obtain

$$\frac{d}{dt}\Delta F_i = \frac{1}{T_{p_i}}(-\Delta F_i + K_{p_i}\Delta P_{G_i} - K_{p_i}\Delta P_{D_i})$$

$$\frac{d}{dt}\Delta P_{G_i} = -\frac{1}{T_{T_2}}\Delta P_{G_i} + \frac{1}{T_{T_i}}\Delta X_{G_i} \tag{4-23}$$

$$\frac{d}{dt}\Delta X_{G_i} = -\frac{1}{T_{G_i}}\Delta X_{G_i} - \frac{1}{T_{Gi}R_i}\Delta F_i + \frac{1}{T_{G_i}}\Delta P_{C_i}$$

where $$K_{pi} = \frac{1}{D_i} \tag{4-24}$$

and $$T_{\nu i} = \frac{2H_i}{F^* D_i} \tag{4-25}$$

For each area, we have this set of three differential equations which describe the dynamic of the power system for any incremental load change. However if the power system area is coupled to other power systems, one more equation is required which relates the tie-line power to the specific areas:

$$\frac{d}{dt} \Delta P_{tie,i} = \sum_{\nu} T_{i\nu} (\Delta F_i - \Delta F_\nu) \tag{4-26}$$

The four equations which describe the single area of the multi-area can be rewritten in terms of state and control variables. Let us define them in the following way:

$$X_{1i} = \Delta F_i$$

$$X_{2i} = \Delta X_{Gi}$$

$$X_{3i} = \Delta P_{Gi}$$

$$X_{4i} = \Delta P_{tie,i}$$

$$u_i = \Delta P_{Gi}$$

So far, each area has a set of four state variables and one control input. However in the two-area problem, the tie-line deviation in the 1st area is proportional to the tie-line deviation

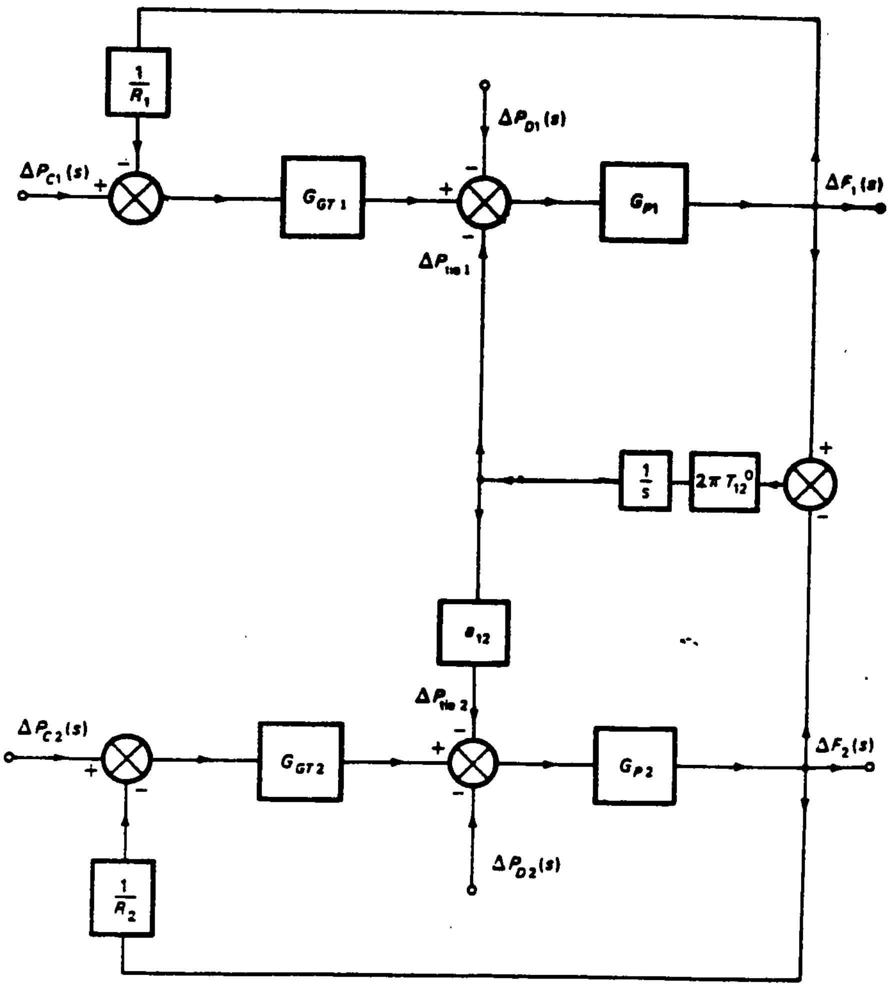

Figure 4.3. Block model of two-area system.

in the second area

$$\Delta P_{tie\ 2} = a_{12}\ \Delta P_{tie\ 1}$$

where $a_{12} = - P_{r_1}/P_{r_2}$

So in this case we need not to define an additional state for the tie-line deviation in area 2. The structure of the two area system is represented in Fig. (4-3).

If more areas are considered it can be calculated in a similar way.

The overall system can be expressed in a more compact way:

$$\dot{x} = Ax + Bu + \Gamma p$$

Where A constitute of the coefficient of all state variable, B consists of the coefficient of all the control inputs and Γ is the coefficient of all disturbance terms.

So A, B & Γ can be easily obtained for any power system using the previous analysis. It can be represented in block form as it is shown in Fig. (4-4).

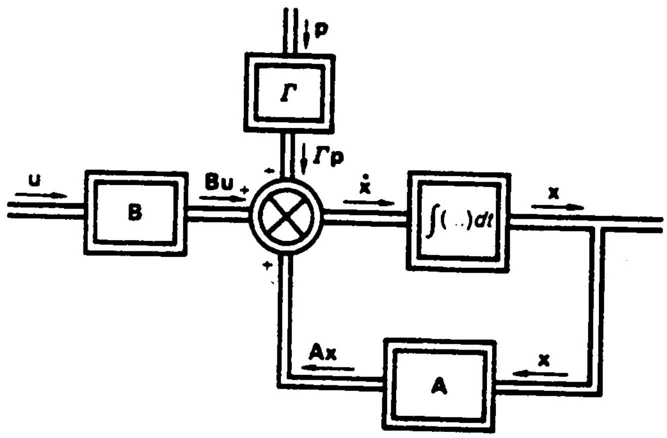

Figure 4.4. Block representation of state model.

The model derived above referred to a two area-system containing only nonreheat turbines. Reheat turbines have more complicated models, and would require additional state variables to describe the system appropriately.

CHAPTER 5

5.1 INTRODUCTION

The method presented in Chapter 3 is applied to a two-area power system to control the deviation of the frequency and tie-line power when the system is subjected to constant disturbances.

The regulator obtained uses only subsystems information to control the deviation of the frequency and tie-line. Each subsystem consists of one area and its external equivalence which is regulated separately of the remaining areas.

The interaction state variables are approximated by a low-order model which is corrected online before to be used for the generation of the control vector. Different crude model matrices are selected and tested on the two-area power system. Near-integrated optimal control was obtained in some cases.

The system was simulated on the digital computer to study its behaviour for different values of S_i, the weighting matrix. The results obtained are compared to the integrated optimal control.

The model of the power system was developed in Chapter 3.

5.2 DYNAMIC SYSTEM IN THE STATE VARIABLE FORM

We define the state and control variables of the single area described in (4-23) as follow:

$$\left.\begin{aligned} x_1 &= \Delta f_1 \\ x_2 &= \Delta X_{E1} \\ x_3 &= \Delta P_{G1} \\ x_4 &= \Delta P_{tie\ 1} \\ u_1 &= \Delta P_{C1} \end{aligned}\right\} \tag{5-1}$$

For each area there is a set of 4 state variables and one control input. However in the two-area problem that we will consider, the tie-line deviation in the first area is proportional to the tie-line deviation in the second, i.e.

$$\Delta P_{tie\ 2} = a_{12}\, \Delta P_{tie\ 1} \tag{5-2}$$

where $a_{12} = -\, P_{r1}/P_{r2}$ (5-3)

is the proportionality constant, P_{r1} and P_{r2} are the MW ratings of areas 1 and 2 respectively.

In this case we need not, define an additional state for the tie-line deviation in area 2.

5.3 MODEL OF TWO-AREA POWER SYSTEM

The two-area power system will be then described by the following states and control variables:

States:

$$\left.\begin{aligned} x_1 &= \Delta F_1 \\ x_2 &= \Delta E_1 \\ x_3 &= \Delta P_{G1} \\ x_4 &= \Delta P_{tie\ 1} \\ x_5 &= \Delta F_2 \\ x_6 &= \Delta X_{E2} \\ x_7 &= \Delta P_{G2} \end{aligned}\right\}$$

Controls:

$$u_1 = \Delta P_{C1}$$

$$u_2 = \Delta P_{C2}$$

Disturbances:

$$P_1 = \Delta P_{D1} \qquad (5\text{-}4)$$

$$P_2 = \Delta P_{D2}$$

Then the model of two-area power system therefore takes the form

$$\dot{x} = Ax + Bu + \Gamma p \qquad (5\text{-}5)$$

where A, B and Γ are given in Table I.

The disturbance matrix Γ has dimension nxp.

To be able to apply the optimal control, the system should be expressed into the form given in Eqn. (3-13) and where all the states and controls have zero steady state values.

Since the disturbance vector is of constant magnitude, then we can define the states in terms of their steady state values, x_{iss}, i.e.

$$x_i^{(1)} = x_i - x_{iss} \tag{5-6}$$

where the states are shifted from their reference positions. The matrices A and B remain unchanged, and the system obtained is of the form

$$\dot{x} = Ax + Bu \tag{5-7}$$

the superscript (1) has been dropped to prevent unnecessary notation confusion.

5.4 SYSTEM SPECIFICATION

Before we define the matrices Q and R, we must define a set of requirements to be satisfied:

TABLE I.

$$
A = \begin{bmatrix}
-1/T_{p1} & 0 & K_{p1}/T_{p1} & -K_{p1}/T_{p1} & 0 & 0 & 0 \\
-1/R_1T_{G1} & -1/T_{G1} & 0 & 0 & 0 & 0 & 0 \\
0 & 1/T_{T1} & -1/T_{T1} & 0 & 0 & 0 & 0 \\
2\pi T^0_{12} & 0 & 0 & 0 & -2\pi T^0_{12} & 0 & 0 \\
0 & 0 & 0 & -a_{12}K_{p2}/T_{p2} & -1/T_{p2} & 0 & K_{p2}/T_{p2} \\
0 & 0 & 0 & 0 & -1/R_2T_{G2} & -1/T_{G2} & 0 \\
0 & 0 & 0 & 0 & 0 & 1/T_{T2} & -1/T_{T2}
\end{bmatrix}
$$

$$
B = \begin{bmatrix}
0 & 1/T_{G1} & 0 & 0 & 0 & 0 & 0 \\
0 & 0 & 0 & 0 & 0 & 1/T_{G2} & 0
\end{bmatrix}^t
$$

$$
\Gamma = \begin{bmatrix}
-K_{p1}/T_{p1} & 0 & 0 & 0 & 0 & 0 & 0 \\
0 & 0 & 0 & 0 & -K_{p2}/T_{p2} & 0 & 0
\end{bmatrix}^t
$$

1) The static frequency deviation following a step-load change must be as minimum as possible.

2) The static tie-line power deviation following a step-load change must be zero.

To define these specifications mathematically requires the introduction of the following terms in the cost function:

$$(\Delta F_1)^2 + (\Delta F_2)^2 + (\Delta P_{tie})^2 \tag{5-8}$$

Defining these variables in terms of their respective states, and putting the product in matrix form $x^t Q x$ specifies Q to be

$$Q = \mathrm{diag}\ (1 \quad 0 \quad 0 \quad 1 \quad 1 \quad 0 \quad 0) \tag{5-9}$$

We penalize for large control effort by adding the term

$$(u_1)^2 + (u_2)^2 \tag{5-10}$$

which requires

$$R = \mathrm{diag}\ (1 \quad 1) \tag{5-11}$$

It is always possible to change the values of the coefficient of the weighting matrices depending on the relative importance of any state. If for example, the variation of the state x_i is to be limited more weight is given to the corresponding entry in the state weighting matrix Q.

5.4 DECOMPOSITION OF THE SYSTEM INTO SUBSYSTEMS

The model of the two-area power system has been already expressed in the form

$$\dot{x} = Ax + Bu \tag{5-12}$$

The system can be split into two subsystems:

The first subsystem comprises the states of Area # 1 and tie-line and control while the second subsystem composes the variables of Area # 2.

The decomposed system will then be described as:

$$x_i = A_i x_i + B_i u_i + C_i Z_i \qquad i = 1,2$$

where

K_{p1}

$$A_1 = \begin{bmatrix} -1/T_{p1} & 0 & K_{p1}/T_{p1} & -K_{p1}/T_{p1} \\ -1/R_1T_{G1} & -1/T_{G1} & 0 & 0 \\ 0 & 1/T_1 & -1/T_1 & 0 \\ 2\pi T_{12} & 0 & 0 & 0 \end{bmatrix}$$

$$B_1 = \begin{bmatrix} 0 \\ 1/T_{G1} \\ 0 \\ 0 \end{bmatrix} \quad , \quad C_1 \begin{bmatrix} 0 \\ 0 \\ 0 \\ -2\pi T_{12} \end{bmatrix}$$

$$A_2 = \begin{bmatrix} -1/T_{p2} & 0 & K_{p2}/T_{p2} \\ -1/R_2T_{G2} & -1/T_{G2} & 0 \\ 0 & 1/T_{T2} & -1/T_{T2} \end{bmatrix}$$

$$B_2 = \begin{bmatrix} 0 \\ 1/T_{G2} \\ 0 \end{bmatrix} \quad , \quad C_2 = \begin{bmatrix} -a_{12}K_{p2}/T_{p2} \\ 0 \\ 0 \end{bmatrix}$$

Using the model following approach, the interaction model for the two subsystems would be

$$A_{z1} = 0.0 \quad \text{and} \quad A_{z2} = -a_{12}\frac{K_{p2}}{T_{p2}} \tag{5-13}$$

In the simulation study presented here, the following typical values were selected:

$$\left.\begin{array}{ll}
T_{p1} = 20 \text{ sec} & T_{p2} = 25 \text{ sec} \\
T_{g1} = 0.08 \text{ sec} & T_{G2} = 0.1 \text{ sec} \\
T_{T1} = 0.03 \text{ sec} & T_{T2} = 0.1 \text{ sec} \\
R_1 = 2.4 \text{Hz/p.u. MW} & R_2 = 3.0 \text{ Hz/p.u. MW} \\
K_{p1} = 120 \text{ Hz/p.u.MW} & K_{p2} = 100 \text{ Hz/p.u. MW} \\
\multicolumn{2}{c}{T_{12} = 0.0866 \text{ p.u. MW}}
\end{array}\right\} \tag{5-14}$$

The weighting matrices S & H are primarily selected equal to the identity matrix.

5.6 SIMULATION AND RESULTS

Using the interaction model suggested by Hassan and Singh [13], the crude model matrices are selected as:

$$A_{z1} = -0.05 \text{ and } A_{z2} = 0.0 \tag{5-15}$$

The Regulator obtained was simulated on the CSMP, with a

1% per unit step load change in area one. The system was badly regulated. The system settles down in more than 10 seconds, which is far from the optimal control, moreover the first overshoot is very high. Thus the model that is chosen is not a good one, since it does not give the desired response. The results are shown in Fig. (5-1).

Analysing the closed loop system, it was found that the modes are:

$-13.3451 + j\ 0.0$	$-13.4022 + j\ 0.0$
$-\ 2.4318 \pm j\ 3.8453$	$-\ 4.5687 + j\ 3.2684$
$-\ 0.6962 + j\ 0.0$	

The modes are spread over a range of -13.345 to -0.4944. Thus we need to choose A_{z1} and A_{z2} within this range, in order to fit the system response.

Changing A_{z1} and A_{z2}, the response obtained was improved and in some cases it was close to the integrated optimal control.

5.7 INVESTIGATION ON THE CRUDE MODEL

It is extremely important to select a better interaction model which fits the system in order to obtain the desired response for the following reasons:

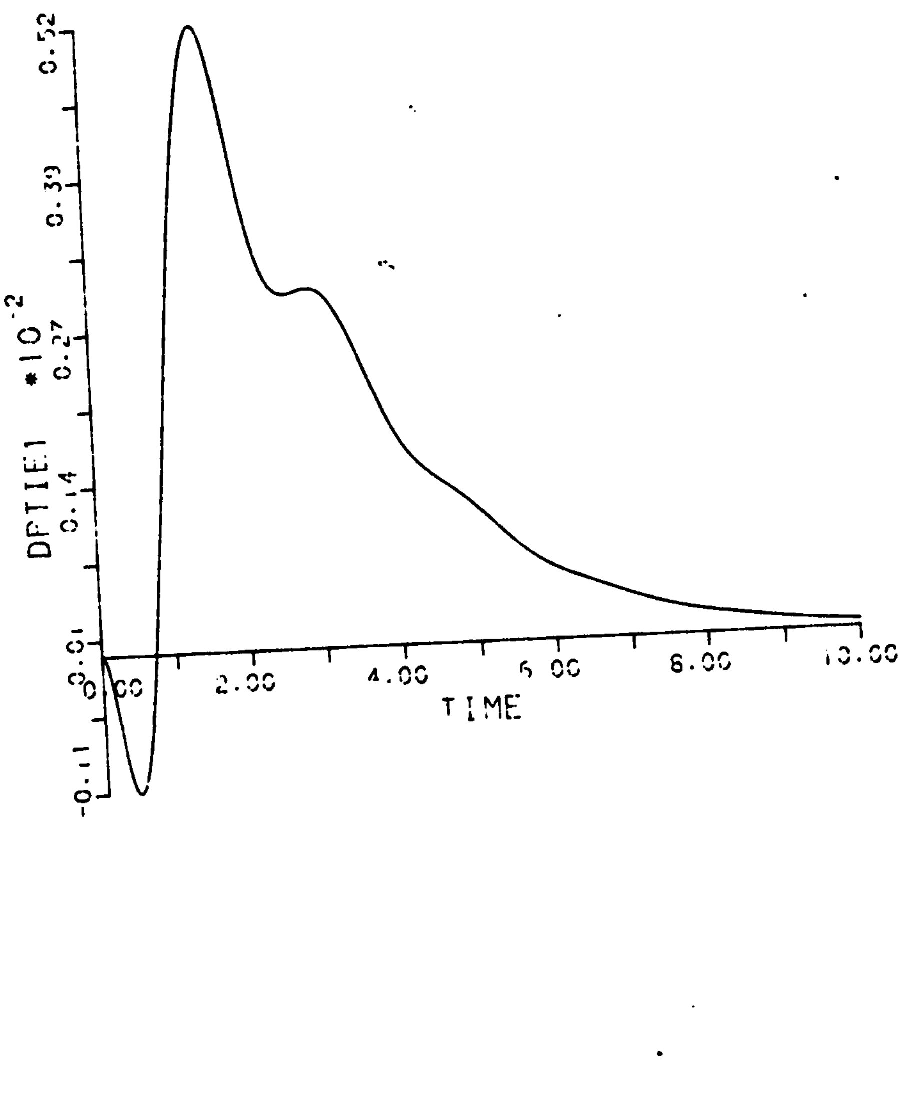

Figure 5-1b. Tie-line deviation in a controlled two-area system following a step load disturbance.

1) The feedback control law is dependent on the crude model.

2) The interaction variables are dependent on the crude model.

The system was simulated for various values of A_{z2} and the results and comments are given below.

The typical values which were tested are:

1) $A_{z1} = A_{z2} = -1.0$ (5-16)

In this case the response was better than the previous one, but still far from the solution. The system has less oscillation, but with large overshoot if compared to the integrated optimal control. The settling time was less than ten seconds which is acceptable. The results are shown in Fig. (5-2).

2) $A_{z1} = A_{z2} = -5.0$. The response was even better. The settling time was very close to the integrated optimal control. The first overshoot had decreased enormously if compared to the previous response. However the system got more secondary oscillations which were quickly damped. The results of the simulation are shown in Fig. (5-3).

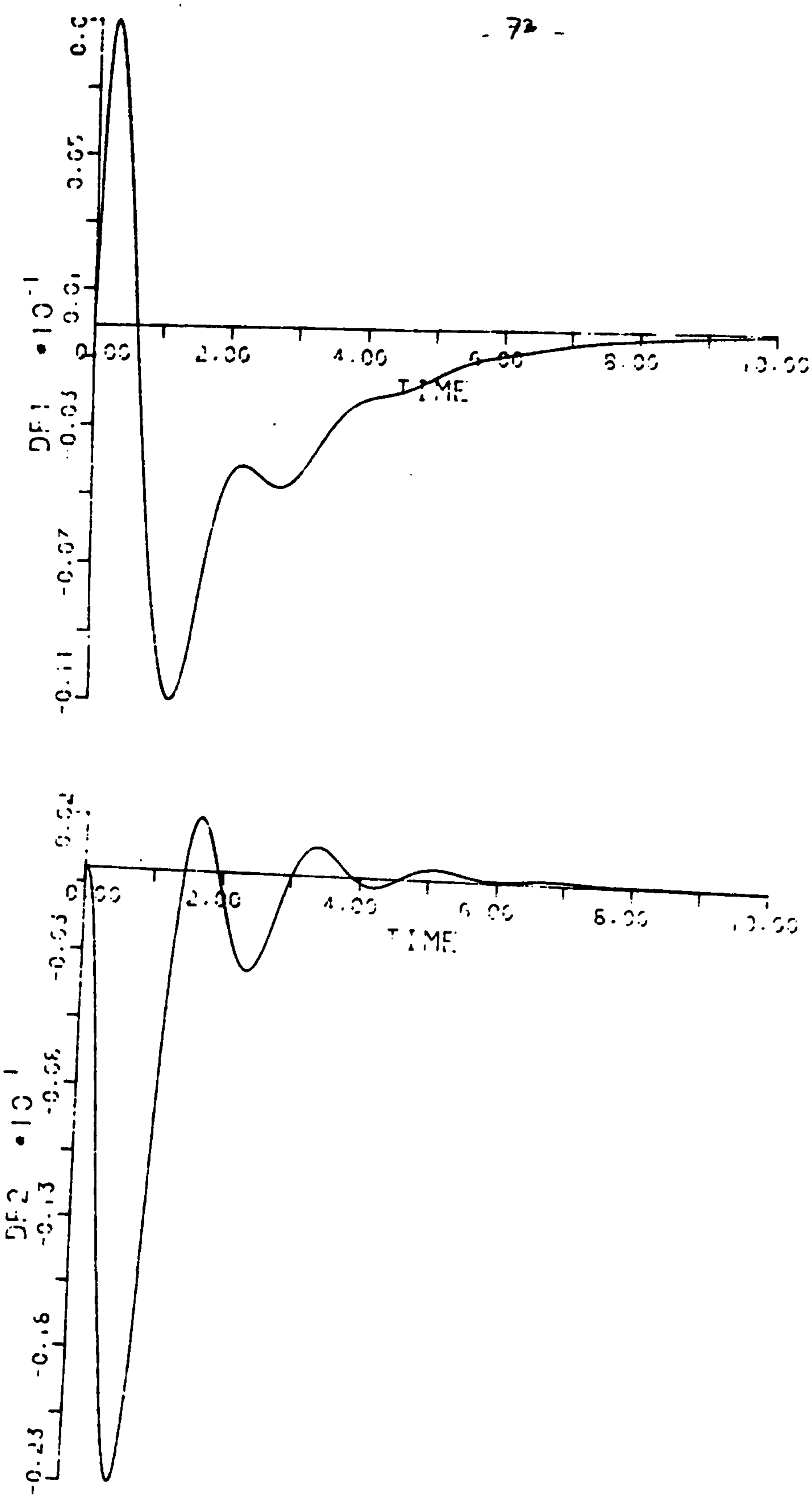

Figure 5-2a. Frequency deviation in a controlled two-area system following a step load.

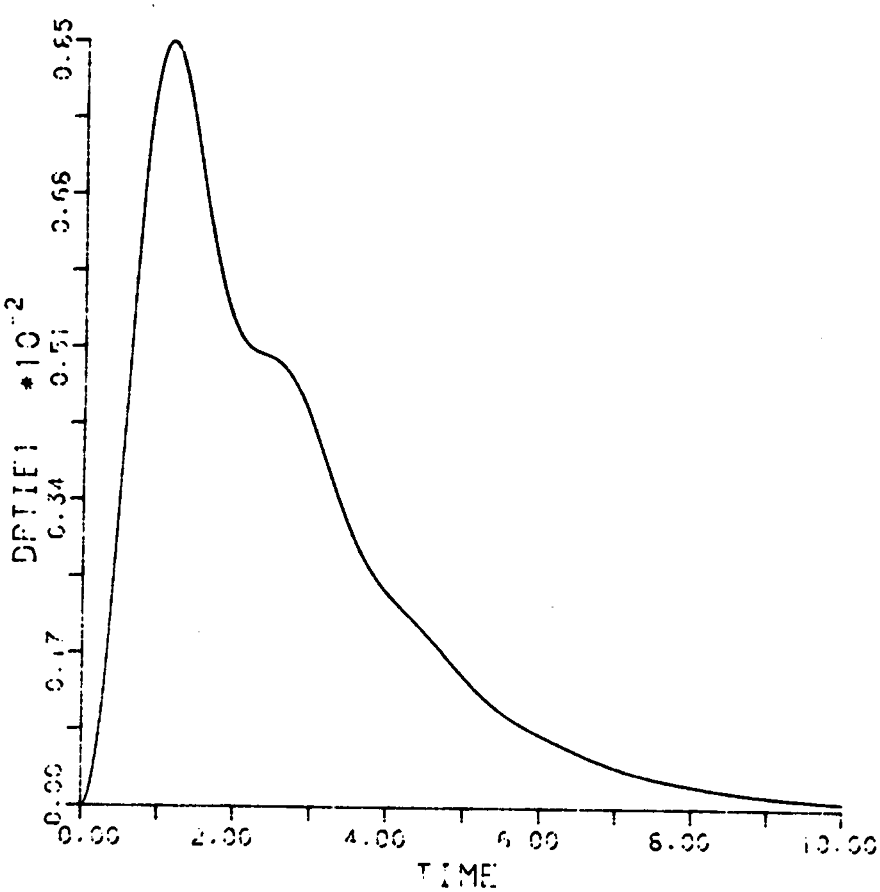

Figure 5-2b. Tie-line power deviation in a controlled two-area system following a step load disturbance.

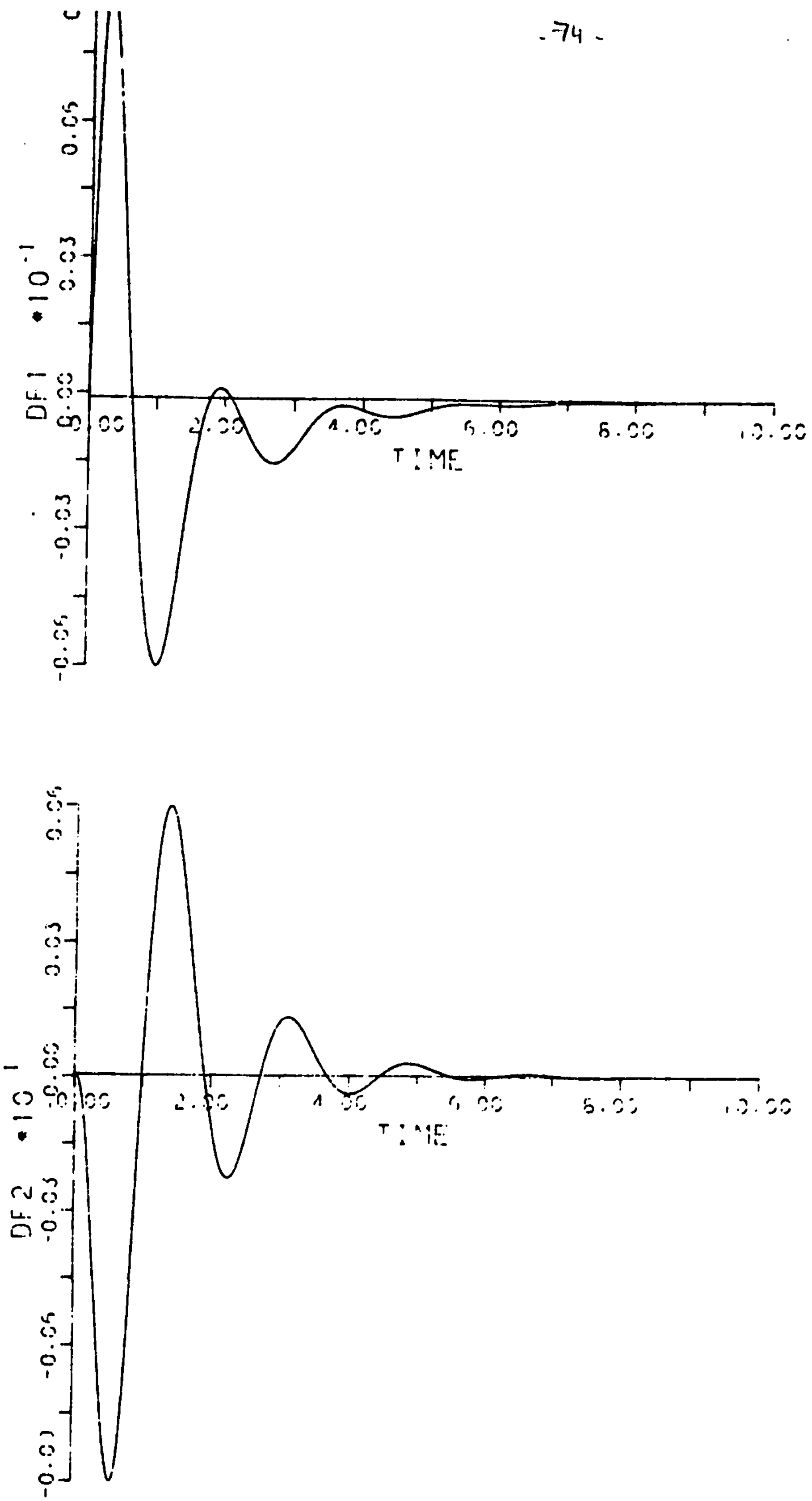

Figure 5-3a. Frequency deviation in a controlled two-area system following a step load disturbance.

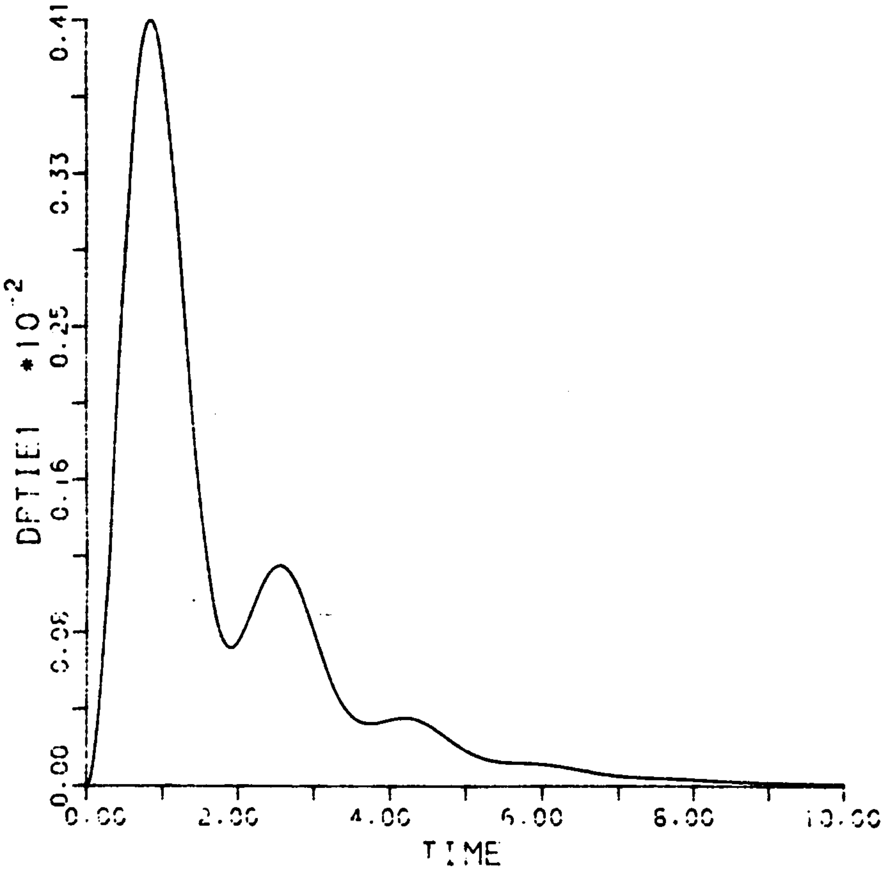

Figure 5-3b. Tie-line power deviation in a controlled two-area system following a step load disturbance.

3) $A_{z1} = A_{z2} = -9$. The response was even better this time. The settling time is nearly identical to the integrated optimal control. Moreover the first overshoot was further improved, and less secondary oscillations were obtained. The simulation results are shown in Fig. (5-4) with the integrated optimal control for comparison.

In all the four cases, the disturbance was taken to be the same i.e. 0.01 per unit.

5.8 COMPARISON AND COMMENTS

In all cases, the controlled system was asymptotically stable. Some of the response was close to the desired response. Table II includes the settling time, first overshoot, secondary overshoot for comparison for all various values of A_{zi}.

We may conclude that the system can always be regulated, even if the crude model is not suitable. The response of the controlled system can be improved by selecting crude model matrices which fits the response of the system.

5.9 INVESTIGATION OF THE WEIGHTING MATRIX S_i

The effect of the weighting matrix S_i is to penalize the error $\hat{z}_i$. The system was implemented for different values of S_i.

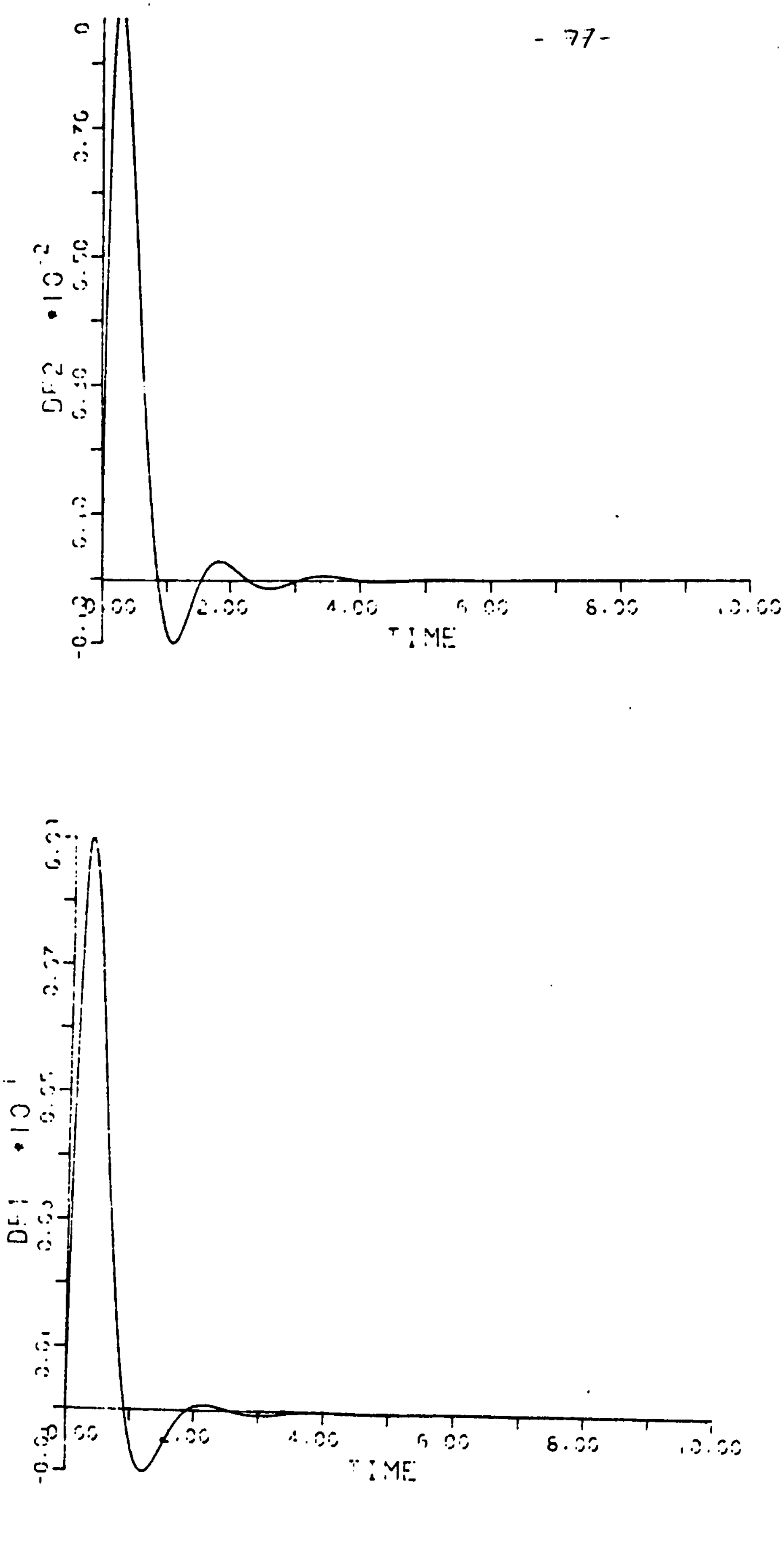

Figure 5-4a. Frequency deviation in a controlled two-area system following a step load disturbance.

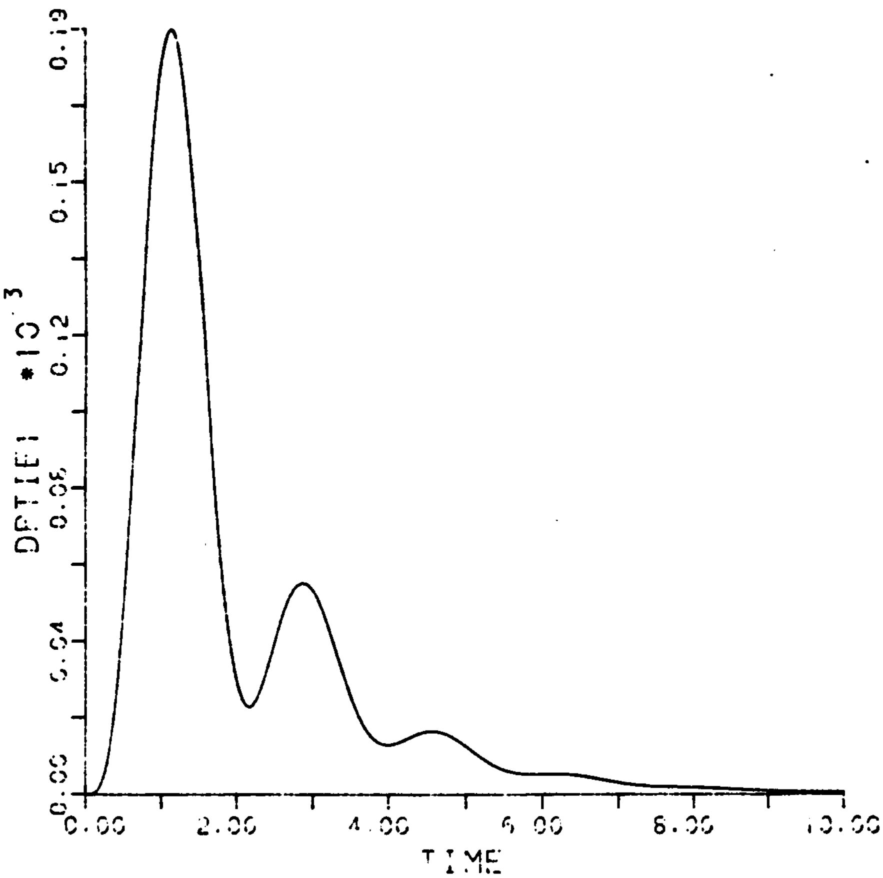

Figure 5-4b. Tie line power deviation of a controlled two area system following a step load disturbance.

TABLE II. Range of Deviation.

$A_{z1} = A_{z2}$	-1.0	-5.0	-9.0	Crude Model suggested by Hassan & Singh
ΔF_1	-0.011 to 0.009	-0.006 to -0.009	-0.001 to 0.009	-0.007 to 0.0014
ΔF_2	-0.023 0.002	-0.009 to 0.006	-0.001 to 0.009	-0.019 to 0.008
ΔP_{tie}	0.0 to 0.0085	0.0 to 0.0041	0.0 to 0.00019	-0.0011 to 0.0052

The system was simulated for $A_{z1} = A_{z2} = -9.0$ for different values of S_i

$$
\left.\begin{array}{lll}
1) & \text{Case} & S_1 = S_2 = 1.0 \\
2) & \text{Case} & S_1 = S_2 = 100.0 \\
3) & \text{Case} & S_1 = S_2 = 1000.0
\end{array}\right\} \qquad (4\text{-}17)
$$

The system is likely to be independent of the weighting matrix S_i, except in those cases where the error is very large, which occurs for bad choice of the crude model.

5.10 INVESTIGATION ON THE INITIAL VALUE OF THE INTERACTION VARIABLE

The system was tested for different initial values of the approximated interaction variables. The system was simulated for the case where

$$A_{z1} = A_{z2} = -9.0 \quad ; \qquad (5\text{-}18)$$

and $S_1 = S_2 = 1000\ I$

and for the following initial values:

$$\left.\begin{array}{ll} \text{Case (1).} & Z_1(0.0) = 0.0,\ Z_2 = 0.01 \\ \text{Case (2).} & Z_1(0.0) = 0.01,\ Z_2 = 0.0 \\ \text{Case (3)} & Z_1(0.0) = Z_2(0.0) = 0.01 \end{array}\right\} \quad (5\text{-}19)$$

In all the cases, the system was regulated, and the response i.e. settling time, overshoot are nearly identical. Thus the decentralized controller response is independent of the initial values of the interaction, this saves the requirement to reset the values of interaction every time.

5.11 INVESTIGATION OF THE COUPLING COEFFICIENT

In our case the coupling coefficient is the synchronizing coefficient T^o_{12} . The system was tested for different values of the coupling coefficient to study the effectiveness of the controller. The following values of the synchronizing coefficient were selected.

$$\left.\begin{array}{ll} \text{Case (1)} & T^o_{12} = 0.17 \text{ p.u. MW} \\ \text{Case (2)} & T^o_{12} = 0.0866 \text{ p.u. MW} \\ \text{Case (3)} & T^o_{12} = 0.4 \text{ p.u. MW} \end{array}\right\} \quad (5\text{-}20)$$

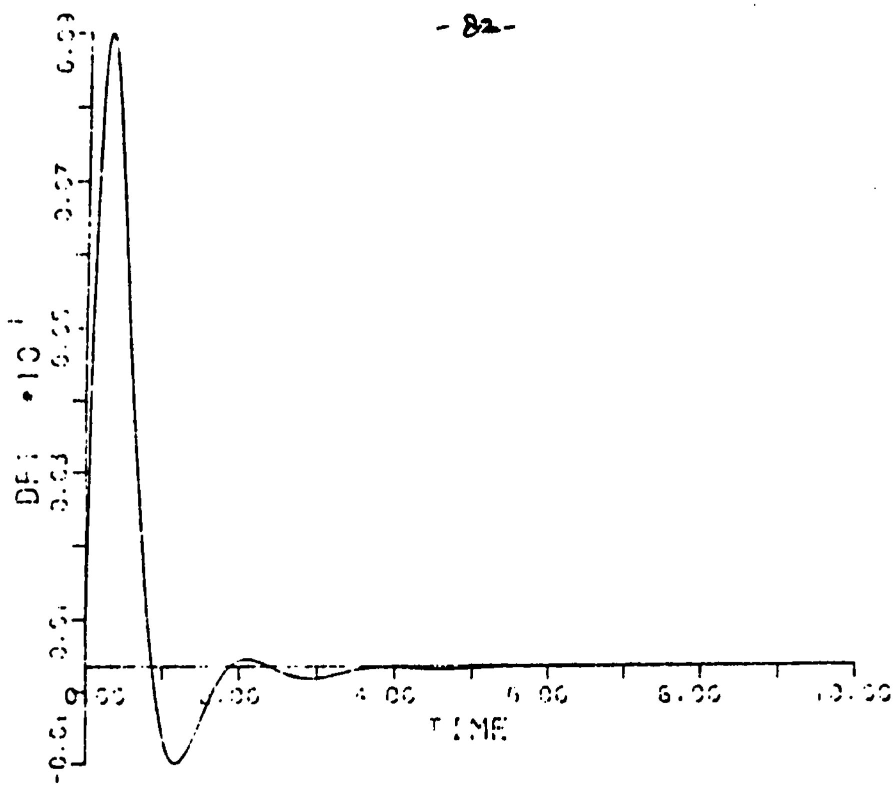

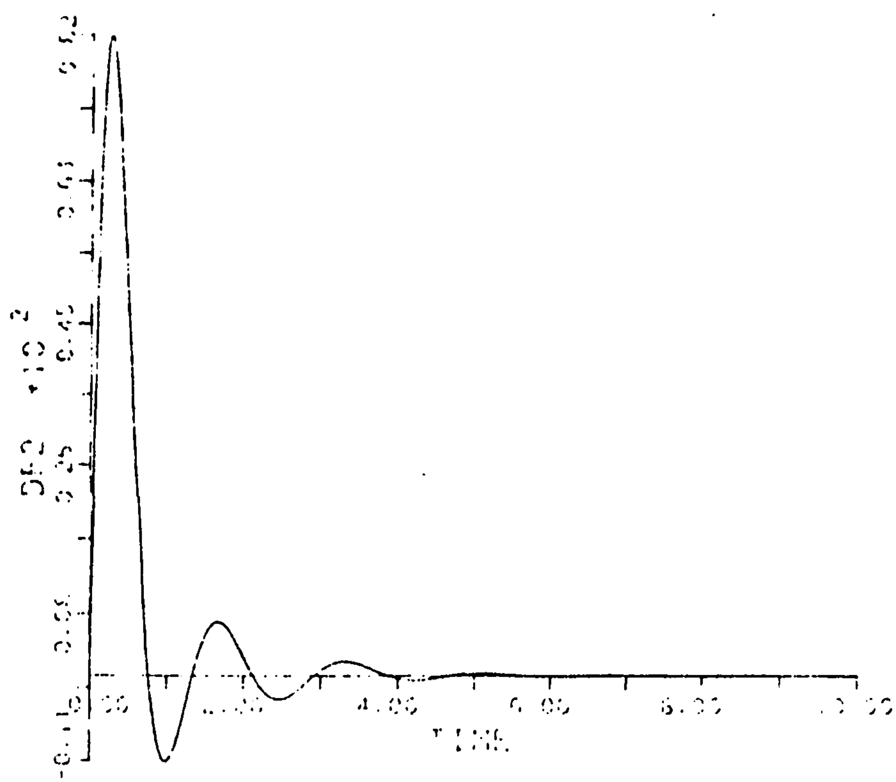

Figure 5.5a. Frequency deviation of a controlled two-area system following a step load disturbance.

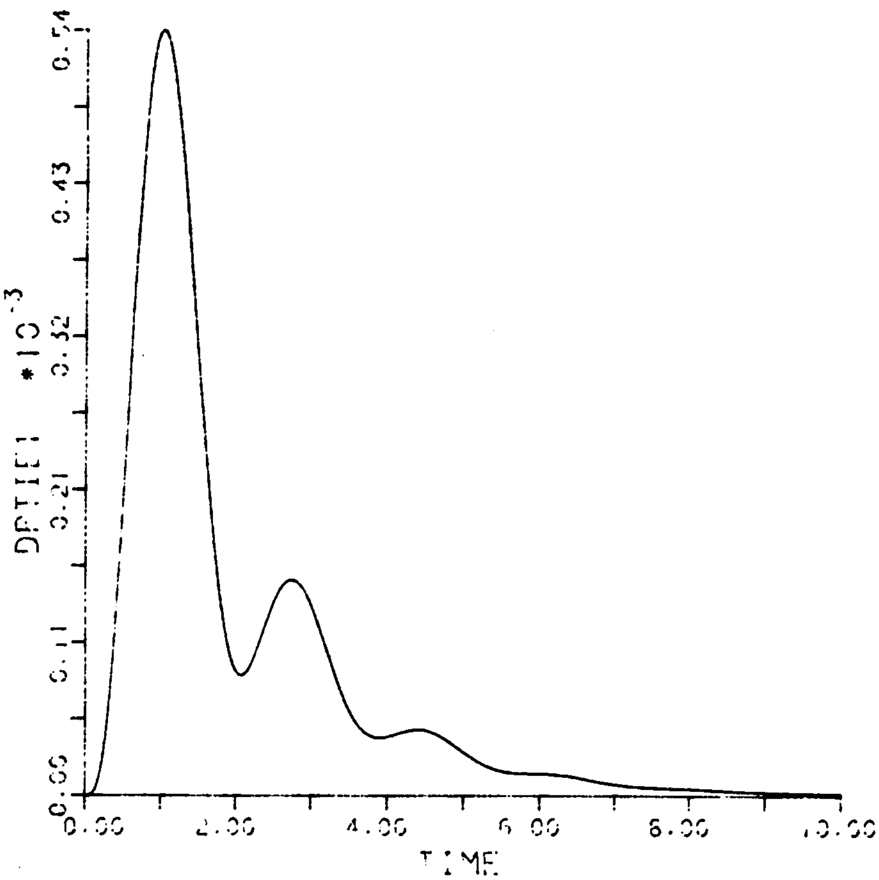

Figure 5-5b. Tie-line deviation of a controlled two-area system following a step load disturbance.

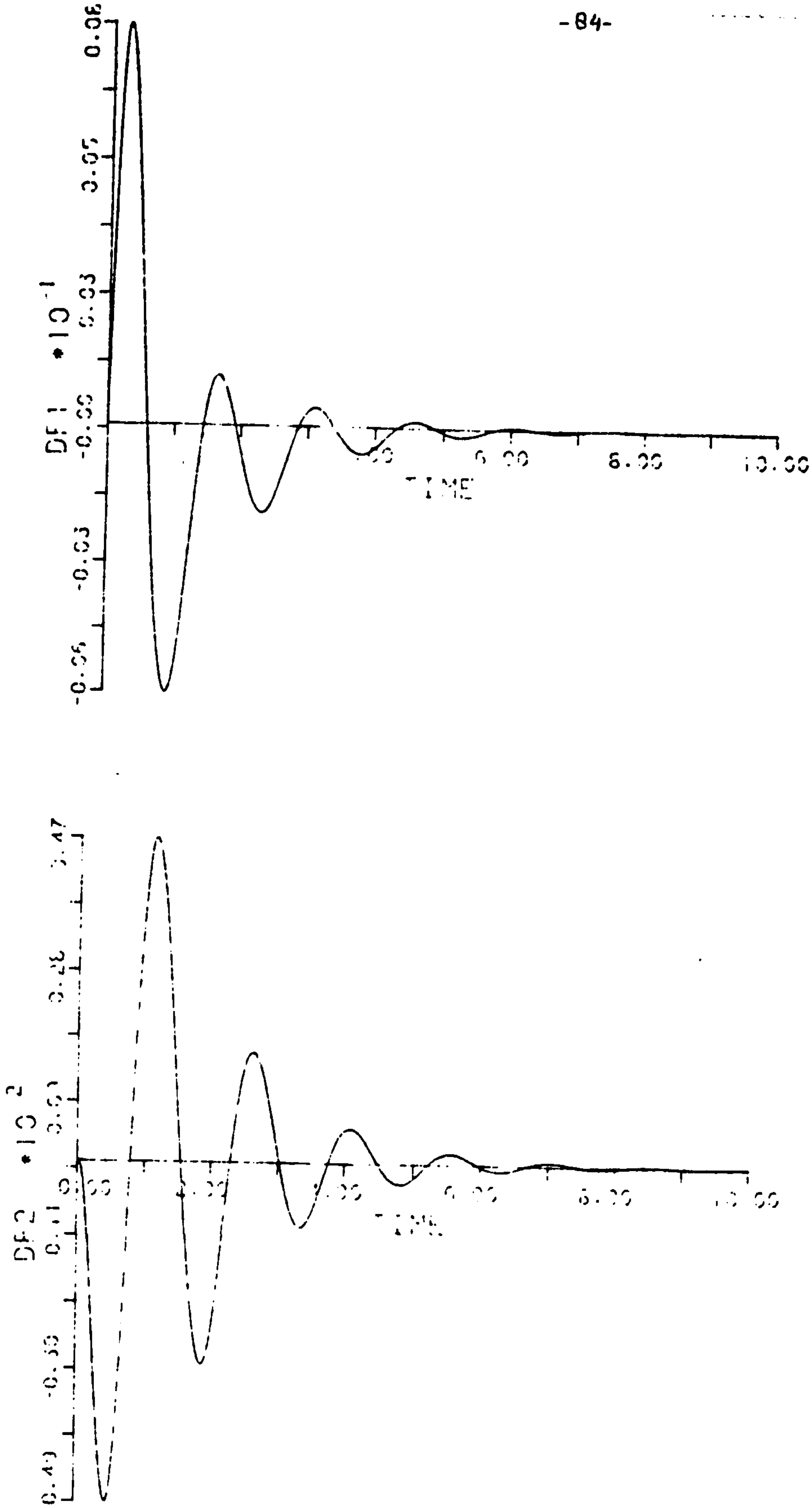

Figure 5-6a. Frequency deviation of a controlled two-area system following a step load change.

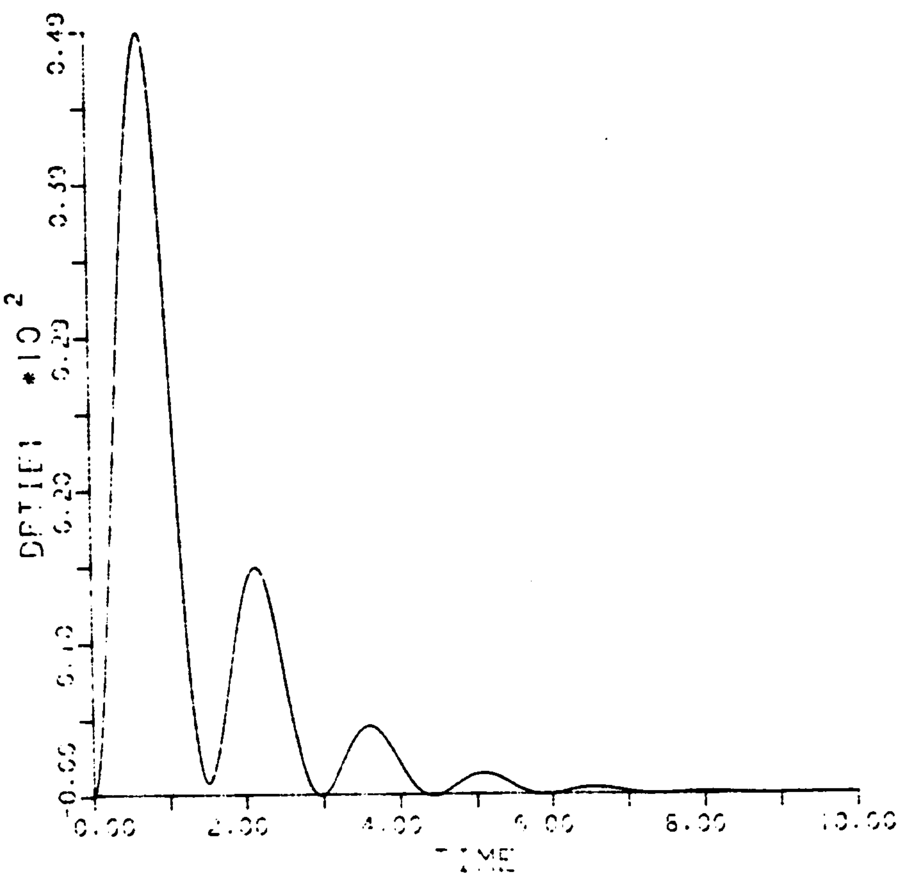

Figure 5-6b. Tie-line power deviation of a controlled two-area system following a step-load disturbance.

5.12 CONTROL CRITERION

The error criterion or so-called integral of the squared errors (ISE) criterion defined mathematically by:

$$ISE = \int_0^\infty [(\Delta F_1)^2 + (\Delta F_2)^2 + (\Delta P_{tie})^2]\, dt \tag{5-21}$$

was computed for different values of the crude models A_{zi}. The values are shown in Table III including the integrated one for comparison.

From the result obtained one concludes that the minimum values of ISE were obtained for the best response which is $A_{z1} = A_{z2} = -9.0$, which was the closest to the integrated.

The performance index was calculated for different values of the crude model matrix. The minimum value of the performance index occurred for the choice of $A_{z1} = A_{z2} = -9.0$.

TABLE III.

A_z	-1.0	-5.0	-9
J	$9.17770*10^{-4}$	$7.2366*10^{-4}$	$1.3666*10^{-4}$

J = performance index = $\frac{1}{2}\int_0^\infty (\Delta F_1^2 + \Delta F_2^2 + \Delta P_{tie}^2)\, dt$

6.0 SIMULATION OF FOUR INTERCONNECTED POWER SYSTEMS

6.1 INTRODUCTION

The decentralized controller was applied successfully to the two-area power system, and promising results were obtained. Next, using the results already obtained, the decentralized approach will be applied to systems consisting of N-area power system instead of only two-area, and of different configuration to confirm the effectiveness of the method. Three different configurations which may occur in power system are considered in this study.

- cascaded area system
- area system containing loops
- radial area system

The model described in Chapter 4 is extended for multi-areas systems. The systems are expressed in the standard form:

$$\underline{\dot{x}} = A\underline{x} + B\underline{u}$$

The simulation results showed, that the system was always regulated when subject to a constant disturbance.

6.2 SIMULATION OF A 4 CASCADED AREA

6.2.1 Model of 4 Cascaded Area

Let us consider 4 cascaded areas, represented as follows:

The equations describing the system are as follow:

$$\frac{d}{dt} \Delta F_1 = \frac{1}{T_{P1}} (-\Delta F_1 + K_P P_{G1} - K_{P1} \Delta P_{tie\ 1} - K_{P1} \Delta P_{D1})$$

$$\frac{d}{dt} \Delta X_{E1} = \frac{1}{T_{G1}} (- \frac{1}{R_1} \Delta F_1 - \Delta X_{E1} + \Delta P_{C1})$$

$$\frac{d}{dt} \Delta P_{G1} = \frac{1}{T_{T1}} (\Delta X_{E1} - \Delta P_{G1})$$

$$\frac{d}{dt} \Delta P_{tie\ 12} = 2\pi\ T_{12}\ (\Delta F_1 - \Delta F_2)$$

$$\frac{d}{dt} \Delta F_2 = \frac{1}{T_{P2}}(-a_{12} K_{P2} \Delta P_{tie\ 12} - \Delta F_2 + K_{P2} \Delta P_{G2} - K_{P2} \Delta P_{D2} - K_{P2} \Delta P_{tie\ 23})$$

$$\frac{d}{dt} \Delta X_{E2} = \frac{1}{T_{G2}} (- \frac{1}{R_2} \Delta F_2 - \Delta X_{E2} + \Delta P_{C2})$$

$$\frac{d}{dt} \Delta P_{G2} = \frac{1}{T_{T2}} (\Delta X_{E2} - \Delta P_{G2})$$

$$\frac{d}{dt}\,\Delta P_{tie\ 23} = 2\pi\ T_{23}\ (\Delta F_2 - \Delta F_3)$$

$$\frac{d}{dt}\,\Delta F_3 = \frac{1}{T_{P3}}(-a_{23}K_{P3}\Delta P_{tie\ 23} - \Delta F_3 + K_{P3}\Delta P_{G3} - K_{P3}\Delta P_{D3} - K_{P3}\Delta P_{tie\ 34})$$

$$\frac{d}{dt}\,\Delta X_{E3} = \frac{1}{T_{G3}}\left(-\frac{1}{R_3}\Delta F_3 - \Delta X_{E3} + \Delta P_{C3}\right)$$

$$\frac{d}{dt}\,\Delta P_{G3} = \frac{1}{T_{T3}}(\Delta X_{E3} - \Delta P_{G3})$$

$$(6\text{-}1)$$

$$\frac{d}{dt}\,\Delta P_{tie\ 34} = 2\pi\ T_{34}\ (\Delta F_3 - \Delta F_4)$$

$$\frac{d}{dt}\,\Delta F_4 = \frac{1}{T_{P4}}(-a_{34}K_{P4}\Delta P_{tie\ 34} - \Delta F_4 + K_{P4}P_{G4} - K_{P4}\ \Delta P\quad)$$

$$\frac{d}{dt}\,\Delta X_{E4} = \frac{1}{T_{G4}}\left(-\frac{1}{R_4}\Delta F_4 - \Delta X_{E4} + \Delta P_{C4}\right)$$

$$\frac{d}{dt}\,\Delta P_{G4} = \frac{1}{T_{T4}}(\Delta X_{E4} - \Delta P_{G4})$$

let us choose the state vector as

$$\underline{x} = [\Delta F_1\ \Delta X_{E1}\ \Delta P_{G1}\ \Delta P_{tie\ 12}\ \Delta F_2\ \Delta X_{E2}\ \Delta P_{G2}\ \Delta P_{tie\ 23}\ \Delta F_3\ \Delta X_{E3}$$
$$\Delta P_{G3}\ \Delta P_{tie\ 34}\ \Delta F_4\ \Delta X_{E4}\ \Delta P_{G4}]^t \qquad (6\text{-}2)$$

the control input vector

$$\underline{u} = [\Delta P_{C1}\quad \Delta P_{G2}\quad \Delta P_{C3}\quad \Delta P_{C4}]^t \qquad (6\text{-}3)$$

and the disturbance vector

$$\underline{P} = [\Delta P_{D1} \ \Delta P_{D2} \ \Delta P_{D3} \ \Delta P_{D4}]^t \tag{6-4}$$

Then, Eqns. (6-1) to (6-4) can be expressed as:

$$\dot{\underline{x}} = A\underline{x} + Bu + \Gamma p \tag{6-5}$$

where A, B and Γ are defined as follows:

$$A = \begin{bmatrix}
-1/T_{P1} & 0 & K_{P1}/T_{P1} & -K_{P1}/T_{P1} & 0 & 0 & 0 & 0 & 0 & 0 & 0 & 0 & 0 & 0 & 0 \\
-1/R_1T_{G1} & -1/T_{G1} & 0 & 0 & 0 & 0 & 0 & 0 & 0 & 0 & 0 & 0 & 0 & 0 & 0 \\
0 & 1/T_{T1} & -1/T_{T1} & 0 & 0 & 0 & 0 & 0 & 0 & 0 & 0 & 0 & 0 & 0 & 0 \\
2\pi T_{12} & 0 & 0 & 0 & -2\pi T_{12} & 0 & 0 & 0 & 0 & 0 & 0 & 0 & 0 & 0 & 0 \\
0 & 0 & 0 & -a_{12}K_{P2}/T_{P2} & -1/T_{P2} & 0 & K_{P2}/T_{P2} & -K_{P2}/T_{P2} & 0 & 0 & 0 & 0 & 0 & 0 & 0 \\
0 & 0 & 0 & 0 & -1/R_2T_{G2} & -1/T_{G2} & 0 & 0 & 0 & 0 & 0 & 0 & 0 & 0 & 0 \\
0 & 0 & 0 & 0 & 0 & 1/T_{T2} & -1/T_{T2} & 0 & 0 & 0 & 0 & 0 & 0 & 0 & 0 \\
0 & 0 & 0 & 0 & 2\pi T_{23} & 0 & 0 & 0 & -2\pi T_{23} & 0 & 0 & 0 & 0 & 0 & 0 \\
0 & 0 & 0 & 0 & 0 & 0 & 0 & -a_{23}K_{P3}/T_{P3} & -1/T_{P3} & 0 & K_{P3}/T_{P3} & -K_{P3}/T_{P3} & 0 & 0 & 0 \\
0 & 0 & 0 & 0 & 0 & 0 & 0 & 0 & -1/R_3T_{G3} & -1/T_{G3} & 0 & 0 & 0 & 0 & 0 \\
0 & 0 & 0 & 0 & 0 & 0 & 0 & 0 & 0 & 1/T_{T3} & -1/T_{T3} & 0 & 0 & 0 & 0 \\
0 & 0 & 0 & 0 & 0 & 0 & 0 & 0 & 2\pi T_{34} & 0 & 0 & 0 & -2\pi T_{34} & 0 & 0 \\
0 & 0 & 0 & 0 & 0 & 0 & 0 & 0 & 0 & 0 & 0 & -a_{34}K_{P4}/T_{P4} & -1/T_{P4} & 0 & K_{P4}/T_{P4} \\
0 & 0 & 0 & 0 & 0 & 0 & 0 & 0 & 0 & 0 & 0 & 0 & -1/R_4T_{G4} & -1/T_{G4} & 0 \\
0 & 0 & 0 & 0 & 0 & 0 & 0 & 0 & 0 & 0 & 0 & 0 & 0 & 1/T_{T4} & -1/T_{T4}
\end{bmatrix}$$

$$B^t = \begin{bmatrix} 0 & \frac{1}{T_{G2}} & 0 & 0 & 0 & 0 & 0 & 0 & 0 & 0 & 0 & 0 & 0 & 0 & 0 \\ 0 & 0 & 0 & 0 & 0 & \frac{1}{T_{G2}} & 0 & 0 & 0 & 0 & 0 & 0 & 0 & 0 & 0 \\ 0 & 0 & 0 & 0 & 0 & 0 & 0 & 0 & 0 & \frac{1}{T_{G3}} & 0 & 0 & 0 & 0 & 0 \\ 0 & 0 & 0 & 0 & 0 & 0 & 0 & 0 & 0 & 0 & 0 & 0 & 0 & \frac{1}{T_{G4}} & 0 \end{bmatrix}$$

$$\Gamma^t = \begin{bmatrix} -K_{P1}/T_{P1} & 0 & 0 & 0 & 0 & 0 & 0 & 0 & 0 & 0 & 0 & 0 & 0 & 0 & 0 \\ 0 & 0 & 0 & 0 & -K_{P2}/T_{P2} & 0 & 0 & 0 & 0 & 0 & 0 & 0 & 0 & 0 & 0 \\ 0 & 0 & 0 & 0 & 0 & 0 & 0 & 0 & -K_{P3}/T_{P3} & 0 & 0 & 0 & 0 & 0 & 0 \\ 0 & 0 & 0 & 0 & 0 & 0 & 0 & 0 & 0 & 0 & 0 & 0 & -K_{P4}/T_{P4} & 0 & 0 \end{bmatrix}$$

The system was simulated for the following typical values of the parameters:

Area # 1:

T_{P1} = 20 sec, K_{P1} = 120 Hz/p.u. MW, R_1 = 2.4 Hz/p.u. MW,
T_{G1} = 0.08 sec, T_{T1} = 0.3 sec

Area # 2:

T_{P2} = 25 sec, K_{P2} = 100.0 Hz/p.u. MW, R_2 = 3.0 Hz/p.u. MW,
T_{G2} = 0.1 sec, T_{T2} = 0.95 sec.

Area # 3:

T_{P3} = 21 sec, K_{P3} = 115 Hz/p.u. MW, R_3 = 2.2 Hz/p.u. MW,
T_{G3} = 0.08 sec, T_{T3} = 0.3 sec.

Area # 4:

T_{P4} = 22 sec, K_{P4} = 110 Hz/p.u. MW, R_4 = 2.4 Hz/p.u. MW,
T_{G4} = 0.25 sec, T_{T4} = 0.1 sec.

The synchronizing coefficients are:

T_{12} = 0.0866 p.u. MW
T_{23} = 0.1 p.u. MW
T_{34} = 0.1 p.u. MW

6.2.2 Area Decomposition

The system is decomposed into 4 subsystems. Each subsystem consists of one area and its external equivalence. The system can be expressed in the following form:

$$\dot{x}_i = A_i x_i + B_i x_i + C_i z_i \qquad (i=1,2,3,4) \qquad (6\text{-}6)$$

where

$$A_1 = \begin{bmatrix} -1/T_{P1} & 0 & K_{P1}/T_{P1} & -K_{P1}/T_{P1} \\ -1/R_1T_{G1} & -1/T_{G1} & 0 & 0 \\ 0 & 1/T_{T1} & -1/T_{T1} & 0 \\ 2\pi T_{12} & 0 & 0 & 0 \end{bmatrix} ; \; B_1 = \begin{bmatrix} 0 \\ 1/T_{G1} \\ 0 \\ 0 \end{bmatrix}$$

$$A_2 = \begin{bmatrix} -1/T_{P2} & 0 & K_{P2}/T_{P2} & -K_{P2}/T_{P2} \\ -1/R_2T_{G2} & -1/T_{G2} & 0 & 0 \\ 0 & 1/T_{T2} & -1/T_{T2} & 0 \\ 2\pi T_{23} & 0 & 0 & 0 \end{bmatrix} ; \; B_2 = \begin{bmatrix} 0 \\ 1/T_{G2} \\ 0 \\ 0 \end{bmatrix}$$

$$A_3 = \begin{bmatrix} -1/T_{P3} & 0 & K_{P3}/T_{P3} & -K_{P3}/T_{P3} \\ -1/R_3T_{G3} & -1/T_{G3} & 0 & 0 \\ 0 & 1/T_{T3} & -1/T_{T3} & 0 \\ 2\pi T_{34} & 0 & 0 & 0 \end{bmatrix} \; ; \; B_3 = \begin{bmatrix} 0 \\ 1/T_{G3} \\ 0 \\ 0 \end{bmatrix}$$

$$A_4 = \begin{bmatrix} -1/T_{P4} & 0 & K_{P4}/T_{P4} \\ -1/R_4T_{G4} & -1/T_{G4} & 0 \\ 0 & 1/T_{T4} & -1/T_{T4} \end{bmatrix} \; ; \; B_4 = \begin{bmatrix} 0 \\ 1/T_{G4} \\ 0 \end{bmatrix}$$

The off-diagonal matrices are as follow:

$$C_1 = \begin{bmatrix} 0 \\ 0 \\ 0 \\ -2\pi T_{12} \end{bmatrix} \quad ; \quad C_2 = \begin{bmatrix} -a_{12}K_{P2}/T_{P2} & 0 \\ 0 & 0 \\ 0 & 0 \\ 0 & -2\pi T_{23} \end{bmatrix}$$

<u>Subsystem # 1</u>:

$-17.840 + j0.0$

$-2.440 + j2.682$

$-2.440 - j2.682$

$-1.160 + j0.0$

<u>Subsystem # 2</u>:

$-10.075 + j0.0$

$-2.827 + j2.062$

$-2.827 - j2.062$

$-1.411 + j0.0$

<u>Subsystem # 3</u>:

$-11.987 + j0.0$

-2.160 ± 2.935

$-1.03914 + j0.0$

<u>Subsystem # 4</u>:

$-10.722 + j0.0$

$-4.220 \pm j2.569$

Then the modes are spread over the range [-17.840 to -1.03914]. We have selected for simplicity diagonal matrices for the crude models and whose eigenvalues are within the range previously mentioned.

$$A_{z1} = [\ -9\ ] \quad , \qquad A_{z2} = \begin{bmatrix} -9 & 0 \\ 0 & -9 \end{bmatrix}$$

$$A_{z3} = \begin{bmatrix} -9 & 0 \\ 0 & -9 \end{bmatrix} \qquad A_{z4} = [\ -9\ ]$$

We have selected also

$$S_i = 1000\ I \qquad i = 1,2,3,4$$

$$H_i = I \qquad I = \text{Indentity matrix}$$

$$\left.\begin{aligned} Q_1 &= \text{diag}\ (1 \quad 0 \quad 0 \quad 1) \\ Q_2 &= \text{diag}\ (1,\ 0\ 0\ 1) \\ Q_3 &= \text{diag}\ (1 \quad 0 \quad 0 \quad 1) \\ Q_4 &= \text{diag}\ (1 \quad 0 \quad 0) \end{aligned}\right\} \qquad (6\text{-}7)$$

6.2.3 Simulation and Results

The above mentioned regulator was tested on the 4 cascaded area under a step-load change of magnitude 0.01. The frequencies and tie-lines deviation of the multi-area system are shown in Fig. (6-1).

The system was found to be asymptotically stable. The steady state is reached in less than 20 seconds. The range of deviations of the frequencies and tie-lines are given in Table IV.

6.3 SIMULATION OF 4 RADIAL AREA

6.3.1 Model of 4 Radial Areas

Let us now consider 4 radial area, represented as follow:

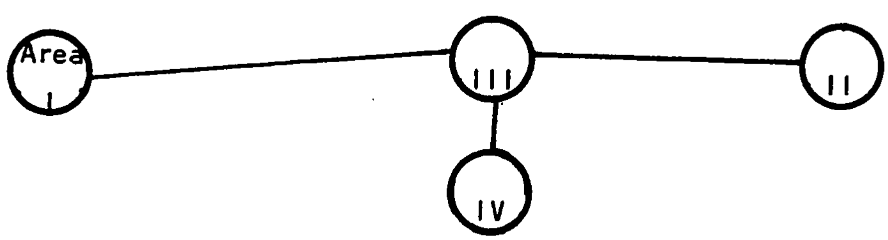

The equations describing the system are:

$$\frac{d}{dt} \Delta F = \frac{1}{T_{P1}} (-\Delta F_1 + K_{P1} \Delta P_{G1} - K_{P1} \Delta P_{tie\ 13} - K_{P1} \Delta P_{D1})$$

$$\frac{d}{dt} \Delta X_{E1} = \frac{1}{T_{G1}} (- \frac{1}{R_1} \Delta F_1 - \Delta X_{E1} + \Delta P_{C1}) \qquad (6\text{-}8)$$

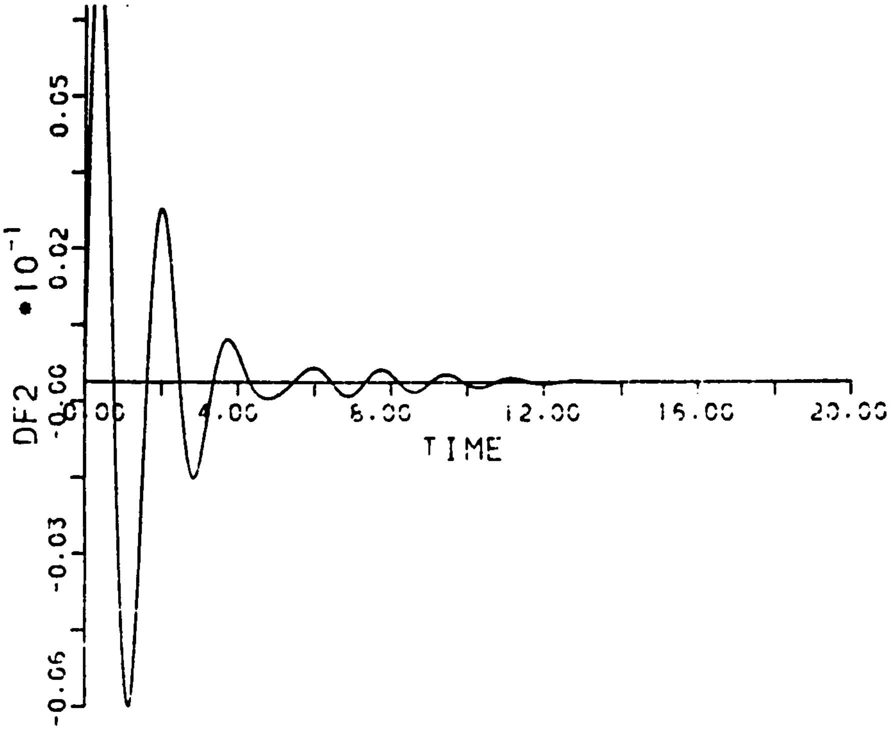

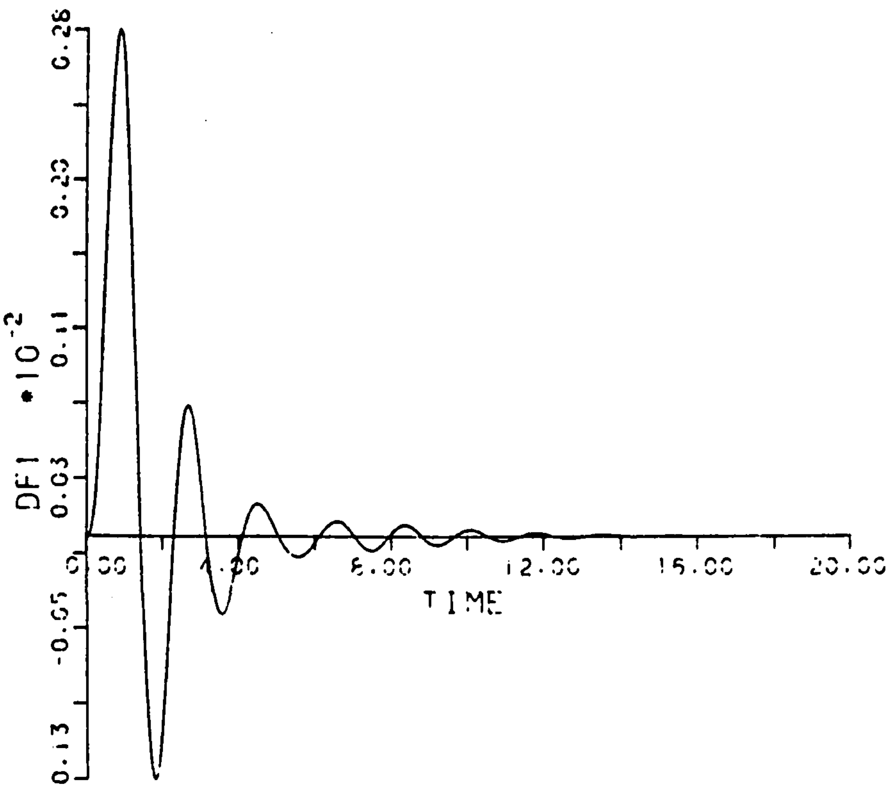

Figure 6-1a. Tie-line deviation in a controlled 4 cascaded area system following a step load disturbance.

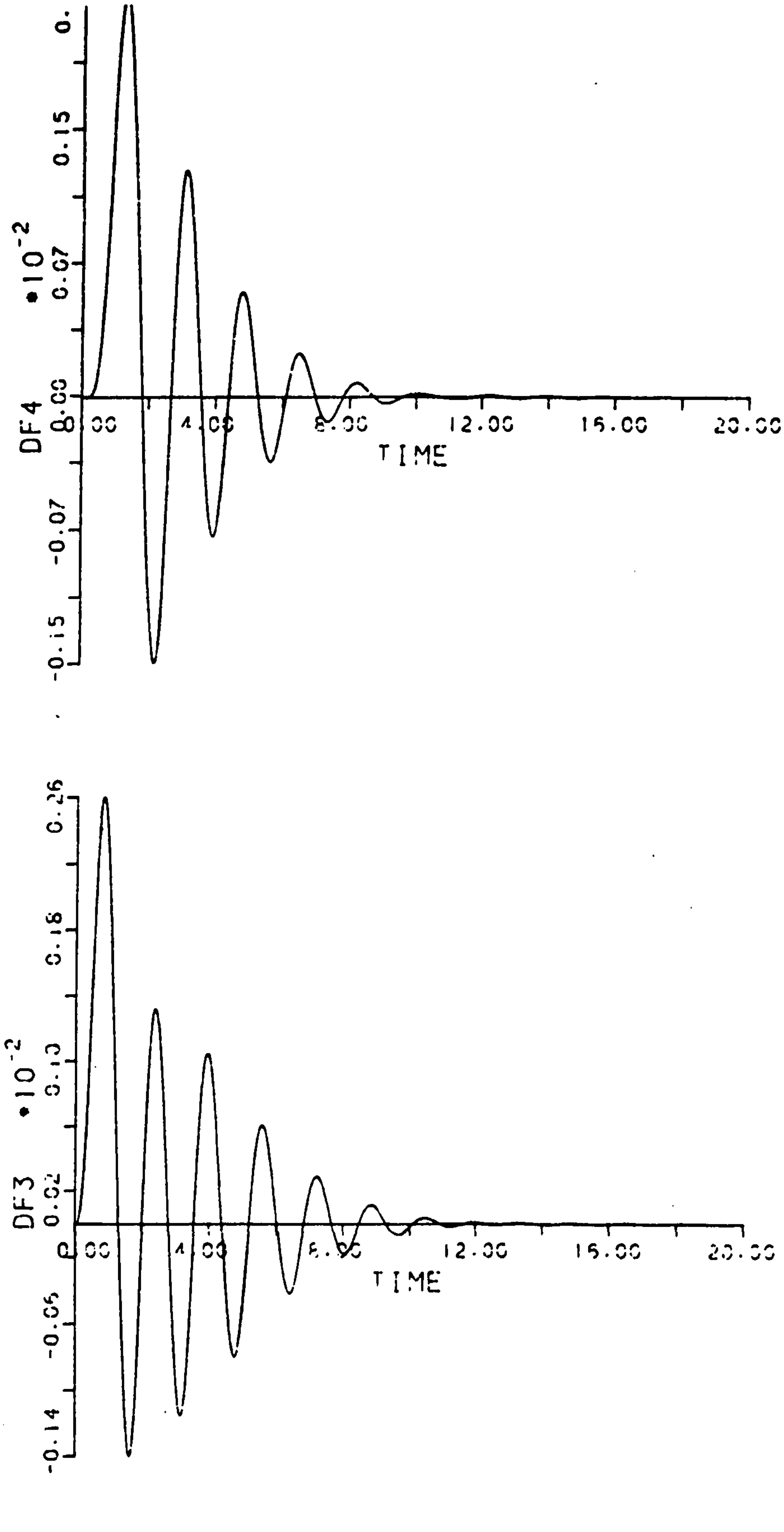

Figure 6.1b. Tie-line deviation in a controlled 4 cascaded area system following a step load disturbance.

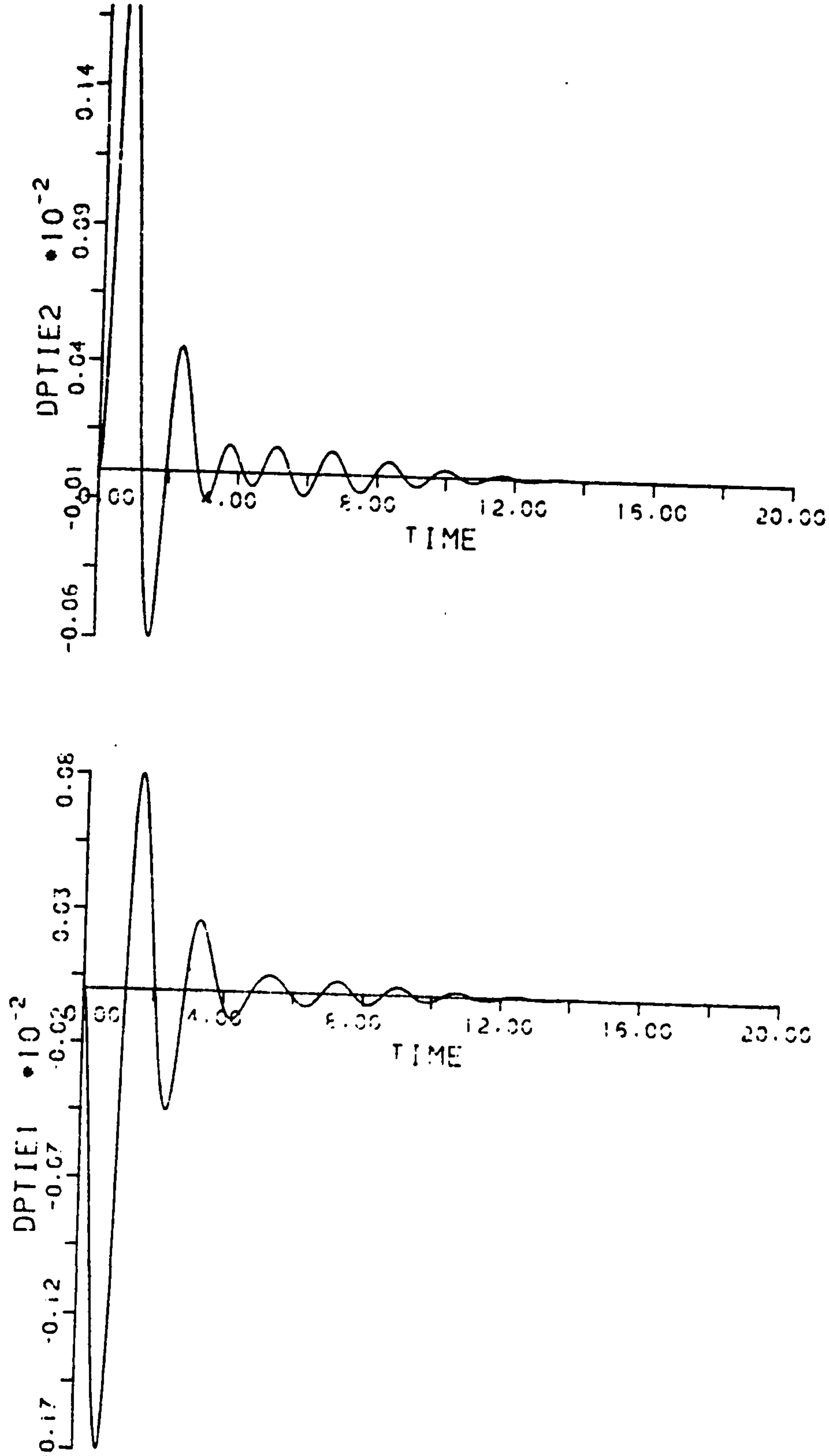

Figure 6-1c. Frequency deviation in a controlled 4 cascaded area system following a step load disturbance.

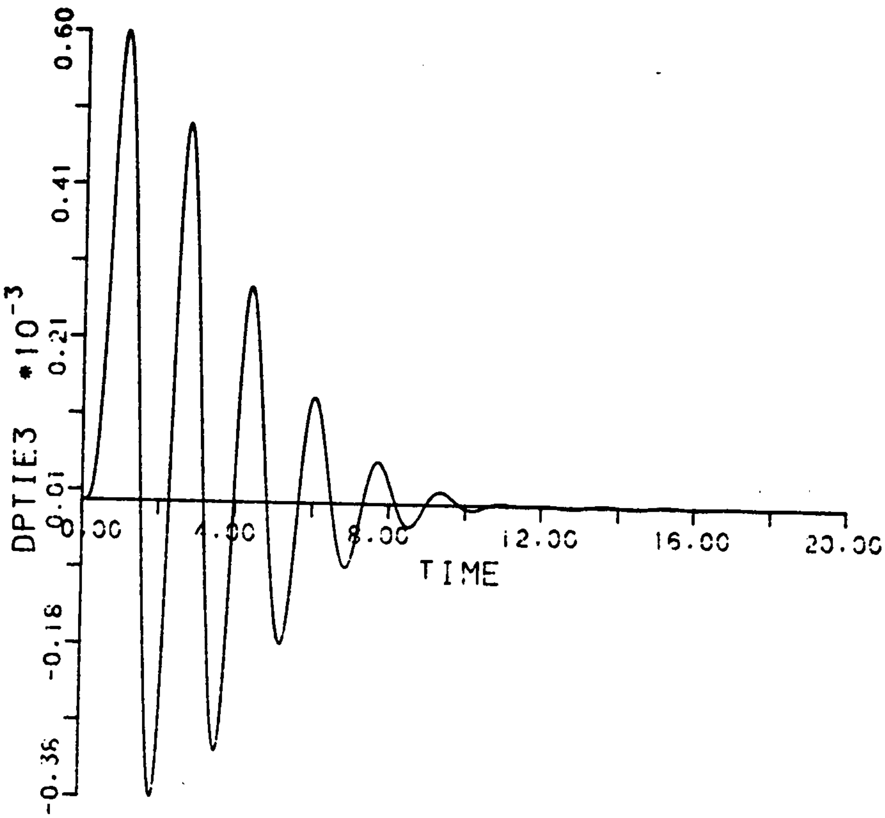

Figure 6-1d. Frequency deviation in a controlled 4 cascaded area system following a step load disturbance.

TABLE IV. Range of Deviation of the Frequency and Tie-Line of a Controlled 4 Area System in Cascad Form.

	Range of Deviation
ΔF_1	$-0.13 * 10^{-2}$ to $0.28 * 10^{-2}$
ΔF_2	$-0.6 * 10^{-2}$ to $0.8 * 10^{-2}$
ΔF_3	$-0.14 * 10^{-2}$ to $0.26 * 10^{-2}$
ΔF_4	$-0.15 * 10^{-2}$ to $0.22 * 10^{-2}$
$\Delta P_{tie\ 12}$	$-0.17 * 10^{-2}$ to $0.08 * 10^{-2}$
$\Delta P_{tie\ 23}$	$-0.06 * 10^{-2}$ to $0.19 * 10^{-2}$
$\Delta P_{tie\ 34}$	$-0.38 * 10^{-3}$ to $0.6 * 10^{-3}$

$$\frac{d}{dt}\Delta P_{G4} = \frac{1}{T_{T4}}(\Delta X_{E4} - \Delta P_{G4}) \tag{6-9}$$

The state vector is selected as follow:

$$x = [\Delta F_1\ \Delta X_{E1}\ \Delta P_{G1}\ \Delta P_{tie\ 13}\ \Delta F_2\ \Delta X_{E2}\ \Delta P_{G2}\ \Delta P_{tie\ 23}\ \Delta F_3\ \Delta X_{E3}$$

$$\Delta P_{G3}\ \Delta P_{tie\ 34}\ \Delta F_4\ \Delta X_{E4}\ \Delta P_{G4}]^t \tag{6-10}$$

The control input:

$$u = [\Delta P_{C1}\quad \Delta P_{C2}\quad \Delta P_{C3}\quad \Delta P_{C4}] \tag{6-11}$$

and the disturbance vector

$$p = [\Delta P_{D1}\quad \Delta P_{D2}\quad \Delta P_{D3}\quad \Delta P_{D4}] \tag{6-12}$$

The system can be written in a compact form, after making use of the definition of the u, x and p vectors,

$$\dot{x} = Ax + Bu + \Gamma p \tag{6-13}$$

where

$$\frac{d}{dt}\Delta P_{G1} = \frac{1}{T_{T1}}(\Delta X_{E1} - \Delta P_{G1})$$

$$\frac{d}{dt}\Delta P_{tie\ 13} = 2\pi\ T_{13}\ (\Delta F_1 - \Delta F_3)$$

$$\frac{d}{dt}\Delta F_2 = \frac{1}{T_{P2}}(-\ \Delta F_2 + K_{P2}\ \Delta P_{G2} - K_{P2}\ \Delta P_{tie\ 23} - K_{P2}\ \Delta P_{D2})$$

$$\frac{d}{dt}\Delta X_{E2} = \frac{1}{T_{G2}}(-\ \frac{1}{R_2}\Delta F_2 - \Delta X_{E2} + \Delta P_{C2})$$

$$\frac{d}{dt}\Delta P_{G2} = \frac{1}{T_{T2}}(\Delta X_{E2} - \Delta P_{G2})$$

$$\frac{d}{dt}\Delta P_{tie\ 23} = 2\pi\ T_{23}\ (\Delta F_2 - \Delta F_3)$$

$$\frac{d}{dt}\Delta F_3 = \frac{1}{T_{P3}}(-a_{13}K_{P3}\Delta P_{tie\ 13} - a_{23}K_{P3}\Delta P_{tie23} - \Delta F_3 + K_{P3}\Delta P_{G3}$$

$$- K_{P3}\ \Delta P_{tie\ 34} - K_{P3}\ \Delta P_{D3})$$

$$\frac{d}{dt}\Delta X_{E3} = \frac{1}{T_{G3}}(-\ \frac{1}{R_3}\Delta F_3 + \Delta X_{E3} + \Delta P_{C3})$$

$$\frac{d}{dt}\Delta P_{G3} = \frac{1}{T_{T3}}(\Delta X_{E3} - \Delta P_{G3})$$

$$\frac{d}{dt}\Delta P_{tie\ 34} = 2\pi T_{34}\ (\Delta F_3 - \Delta F_4)$$

$$\frac{d}{dt}\Delta F_4 = \frac{1}{T_{P4}}(-a_{34}K_{P4}\Delta P_{tie\ 34} - \Delta F_4 + K_{P4}\ \Delta P_{G4} - K_{P3}\ \Delta P_{D4})$$

$$\frac{d}{dt}\Delta X_{E4} = \frac{1}{T_{G4}}(-\ \frac{1}{R_4}\Delta F_4 - \Delta X_{E4} + \Delta P_{G4})$$

$$
A = \begin{bmatrix}
-1/T_{p1} & 0 & K_{P1}/T_{P1} & -K_{P1}/T_{P1} & 0 & 0 & 0 & 0 & 0 & 0 & 0 & 0 & 0 & 0 & 0 \\
-1/R_1T_{G1} & -1/T_{G1} & 0 & 0 & 0 & 0 & 0 & 0 & 0 & 0 & 0 & 0 & 0 & 0 & 0 \\
0 & 1/T_{T1} & -1/T_{T1} & 0 & 0 & 0 & 0 & 0 & 0 & 0 & 0 & 0 & 0 & 0 & 0 \\
2\pi T_{13} & 0 & 0 & 0 & 0 & 0 & 0 & 0 & -2\pi T_{13} & 0 & 0 & 0 & 0 & 0 & 0 \\
0 & 0 & 0 & 0 & -1/T_{P2} & 0 & K_{P2}/T_{P2} & -K_{P2}/T_{P2} & 0 & 0 & 0 & 0 & 0 & 0 & 0 \\
0 & 0 & 0 & 0 & -1/R_2/T_{G2} & -1/T_{G2} & 0 & 0 & 0 & 0 & 0 & 0 & 0 & 0 & 0 \\
0 & 0 & 0 & 0 & 0 & -1/T_{T2} & -1/T_{T2} & 0 & 0 & 0 & 0 & 0 & 0 & 0 & 0 \\
0 & 0 & 0 & 0 & 2\pi T_{23} & 0 & 0 & 0 & -2\pi T_{23} & 0 & 0 & 0 & 0 & 0 & 0 \\
0 & 0 & 0 & -a_{13}K_{P3}/T_{P3} & 0 & 0 & 0 & -a_{23}K_{p3}/T_{p3} & -\frac{1}{T_{P3}} & 0 & K_{P3}/T_{P3} & -K_{P3}/T_{P3} & 0 & 0 & 0 \\
0 & 0 & 0 & 0 & 0 & 0 & 0 & 0 & -1/R_3T_{G3} & -1/T_{G3} & 0 & 0 & 0 & 0 & 0 \\
0 & 0 & 0 & 0 & 0 & 0 & 0 & 0 & 0 & 1/T_{T3} & -1/T_{T3} & 0 & 0 & 0 & 0 \\
0 & 0 & 0 & 0 & 0 & 0 & 0 & 0 & 2\pi T_{34} & 0 & 0 & 0 & -2\pi T_{34} & 0 & 0 \\
0 & 0 & 0 & 0 & 0 & 0 & 0 & 0 & 0 & 0 & 0 & -a_{34}K_{P4}/T_{P4} & -1/T_{P4} & 0 & K_{P4}/T_{P4} \\
0 & 0 & 0 & 0 & 0 & 0 & 0 & 0 & 0 & 0 & 0 & 0 & -1/R_4T_{P4} & -1/T_{P4} & 0 \\
0 & 0 & 0 & 0 & 0 & 0 & 0 & 0 & 0 & 0 & 0 & 0 & 0 & 1/T_{T4} & -1/T_{T4}
\end{bmatrix}
$$

$$B_{ij} = 0,\ B_{2,1} = 1/T_{G1} \quad ; \quad B_{10,3} = 1/T_{G3}$$

$$B_{6,2} = 1/T_{G2} \quad ; \quad B_{14,4} = 1/T_{G4}$$

$$\Gamma_{ij} = 0,\ \Gamma_{1,1} = -K_{P1}/T_{P1} \ ; \ \Gamma_{5,2} = -K_{P2}/T_{P2}$$

$$\Gamma_{g,3} = -K_{P3}/T_{P3} \quad ; \ \Gamma_{13,4} = -K_{P4}/T_{P4}$$

The system was simulated for the following typical values of the parameters:

$T_{P1} = 20,\ T_{P2} = 25,\ T_{P3} = 21,\ T_{P4} = 22$ (Sec.)

$K_{P1} = 120,\ K_{P2} = 100,\ K_{P3} = 115,\ K_{P4} = 110$ (Hz/pu MW)

$R_1 = 2.4,\ R_2 = 3.0,\ R_3 = 2.2,\ R_4 = 2.4$ (Hz/pu MW)

$T_{G1} = 0.08,\ T_{G3} = 0.08,\ T_{G2} = 0.1,\ T_{G4} = 0.25$ (Sec.)

$T_{T1} = 0.3,\ T_{T2} = 0.25,\ T_{T3} = 0.3,\ T_{T4} = 0.1$ (Sec.)

$T_{23} = 0.1,\ T_{13} = 0.0866,\ T_{34} = 0.1$ (pu MW/Hz)

6.3.2 Area Decomposition

The system is partitioned into 4 subsystems which are expressed into the standard form:

$$x_i = A_i x_i + B_i u_i + C_i z_i \qquad (i = 1,2,3,4) \tag{6-14}$$

where

$$A_1 = \begin{bmatrix} -1/T_{P1} & 0 & K_{P1}/T_{P1} & -K_{P1}/T_{P1} \\ -1/R_1T_{G1} & -1/T_{G1} & 0 & 0 \\ 0 & 1/T_{T1} & -1/T_{T1} & 0 \\ 2\pi T_{13} & 0 & 0 & 0 \end{bmatrix} ; \; B = \begin{bmatrix} 0 \\ 1/T_{G1} \\ 0 \\ 0 \end{bmatrix}$$

$$A_2 = \begin{bmatrix} -1/T_{P2} & 0 & K_{P2}/T_{P2} & -K_{P2}/T_{P2} \\ -1/R_2T_{G2} & -1/T_{G2} & 0 & 0 \\ 0 & 1/T_{T2} & -1/T_{T2} & 0 \\ 2\pi T_{23} & 0 & 0 & 0 \end{bmatrix} ; \; B = \begin{bmatrix} 0 \\ 1/T_{G2} \\ 0 \\ 0 \end{bmatrix}$$

$$A_3 = \begin{bmatrix} -1/T_{P3} & 0 & K_{P3}/T_{P3} & -K_{P3}/T_{P3} \\ -1/R_3T_{G3} & -1/T_{G3} & 0 & 0 \\ 0 & 1/T_{T3} & -1/T_{T3} & 0 \\ 2\pi T_{34} & 0 & 0 & 0 \end{bmatrix} \quad ; \; B_3 = \begin{bmatrix} 0 \\ 1/T_{G3} \\ 0 \\ 0 \end{bmatrix}$$

$$A_4 = \begin{bmatrix} -1/T_{P4} & 0 & K_{P4}/T_{P4} \\ -1/R_4T_{P4} & -1/T_{P4} & 0 \\ 0 & 1/T_{T4} & -1/T_{T4} \end{bmatrix} \quad ; \; B = \begin{bmatrix} 0 \\ 1/T_{G4} \\ 0 \end{bmatrix}$$

The off-diagonal matrices are:

$$C_1 = \begin{bmatrix} 0 \\ 0 \\ 0 \\ -2\pi T_{13} \end{bmatrix} \quad , \; C_2 = \begin{bmatrix} 0 \\ 0 \\ 0 \\ -2\pi T_{23} \end{bmatrix} \quad ; \; C_4 = \begin{bmatrix} -a_{34}K_{P4}/T_{P4} \\ 0 \\ 0 \end{bmatrix}$$

$$C_3 = \begin{bmatrix} -a_{13}K_{p3}/T_{p3} & -a_{23}K_{p3}/T_{p3} & 0 \\ 0 & 0 & 0 \\ 0 & 0 & 0 \\ 0 & 0 & -2\pi T_{34} \end{bmatrix}$$

A preliminary study shows that for the following values of:

$$Z_i = 1000 \ I \qquad i = 1, 2, 3, 4$$

$$H_i = I \qquad I = \text{Identity matrix} \tag{6-15}$$

The eigenvalues obtained of the system are:

<u>Subsystem # 1</u>:

$-17.840 + j\ 0.0$

$-\ 2.437 \pm j\ 2.682$

$-\ 1.160 + j\ 0.0$

Subsystem # 2:

$-14.146 + j0.0$

$-2.853 + j0.0$

$-1.782 \pm j1.344$

Subsystem # 3:

$-17.835 + j0.0$

$-2.256 \pm j2.588$

$-1.363 + j0.0$

Subsystem # 4:

$-3.886 \pm j2.158$

$-10.903 + j0.0$

Then the modes are spread over the range (-17.840 to -1.160). The following crude model matrices have been chosen:

$$A_{Z1} = [-9] \quad , \quad A_{Z2} = \begin{bmatrix} -9 & 0 \\ 0 & -9 \end{bmatrix} \quad , \quad A_{Z3} = \begin{bmatrix} -9 & 0 \\ 0 & -9 \end{bmatrix}$$

$$A_{Z4} = [-9] \tag{6-16}$$

$$S_i = 1000\ I \qquad i = 1, 2, 3, 4$$

$H_i = I \qquad\qquad I = \text{Identity matrix.}$

The weighting matrices are selected to be:

$$Q_1 = Q_2 = Q_3 = \text{diag}\ (1 \quad 0 \quad 0 \quad 1)$$
$$Q_4 = \text{diag}\ (1 \quad 0 \quad 0) \tag{6-17}$$

6.3.3 Simulation and Results

Simulation results using the above numerical values show that the system is asymptotically stable. The deviation of the frequency and tie-lines are within the acceptable limits. The frequency and tie-line deviation are shown in Fig. (5-2). The range of the frequency and tie-lines deviations are given in Table V.

6.4 SIMULATION OF 4 AREA SYSTEM CONTAINING A LOOP

6.4.1 Model of 4 Area System Containing a Loop

Let us assume a 4 area system containing one loop. The system is represented as follow:

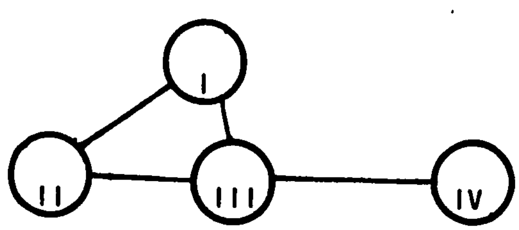

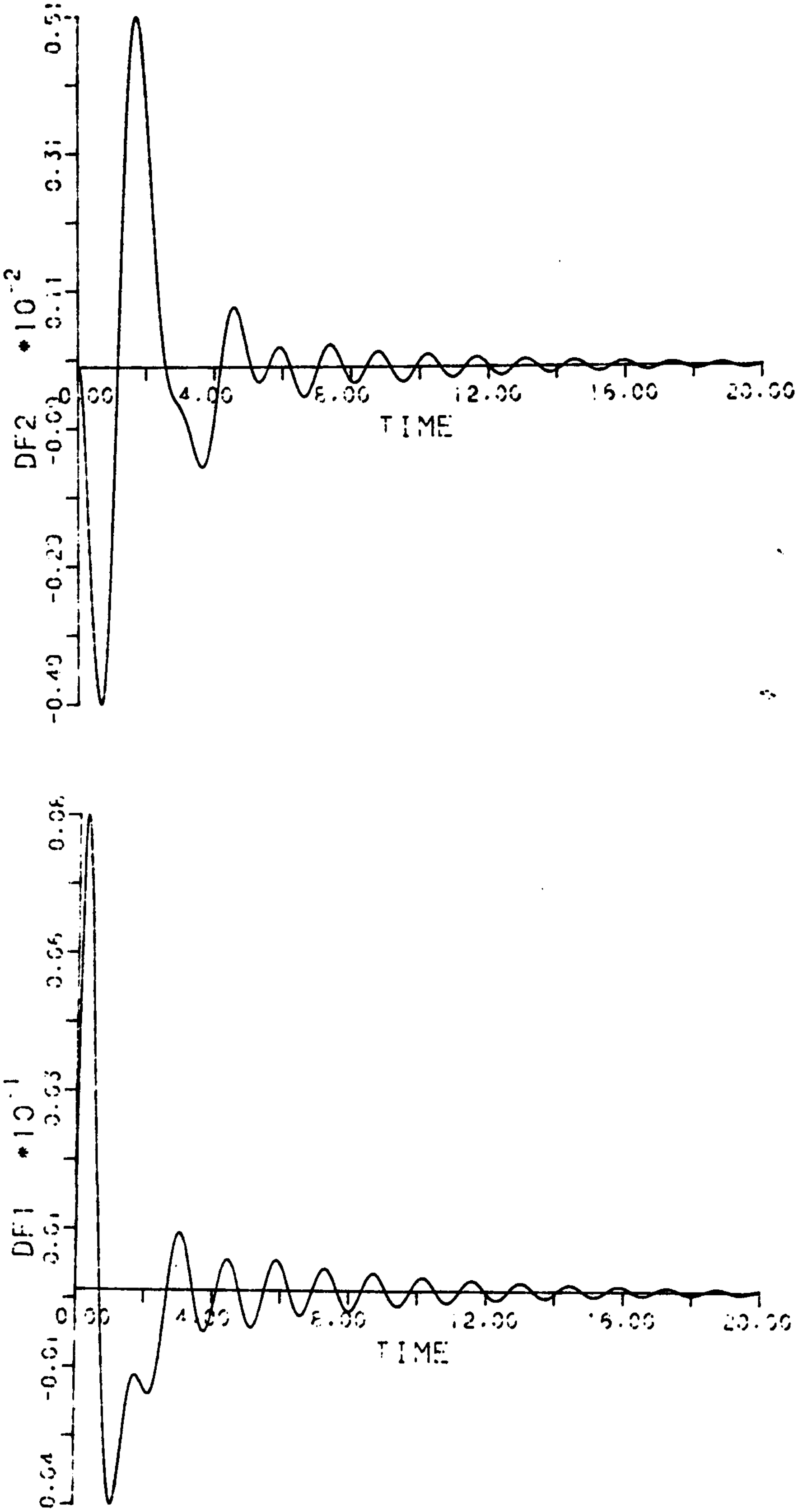

Figure 6-2a. Tie-line deviation in a controlled 4 area radial system following a step load change.

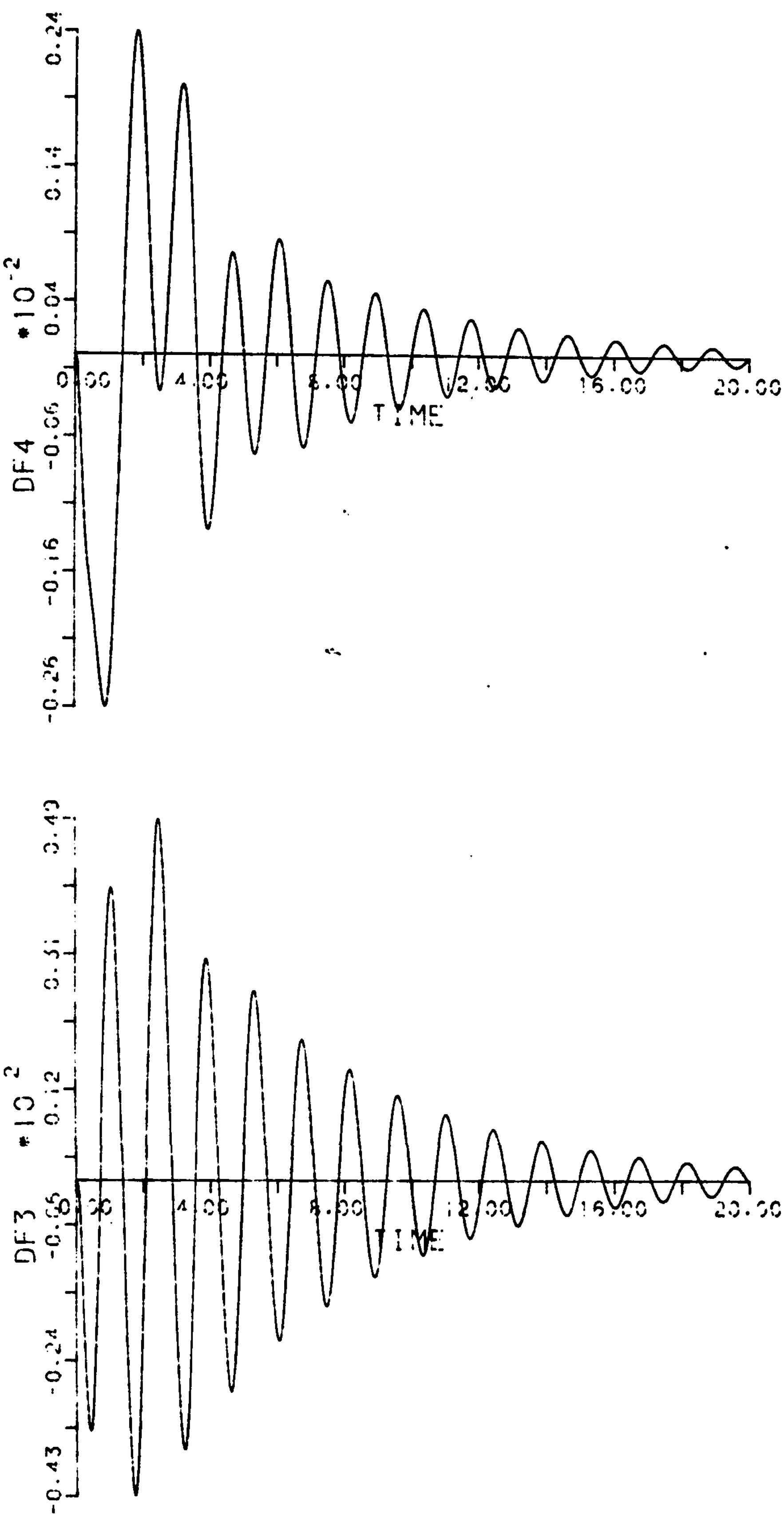

Figure 6-2b. Frequency deviation in a controlled 4 area radial system following a step load disturbance.

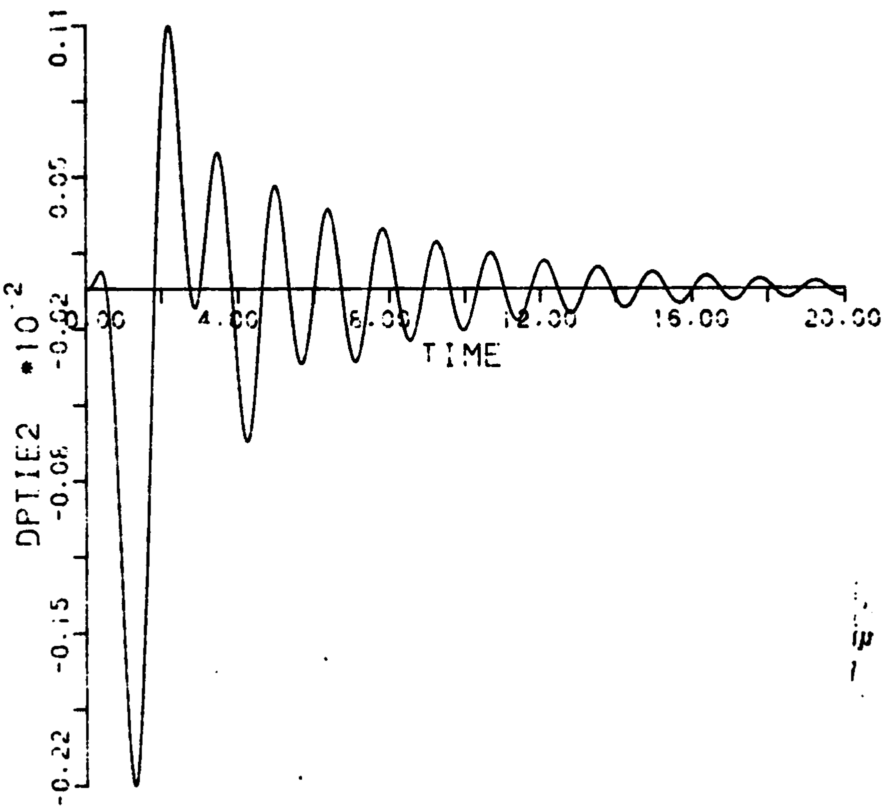

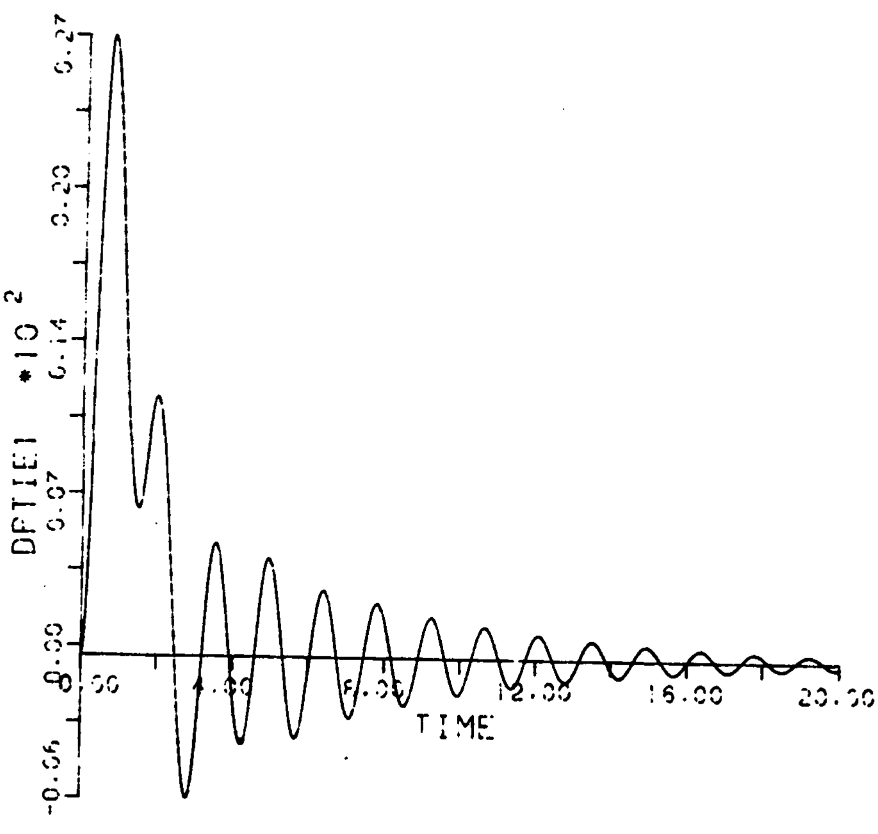

Figure 6-2c. Frequency deviaiton in a controlled 4 area radial system following a step load disturbance.

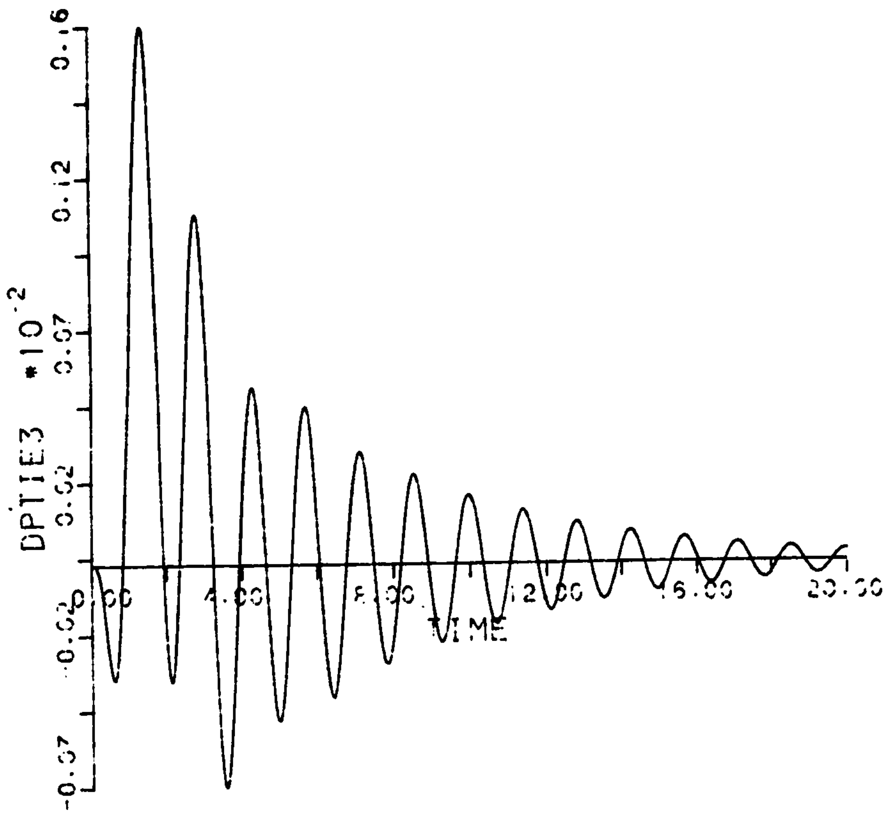

Figure 6-2d. Tie-line deviation in a controlled 4 area radial system following a step load disturbance.

The system of equations describing the multi-area system are:

$$\frac{d}{dt} = \Delta F = \frac{1}{T_{P1}} (- \Delta F_1 + K_{P1}\Delta P_{G1} - K_{P1}\Delta P_{tie\ 12} - K_{P1}\Delta P_{tie\ 13} - K_{P1}\Delta P_{D1})$$

$$\frac{d}{dt} \Delta X_{E1} = \frac{1}{T_{G1}} (- \frac{1}{R_1} \Delta F_1 - \Delta X_{E1} + \Delta P_{C1})$$

$$\frac{d}{dt} \Delta P_{G1} = \frac{1}{T_{T1}} (\Delta X_{E1} - \Delta P_{G1})$$

$$\frac{d}{dt} \Delta P_{tie\ 12} = 2\pi\ T_{12}\ (\Delta F_1 - \Delta F_2)$$

$$\frac{d}{dt} \Delta F_2 = \frac{1}{T_{P2}} (-a_{12}K_{P2}\Delta P_{tie\ 12} - \Delta F_3 + K_{P2}\Delta P_{G2} - K_{P2}\Delta P_{tie\ 23} - K_{P2}\Delta P_{D2})$$

$$\frac{d}{dt} \Delta X_{Q2} = \frac{1}{T_{G2}} (- \frac{1}{R_2} \Delta F_2 - \Delta X_{E2} + \Delta P_{C2})$$

$$(6\text{-}18)$$

$$\frac{d}{dt} \Delta P_{G2} = \frac{1}{T_{T2}} (\Delta X_{E2} - \Delta P_{G2})$$

$$\frac{d}{dt} \Delta P_{tie\ 23} = 2\pi\ T_{23}\ (\Delta F_2 - \Delta F_3)$$

$$\frac{d}{dt} \Delta F_3 = \frac{1}{T_{P3}} (-a_{23}K_{P3}\Delta P_{tie\ 23} - \Delta F_3 + K_{P3}\Delta P_{G3} - a_{13}K_{P3}\Delta P_{tie\ 13} - K_{P3}\Delta P_{tie\ 34} - K_{P3}\Delta P_{D3})$$

$$\frac{d}{dt} \Delta X_{E3} = \frac{1}{T_{G3}} (- \frac{1}{R_3} \Delta F_3 - \Delta X_{E3} + \Delta P_{C3})$$

$$\frac{d}{dt} \Delta P_{G3} = \frac{1}{T_{T3}} (\Delta X_{E3} - \Delta P_{G3})$$

$$\frac{d}{dt}\Delta P_{tie\ 13} = 2\pi T_{13}\ (\Delta F_1 - \Delta F_3)$$

$$\frac{d}{dt}\Delta F_4 = \frac{1}{T_{P4}}\ (-a_{34}K_{P4}\Delta P_{tie\ 34} - \Delta F_4 + K_{P4}\Delta P_{G4} - K_{P4}\Delta P_{D4})$$

$$\frac{d}{dt}\Delta X_{E4} = \frac{1}{T_{G4}}\ (-\frac{1}{R_4}\Delta F_4 - \Delta X_{E4} + \Delta P_{G4}) \tag{6-18}$$

$$\frac{d}{dt}\Delta P_{G4} = \frac{1}{T_{T4}}\ (\Delta X_{E4} - \Delta P_{G4})$$

If we assume the state variable by

$$x = (\Delta F_1\ \ \Delta X_{E1}\ \ \Delta P_{G1}\ \ \Delta P_{tie\ 12}\ \ \Delta F_2\ \ \Delta X_{E2}\ \ \Delta P_{G2}\ \ \Delta P_{tie\ 23}$$

$$\Delta F_3\ \ \Delta X_{E3}\ \ \Delta P_{G3}\ \ \Delta P_{tie\ 13}\ \ \Delta P_{tie\ 34}\ \ \Delta F_4\ \ \Delta X_{E4}\ \ \Delta P_{G4})^t \tag{6-19}$$

and the control input by

$$u = (\Delta P_{C1}\ \ \Delta P_{C2}\ \ \Delta P_{C3}\ \ \Delta P_{C4})^t \tag{6-20}$$

and the disturbance vector by

$$p = (\Delta P_{D1}\ \ \Delta P_{D2}\ \ \Delta P_{D3}\ \ \Delta P_{D4}) \tag{6-21}$$

The system can be expressed in a compact form:

$$\dot{x} = Ax + Bu + \Gamma p \tag{6-22}$$

where

$$A=\begin{bmatrix}
-\frac{1}{T_{P1}} & 0 & K_{P1}/T_{P1} & -K_{P1}/T_{P1} & 0 & 0 & 0 & 0 & 0 & 0 & 0 & -K_{P1}/T_{P1} & 0 & 0 & 0 & 0 \\
-\frac{1}{R_1 T_{G1}} & -\frac{1}{T_{G1}} & 0 & 0 & 0 & 0 & 0 & 0 & 0 & 0 & 0 & 0 & 0 & 0 & 0 & 0 \\
 & \frac{1}{T_{T1}} & -1/T_{T1} & 0 & 0 & 0 & 0 & 0 & 0 & 0 & 0 & 0 & 0 & 0 & 0 & 0 \\
2\pi T_{12} & 0 & 0 & 0 & -2\pi T_{12} & 0 & 0 & 0 & 0 & 0 & 0 & 0 & 0 & 0 & 0 & 0 \\
0 & 0 & 0 & -a_{12}K_{P2}/T_{P2} & -1/T_{P2} & 0 & K_{P2}/T_{P2} & -K_{P2}/T_{P2} & 0 & 0 & 0 & 0 & 0 & 0 & 0 & 0 \\
0 & 0 & 0 & 0 & -1/R_2T_{G2} & -1/T_{G2} & 0 & 0 & 0 & 0 & 0 & 0 & 0 & 0 & 0 & 0 \\
0 & 0 & 0 & 0 & 0 & 1/T_{T2} & -1/T_{T2} & 0 & 0 & 0 & 0 & 0 & 0 & 0 & 0 & 0 \\
0 & 0 & 0 & 0 & 2\pi T_{23} & 0 & 0 & 0 & -2\pi T_{23} & 0 & 0 & 0 & 0 & 0 & 0 & 0 \\
0 & 0 & 0 & 0 & 0 & 0 & 0 & -a_{23}K_{P3}/T_{P3} & -1/T_{P3} & 0 & K_{P3}/T_{P3} & -a_{13}K_{P3}/T_{P3} & -K_{P3}/T_{P3} & 0 & 0 & 0 \\
0 & 0 & 0 & 0 & 0 & 0 & 0 & 0 & -1/R_3T_{G3} & -1/T_{G3} & 0 & 0 & 0 & 0 & 0 & 0 \\
0 & 0 & 0 & 0 & 0 & 0 & 0 & 0 & 0 & 1/T_{T3} & -1/T_{T3} & 0 & 0 & 0 & 0 & 0 \\
2\pi T_{13} & 0 & 0 & 0 & 0 & 0 & 0 & 0 & -2\pi T_{13} & 0 & 0 & 0 & 0 & 0 & 0 & 0 \\
0 & 0 & 0 & 0 & 0 & 0 & 0 & 0 & 2\pi T_{34} & 0 & 0 & 0 & 0 & -2\pi T_{34} & 0 & 0 \\
0 & 0 & 0 & 0 & 0 & 0 & 0 & 0 & 0 & 0 & 0 & 0 & -a_{34}K_{P4}/T_{P4} & -1/T_{P4} & 0 & \frac{K_{P4}}{T_{P4}} \\
0 & 0 & 0 & 0 & 0 & 0 & 0 & 0 & 0 & 0 & 0 & 0 & 0 & -1/R_4T_{G4} & -1/T_{G4} & 0 \\
0 & 0 & 0 & 0 & 0 & 0 & 0 & 0 & 0 & 0 & 0 & 0 & 0 & 0 & 1/T_{T4} & -\frac{1}{T_{T4}}
\end{bmatrix}$$

$B_{ij} = 0 \qquad B_{2,1} = 1/T_{G1}\ ,\ B_{6,2} = 1/T_{G2}$

$B_{10,3} = 1/T_{G3}\ ,\ B_{15,4} = 1/T_{G4}$

$\Gamma_{ij} = 0 \qquad \Gamma_{1,1} = K_{P1}/T_{P1},\ \Gamma_{5,2} = -K_{P2}/T_{P2}$

$\Gamma_{9,3} = -K_{P3}/T_{P3}\ ,\ \Gamma_{12,4} = -K_{P4}/T_{P4}$

The system is simulated for the following typical values:

$T_{P1} = 20,\ T_{P2} = 25,\ T_{P3} = 21\ ,\ T_{P4} = 22$ (Sec.)

$K_{P1} = 120,\ K_{P2} = 100,\ K_{P3} = 115,\ K_{P5} = 110$ (Hz/pu MW)

$R_1 = 2.4,\ R_2 = 3.0,\ R_3 = 2.2,\ R_4 = 2.4$ (Hz/pu MW)

$T_{G1} = 0.08,\ T_{G2} = 0.1,\ T_{G3} = 0.08,\ T_{G4} = 0.25$ (Sec.)

$T_{T1} = 0.3,\ T_{T2} = 0.25,\ T_{T3} = 0.3,\ T_{T4} = 0.1$ (Sec.)

$T_{12} = 0.0866,\ T_{23} = 0.1,\ T_{13} = 0.1,\ T_{34} = 0.1$ (pu MW/Hz)

6.4.2 Area Decomposition

The system is decomposed into 4 subsystems. Each subsystem consists of one area and is expressed into the following form:

$$x_i = A_i x_2 + B_i u_i + C_i z_i \qquad (i=1,2,3,4) \tag{6-24}$$

where

$$A_1 = \begin{pmatrix} -1/T_{P1} & 0 & K_{P1}/T_{P1} & -K_{P1}/T_{P1} \\ -1/R_1T_{G1} & -1/T_{G1} & 0 & 0 \\ 0 & 1/T_{T1} & -1/T_{T1} & 0 \\ 2\pi T_{12} & 0 & 0 & 0 \end{pmatrix}, \quad B_1 = \begin{pmatrix} 0 \\ 1/T_{G1} \\ 0 \\ 0 \end{pmatrix}$$

$$A_2 = \begin{pmatrix} -1/T_{P2} & 0 & K_{P2}/T_{P2} & -K_{P2}/T_{P2} \\ -1/R_2/T_{G2} & -1/T_{G2} & 0 & 0 \\ 0 & 1/T_{T2} & -1/T_{T2} & 0 \\ 2\pi T_{23} & 0 & 0 & 0 \end{pmatrix}, \quad B_2 = \begin{pmatrix} 0 \\ 1/T_{G2} \\ 0 \\ 0 \end{pmatrix}$$

$$A_3 = \begin{pmatrix} -1/T_{P3} & 0 & K_{P3}/T_{P3} & -a_{13}K_{p3}/T_{p3} \\ -1/R_3T_{G3} & -1/T_{G3} & 0 & 0 \\ 0 & 1/T_{T3} & -1/T_{T3} & 0 \\ -2\pi T_{13} & 0 & 0 & 0 \end{pmatrix}, \quad B_3 = \begin{pmatrix} 0 \\ 1/T_{G3} \\ 0 \\ 0 \end{pmatrix}$$

$$A_4 = \begin{pmatrix} 0 & -2\pi T_{34} & 0 & 0 \\ -a_{34}K_{P4}/T_{P4} & -1/T_{P4} & 0 & K_{P4}/T_{P4} \\ 0 & -1/R_4T_{G4} & -1/T_{G4} & 0 \\ 0 & 0 & 1/T_{T4} & -1/T_{T4} \end{pmatrix} \; ; \; B_4 = \begin{pmatrix} 0 \\ 0 \\ 1/T_{G4} \\ 0 \end{pmatrix}$$

The off-diagonal m atrices are:

$$C_2 = \begin{pmatrix} -a_{12}K_{P2}/T_{P2} & 0 \\ 0 & 0 \\ 0 & 0 \\ 0 & -2\pi T_{23} \end{pmatrix}$$

$$C_3 = \begin{pmatrix} 0 & -a_{23}K_{P3}/T_{P3} & -K_{P3}/T_{P3} \\ 0 & 0 & 0 \\ 0 & 0 & 0 \\ 2\pi T_{13} & 0 & 0 \end{pmatrix}$$

$$C_4 = \begin{bmatrix} 2\pi T_{34} \\ 0 \\ 0 \\ 0 \end{bmatrix} \quad ; \quad C_1 = \begin{bmatrix} 0 & -K_{P1}/T_{P1} \\ 0 & 0 \\ 0 & 0 \\ -2\pi T_{12} & 0 \end{bmatrix}$$

The preliminary calculation was done with the following numerical values:

$$S_i = 1000\ I$$

$$H_i = I \qquad\qquad i = 1,2,3,4 \quad (I = \text{Indentity matrix})$$

$$R_i = 1 \tag{6-25}$$

$$Q_1 = Q_2 = Q_3 = \text{diag}\ (1 \quad 0 \quad 0 \quad 1)$$

$$Q_4 = \text{diag}\ (1 \quad 1 \quad 0 \quad 0)$$

The eigenvalues were found to range from -17.839 to -1.160.

Then the proposed crude model matrices were selected as follow:

$$A_{z1} = A_{z2} = \text{diag}\ (-9,\ -9)$$

$$A_{z3} = \text{diag}\ (-9,\ -9,\ -9) \qquad (6\text{-}26)$$

$$A_{z4} = (-9)$$

6.4.3 Simulation Results

The developed decentralized regulator with the characteristics explained in Section 3.13, has been simulated to control the system with a step-change in power demand. The simulation was performed to study the dynamic behaviour of the 4 area-power system containing a loop. The frequency and tie-line deviations are shown in Fig. (6-3). In Table VI is shown the range of the frequency deviation and tie-line under step change in the demand.

The states reached their steady-state values in less than 20 seconds. The range of the frequency and tie-line deviations are within the acceptable range.

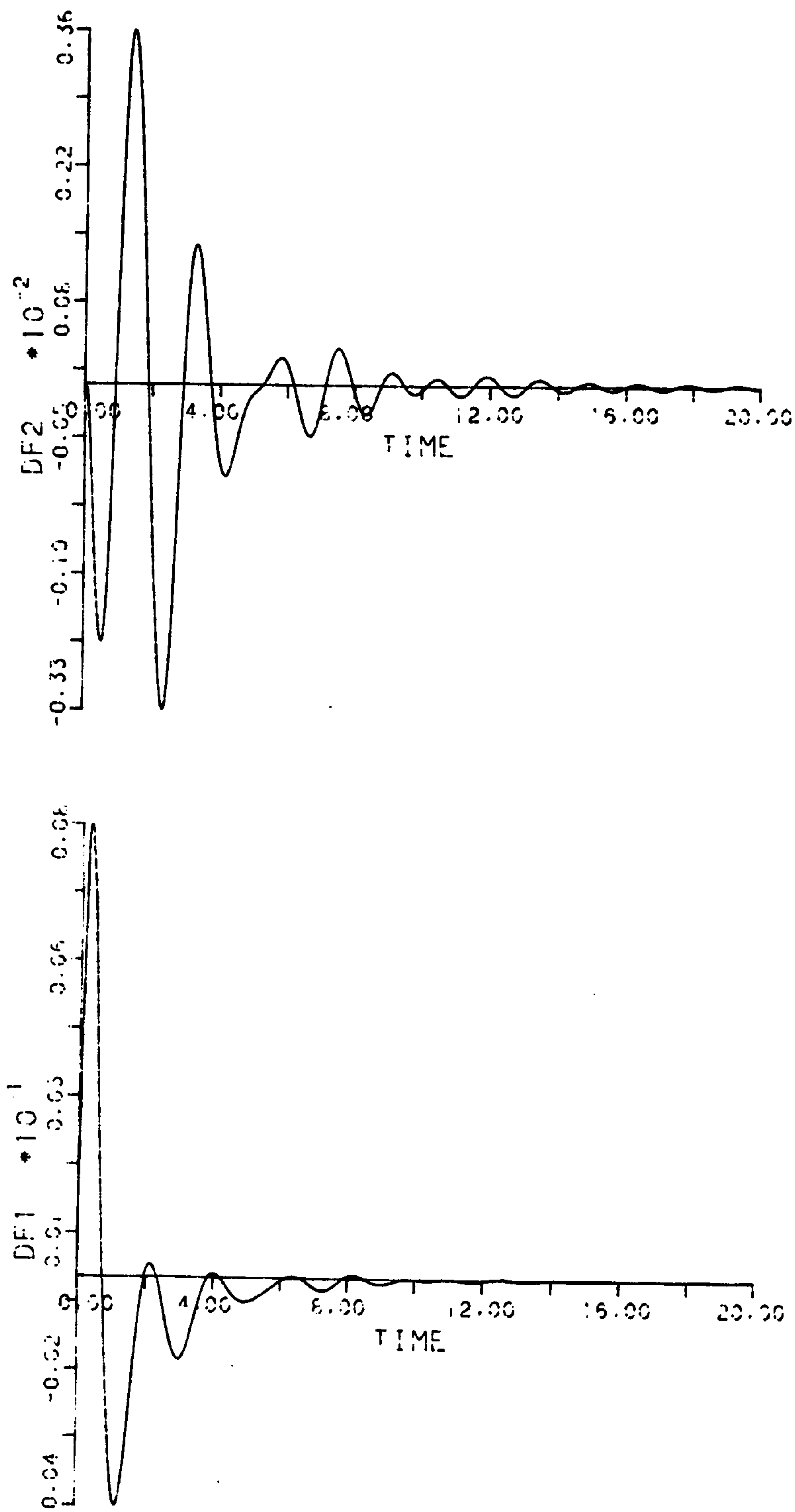

Figure 6-3a. Frequency deviation in a controlled 4 area system containing a loop following a step load disturbance.

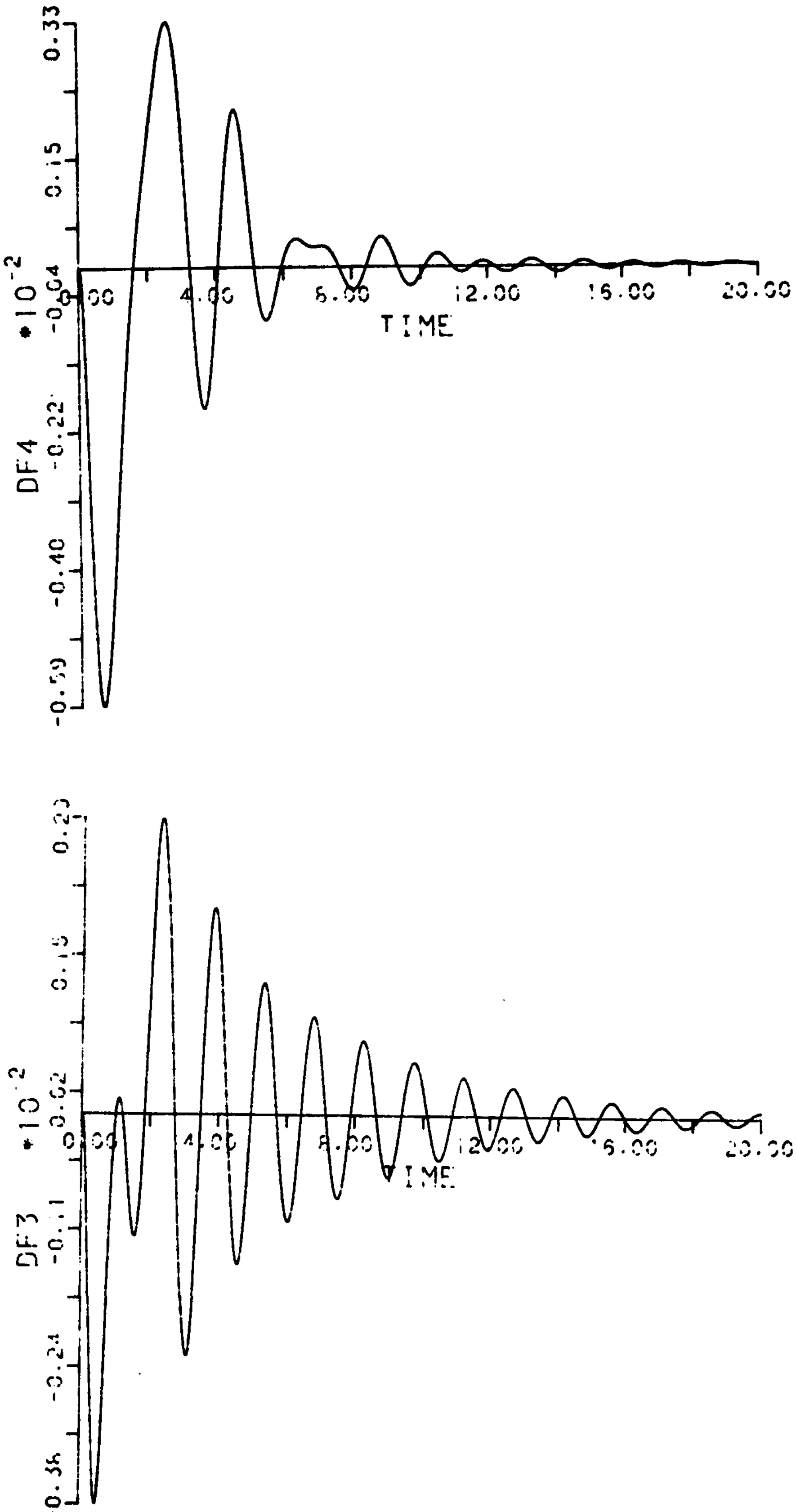

Figure 6-3b. Frequency deviation in a controlled 4 area system containing a loop following a step load disturbance.

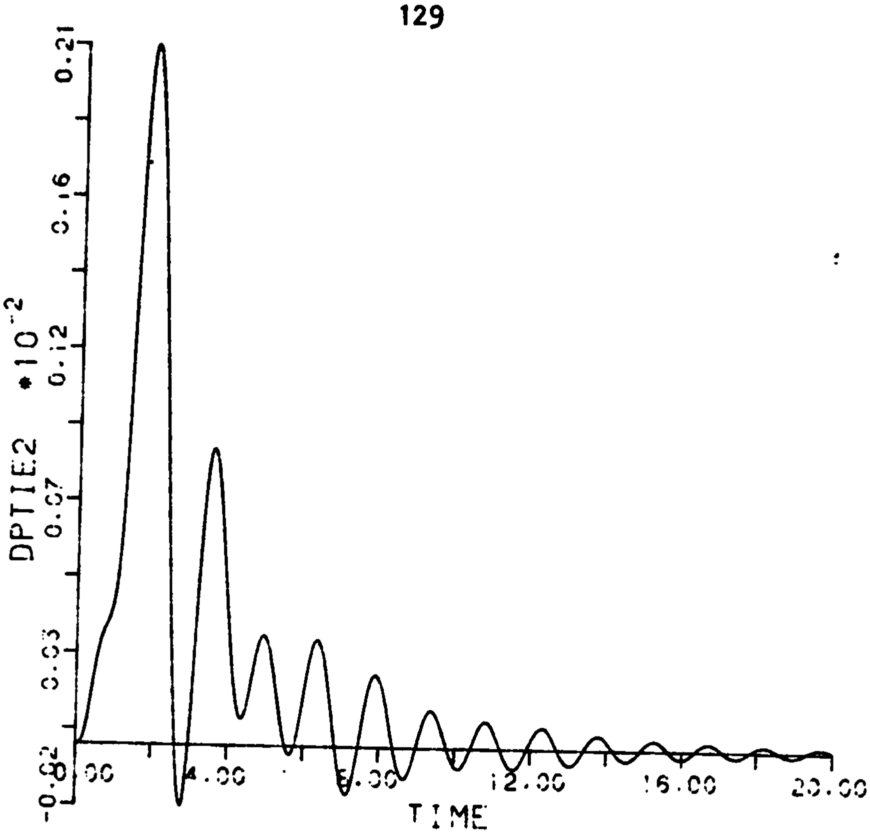

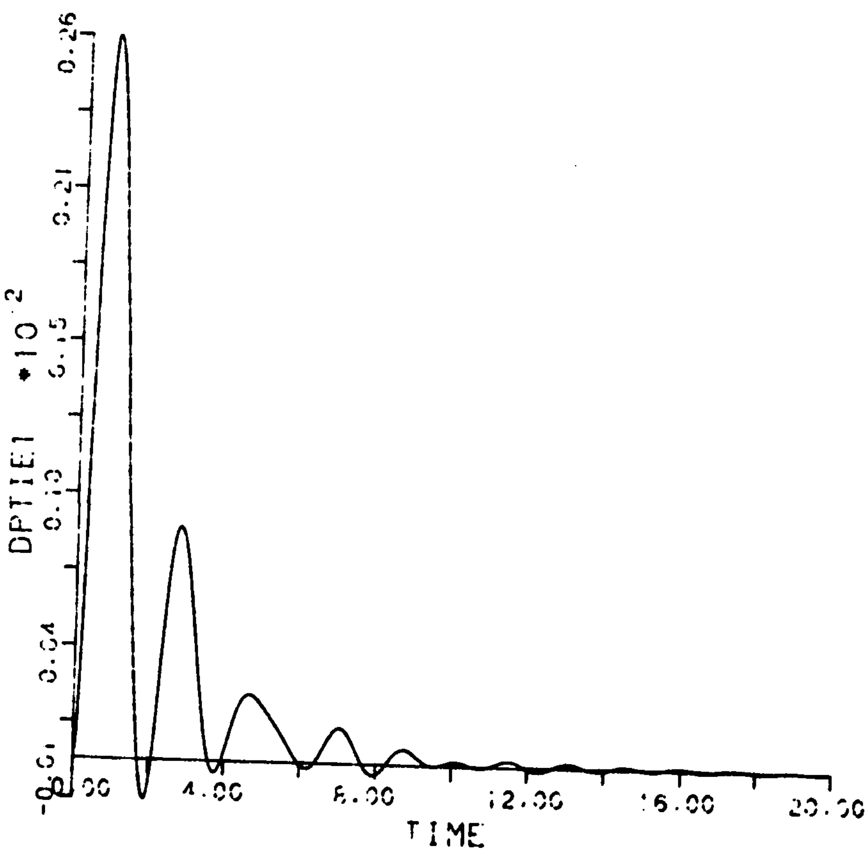

Figure 6-3c. Tie-line deviation in a controlled 4 area system containing a loop following a step load disturbance.

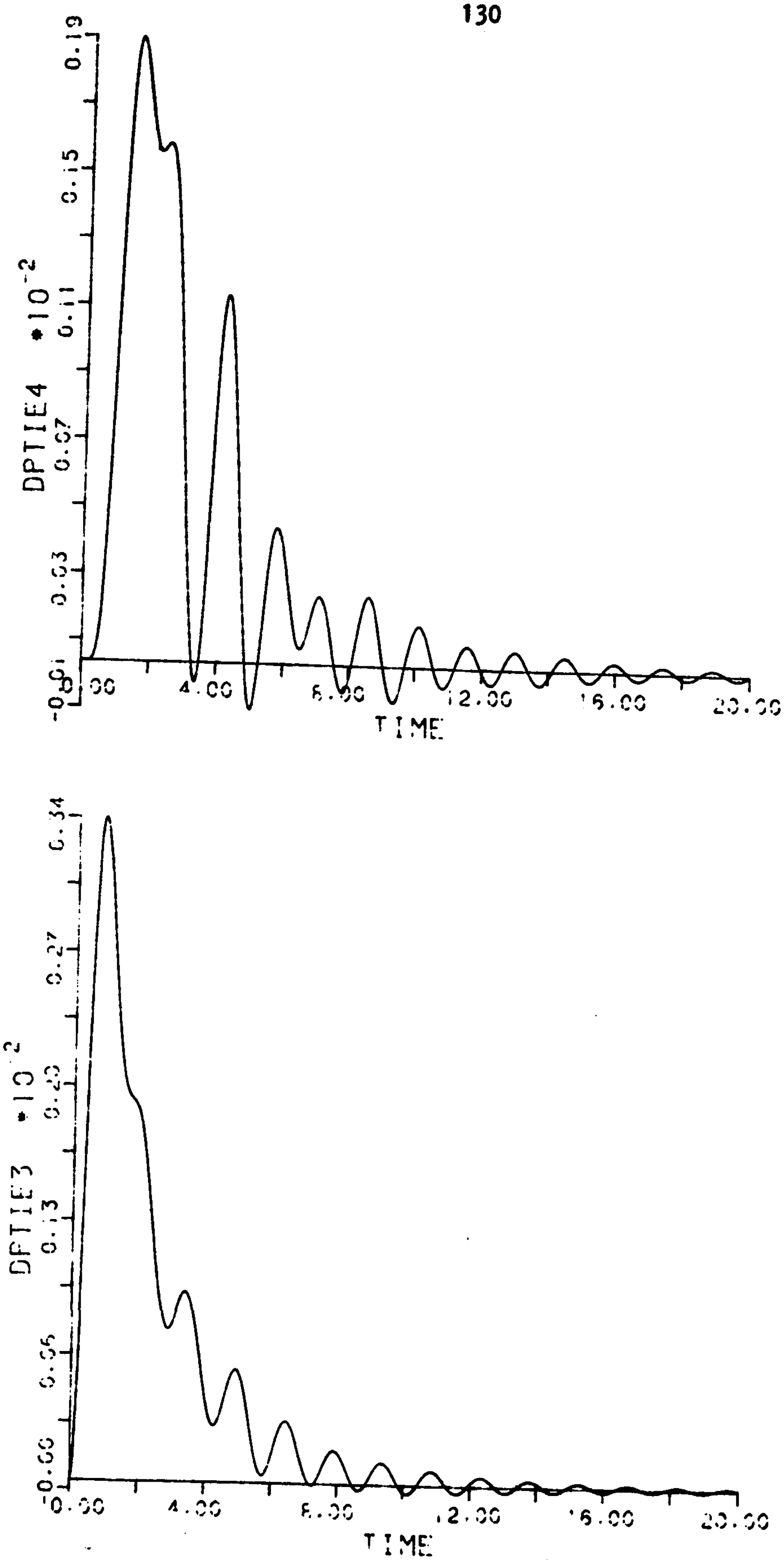

Figure 6-3d. Tie-line deviation in a controlled 4 area system containing a loop following a step load disturbance.

TABLE V. Range of Deviation of the Frequency and Tie-Line of a Controlled 4 Area Radial System.

	Range of Deviation
ΔF_1	$-0.4 * 10^{-2}$ to $0.8 * 10^{-2}$
ΔF_2	$-0.49 * 10^{2}$ to $0.51 * 10^{-2}$
ΔF_3	$-0.43 * 10^{-2}$ to $0.49 * 10^{-2}$
ΔF_4	$-0.26 * 10^{-2}$ to $0.24 * 10^{-2}$
$\Delta P_{tie\ 13}$	$-0.6 * 10^{-3}$ to $0.24 * 10^{-3}$
$\Delta P_{tie\ 23}$	$0.22 * 10^{-2}$ to $0.11 * 10^{-2}$
$\Delta P_{tie\ 32}$	$0.7 * 10^{-2}$ to $0.16 * 10^{-2}$

CONCLUSION

The load frequency control problem of power system has been considered under the assumption that a linear mathematical model of the power system is available in state space form. The method of solution adapted to solve the problem is based on decentralized control theory (13). In this method of design, the interaction between subsystems not available to the controller are obtained from a low-order crude model appropriately selected. The trajectories of the interaction vector are improved online before being used to generate the appropriate control force.

This design method has been applied to a multi-area power system to control the deviations of the frequency and tie-line power. It was found that the resultant load and frequency controller obtained provides a near-optimal solution.

The controller is easy to design and can be worked out subsystem by subsystem. No information transfer between subsystems is necessary. This results in a low implementation cost of the controller. Moreover the design method can be worked out by minicomputers.

The program developed for the purpose of this design method can handle system of any order.

The thesis consists of six chapters. In the first chapter, an introduction to large interconnected power system is presented. It also includes the advantages of interconnecting the power system into large interconnected system. The second chapter gives a literature review of various existing control methods applied to LFC. The third presents the model following algorithms. It also includes the design of the Robust decentralized controller. In chapter four, a description of the power system is considered. It also includes the state space representation of the model. The fifth chapter presents complete simulation of a two-area power system. In chapter six the algorithm is applied to a four-areas power system of different configurations.

It was found that the performance of the controller depends mainly on the following two factors:

(1) The crude model matrix, A_z has to be selected in such a way that all the eigenvalues of A_z lie on the left half plane. However, if the crude model matrix is not chosen as mentioned above the algorithm corrects the trajectories to a considerable extent.

(2) Appropriate selection of the weighting matrix, S, which minimizes the error of the output of the crude model also improved the performance of the controller..

The work done in this thesis could be extended without much difficulties, to take into consideration of the non-linearities in the power system.

Further research is also recommended to study the problem assuming interaction between load frequency and megavar, voltage control channels.

REFERENCES

[1] C.E. Fosha & O.I. Elgerd, "The megawatt-frequency control: a new approach via optimal control theory", IEEE Trans. on Power Apparatus & System, Vol. PAS-89, No. 4, April 1970, pp. 563-577.

[2] Y. Yu, K. Vongsuniya & L. Wedman, "Application of an optimal control theory to a power system", Trans. Paper, Paper No. 69 Tp. 104 - pwr, February 1969.

[3] T. Hiyama, "Load frequency regulators for interconnected power systems", IEE Proc., Vol. 129, No. 1, January 1982, pp. 18-23.

[4] E.J. Davison & N.K. Tripathi, "Decentralised tuning regulators: application to solve the load and frequency control problem for a large power system", IEEE, 1979.

[5] S.C. Tripathy & O.P. Malik, "Optimisation of load frequency control parameters for power systems with reheat steam turbines & governor deadband nonlinearity", IEE Proc., Vol. 129, No. 1, January 1982, pp. 10-16.

[6] Y. Misutani, "Sub-optimal control for load frequency control system using an area decomposition method", Electrical Engg. in Japan, Vol. 98, No. 6, December 1978, pp. 971-978.

[7] E.J. Davison & N.K. Tripathi, "Optimal decentralized control of large power system: load and frequency control", IEEE Trans. on Automatic Control, Vol. AC-23, No. 2, April 1978, pp. 312-324.

[8] G.M. Aly & Y.L. Abdel-Magid, "Two-level L.F.C. of interconnected power system", IECI 1981, San Francisco, CA, USA.

[9] S.A. Arafeh, "Hierarchical control of power distribution systems", IEE Trans. on Automatic Control, Vol. AC-23, No. 2, April 1978, pp. 333-343.

[10] R.K. Cavin, M.C. Budge & P. Rasmussen, "An optimal linear systems approach via load frequency control", IEE, December 1970.

[11] S.M. Miniesty & E.V. Bohn, "Optimum load frequency continuous control with unknown deterministic power demand", IEEE, February 1971.

[12] M. Singh & M. Hassan, "Decentralised controller with online interaction trajectory improvement", IEE Proceeding, Vol. 127, No. 3, May 1980, pp. 142-148.

[13] M. Singh & M. Hassan, "Controller for linear interconnected dynamical systems with prespecified degree of stability", Int. J. System Sci, Vol. 10, No. 3, May 1979, pp. 339-350.

[14] M.G. Singh & M. Hassan, "Robust decentralized controller linear-interconnected dynamical system", Proc. IEE, Vol. 125, No. 56, May 1978, pp. 429-432.

[15] M.G. Singh & M. Hassan, "A comparison of two hierarchical optimization methods", Int. J. System Sci., Vol. 7, No. 6, May 1975, pp. 603-611.

[16] C.A. Markland, "Optimal model following control synthesis techniques", IEE Proc., Vol. 117, No. 3, March 1970, pp. 623-627.

[17] C. Yuliu & M. Singh, "Certain practical considerations in the model-following method of decentralized control", IEE Proc., Vol. 128, No. 4,

July 1981, pp. 149-155.

[18] E. J. Davison, "Decentralized robust control of unknown systems using regulators", IEEE Transaction on Automatic Control, Vol. AC-23, No. 2, April 1978, pp. 276-288.

[19] M.S. Mahmoud, "A quantitative comparison between two decentralised control approach", Int. J. Control, Vol. 28, No. 2, June 1977, pp. 261-275.